Electronic Supplementary Material (ESI) for ChemComm.

Supporting Information

Catalyst-free nucleophilic borylation of fluorobenzenes with reduced arylboranes

Hendrik Budy, Sven E. Prey, Christoph D. Buch, Michael Bolte, Hans-Wolfram Lerner, and Matthias Wagner

Table of contents:

1. Experimental details and characterization data

General considerations. All reactions, manipulations, and analyses were carried out in an argon-filled glovebox or by applying standard Schlenk techniques under an argon atmosphere. Toluene, Et_2O, and THF were dried over Na/benzophenone; *n*-hexane was dried over Na; 1,2-dimethoxyethane (DME) and THF-d_8 were dried over Na-K alloy without benzophenone. Prior to use, the solvents were distilled from the drying agent and then degassed by applying three freeze-pump-thaw cycles. Fluorobenzene, 1,3,5-trifluorobenzene, and hexafluorobenzene were degassed by applying three freeze-pump-thaw cycles and were stored over molecular sieves (3 Å) several days prior to use. Me_3SiCl (TMSCl) was dried over CaH_2 and also degassed by applying three freeze-pump-thaw cycles prior to use. Compounds $[Na_2(dme)_{3.75}][\mathbf{2}]$,[S1] $Na_2[\mathbf{2'}]$,[S1] $[Li_2(thf)_{2.5}][\mathbf{3}]$,[S2] $[Na_2(thf)_{4.5}][\mathbf{3}]$,[S2] **4**,[S3] $\mathbf{4^H}$,[S4] $\mathbf{4^{Tol}}$,[S5] their respective dilithio and disodio salts,[S3,S5] and *p*-tolyllithium[S6] were synthesized according to literature procedures. Carbon atoms marked with asterisks bear *t*Bu substituents.

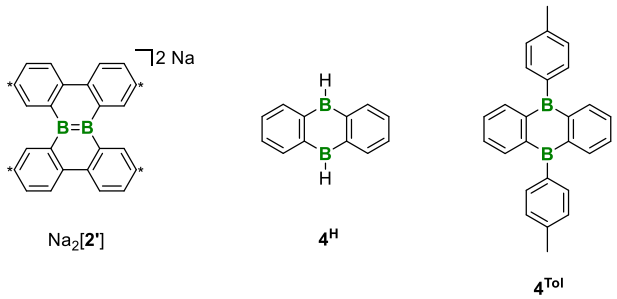

$Na_2[\mathbf{2'}]$ $\mathbf{4^H}$ $\mathbf{4^{Tol}}$

Figure S1. Compounds $Na_2[\mathbf{2'}]$, $\mathbf{4^H}$, and $\mathbf{4^{Tol}}$ (see the actual Communication for structural formulae of all other compounds).

NMR spectra were recorded at 298 K using the following Bruker spectrometers: Avance-300, Avance-400, or Avance-500.

Chemical shifts are referenced to (residual) solvent signals ($^1H/^{13}C\{^1H\}$ and $^{13}C\{^{19}F\}$: THF-d_8: δ = 3.58/67.21 ppm)[S7] or external $BF_3{\cdot}OEt_2$ (^{11}B: δ = 0.00 ppm) and $CFCl_3$ (^{19}F: δ = 0.00 ppm). Abbreviations: s = singlet, d = doublet, t = triplet, vt = virtual triplet, q = quartet, m = multiplet, br = broad, n.o. = not observed.

Note: Whenever a salt of $[\mathbf{3}]^{2-}$ was used as a reactant, the formation of $[\mathbf{3}H]^-$ and $[\mathbf{3}_2]^{2-}$ as minor side products was observed; these compounds were identified by their characteristic signals in the ^{11}B NMR spectra (cf. Figure S2).[S2] $[\mathbf{3}H]^-$ and $[\mathbf{3}_2]^{2-}$ are known side products of *open shell* reaction pathways during the conversions of $[\mathbf{3}]^{2-}$.[S2]

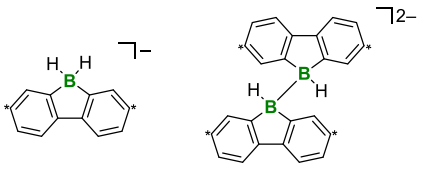

$[\mathbf{3}H]^-$ $[\mathbf{3}_2]^{2-}$

Figure S2. Anions $[\mathbf{3}H]^-$ and $[\mathbf{3}_2]^{2-}$.

1.1 Synthesis of Li[5]

Neat hexafluorobenzene (5.5 μL, 0.048 mmol, 1.5 equiv) was added with stirring at room temperature *via* syringe to a deep green solution of $[Li_2(thf)_{2.5}][\mathbf{3}]$ (15 mg, 0.032 mmol) in THF (1.5 mL). The color of the solution quickly faded. After approx. 30 min, all volatiles were removed *in vacuo*. The solid, off-white residue was dissolved in THF-d_8 (0.5 mL), the solution was transferred to an NMR tube, and the tube was flame-sealed. NMR spectroscopy revealed the selective formation of Li[**5**]. *Note*: A small excess of the fluorobenzene was used to suppress any two-fold substitution (cf. the synthesis of Li_2[**9**] below).

X-ray quality crystals of $[Li(thf)_4][\mathbf{5}]$ were grown from a THF solution of Li[**5**] at –30 °C. Mainly due to severely disordered thf ligands and *t*Bu groups, the quality of the crystals was poor. Nevertheless, the crystal structure determination can be taken as reliable proof of the general constitution of the molecule.[S8]

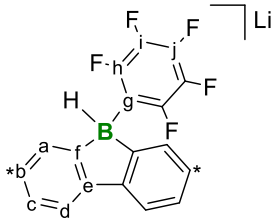

^{1}H NMR (500.2 MHz, THF-d_8): δ = 7.38 (br, 2H; H-a), 7.38 (d, ^3J(H,H) = 7.9 Hz, 2H; H-d), 6.95 (dd, ^3J(H,H) = 7.9 Hz, ^4J(H,H) = 2.0 Hz, 2H; H-c), 3.23 (q, ^1J(H,B) = 79 Hz, 1H; B*H*), 1.27 (s, 18H; C(CH_3)$_3$).

^{11}B NMR (160.5 MHz, THF-d_8): δ = –17.5 (d, ^1J(B,H) = 79 Hz; *B*H).

^{13}C{^{1}H} NMR (125.8 MHz, THF-d_8): δ = 165.3 (br; C-f), 149.0* (br d, ^1J(C,F) = 236 Hz; C-h), 147.2 (C-e), 145.5 (C-b), 137.3* (br d, ^1J(C,F) = 239 Hz; C-i or C-j), 137.0* (br d, ^1J(C,F) = 246 Hz; C-i or C-j), 127.8 (C-a), 120.1 (C-c), 117.3 (C-d), 34.8 (*C*(CH$_3$)$_3$), 32.3 (C(*C*H$_3$)$_3$), n.o. (C-g).

^{19}F NMR (470.6 MHz, THF-d_8): δ = –130.2 (br d, ^3J(F,F) = 24 Hz, 2F; F-h), –168.5 (t, ^3J(F,F) = 20 Hz, 1F; F-j), –169.2 – (–169.4) (m, 2F; F-i).

* These signals gave singlets in an ^{13}C{^{19}F} NMR experiment (cf. Figure S6).

1.2 Synthesis of Na[5]

Neat hexafluorobenzene (3.7 μL, 0.032 mmol, 2 equiv) was added with stirring at room temperature *via* syringe to a deep green solution of $[Na_2(thf)_{4.5}][\mathbf{3}]$ (10 mg, 0.016 mmol) in THF (1.5 mL) under stirring. Upon addition, the color of the solution quickly faded. All volatiles were removed *in vacuo*. The solid, off-white residue was dissolved in THF-d_8 (0.5 mL), the solution transferred to an NMR tube, and the tube was flame-sealed. NMR spectroscopy revealed the selective formation of Na[**5**]. *Note*: An excess of the fluorobenzene was used to suppress any two-fold substitution (cf. the synthesis of Na_2[**9**] below).

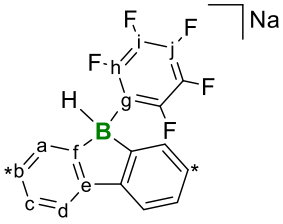

^{1}H NMR (500.2 MHz, THF-d_8): δ = 7.45 (d, ^3J(H,H) = 7.9 Hz, 2H; H-d), 7.42 (br, 2H; H-a), 7.02 (dd, ^3J(H,H) = 7.9 Hz, ^4J(H,H) = 2.0 Hz, 2H; H-c), 3.09 (q, ^1J(H,B) = 79 Hz, 1H; B*H*), 1.28 (s, 18H; C(CH_3)$_3$).

^{11}B NMR (160.5 MHz, THF-d_8): δ = –17.6 (d, ^1J(B,H) = 79 Hz; *B*H).

^{13}C{^{1}H} NMR (125.8 MHz, THF-d_8): δ = 163.8 (br; C-f), 149.0* (br d, ^1J(C,F) = 236 Hz; C-h), 147.0 (C-e), 146.2 (C-b), 137.5* (d, ^1J(C,F) = 239 Hz; C-i or C-j), 137.0* (d, ^1J(C,F) = 246 Hz; C-i or C-j), 127.9 (C-a), 120.9 (C-c), 117.9 (C-d), 34.9 (*C*(CH$_3$)$_3$), 32.2 (C(*C*H$_3$)$_3$), n.o. (C-g).

^{19}F NMR (470.6 MHz, THF-d_8): δ = –130.9 (br d, ^3J(F,F) = 24 Hz, 2F; F-h), –167.8 (t, ^3J(F,F) = 20 Hz, 1F; F-j), –168.8 – (–169.0) (m, 2F; F-i).

* These signals gave singlets in an ^{13}C{^{19}F} NMR experiment (cf. Figure S11).

1.3 Synthesis of Li[6]

Neat 1,3,5-trifluorobenzene (2.2 µL, 0.021 mmol, 1.0 equiv) was added with stirring at room temperature *via* syringe to a deep green solution of [Li$_2$(thf)$_{2.5}$][**3**] (10 mg, 0.021 mmol) in THF-d$_8$ (0.5 mL). Upon addition, the color of the solution quickly faded. The reaction solution was placed in an NMR tube and the tube was flame-sealed. NMR spectroscopy revealed the selective formation of Li[**6**].

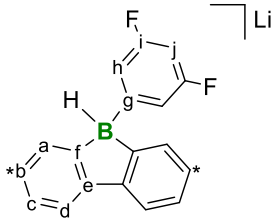

^{1}H NMR (500.2 MHz, THF-d_8): δ = 7.53 (br, 2H; H-a), 7.37 (d, ^3J(H,H) = 7.8 Hz, 2H; H-d), 6.94 (dd, ^3J(H,H) = 7.8 Hz, ^4J(H,H) = 2.0 Hz, 2H; H-c), 6.91 (br, 2H; H-h), 6.15 (tt, ^3J(H,F) = 9.4 Hz, ^4J(H,H) = 2.5 Hz, 1H; H-j) 3.10 (q, ^1J(H,B) = 81 Hz, 1H; B*H*), 1.31 (s, 18H; C(C*H*$_3$)$_3$).

^{11}B NMR (160.5 MHz, THF-d_8): δ = –11.6 (d, ^1J(B,H) = 81 Hz; *B*H).

^{13}C{^{1}H} NMR (125.8 MHz, THF-d_8): δ = 170.2 (q, ^1J(C,B) = 51 Hz; C-g), 166.6 (q, ^1J(C,B) = 49 Hz; C-f), 162.7 (br d, ^1J(C,F) = 241 Hz; C-i), 147.2 (C-e), 145.5 (C-b), 128.3 (C-a), 120.0 (C-c), 117.3 (C-d), 115.6* (br d, ^2J(C,F) = 15 Hz; C-h), 96.2* (t, ^2J(C,F) = 25 Hz; C-j), 34.9 (*C*(CH$_3$)$_3$), 32.3 (C(*C*H$_3$)$_3$).

^{19}F NMR (470.6 MHz, THF-d_8): δ = –117.8 (vt, ^3J(F,H) = 9 Hz; F-i).

* These signals gave doublets in an ^{13}C{^{19}F} NMR experiment with a coupling constant of ^1J(C,H) = 160 Hz (cf. Figure S16).

1.4 Synthesis of Na[6]

Neat 1,3,5-trifluorobenzene (3.3 µL, 0.032 mmol, 2.1 equiv) was added with stirring at room temperature *via* syringe to a deep green solution of [Na$_2$(thf)$_{4.5}$][**3**] (10 mg, 0.015 mmol) in THF (2 mL). Upon addition, the color of the solution quickly faded. All volatiles were removed *in vacuo*. The solid, off-white residue was dissolved in THF-d_8 (0.5 mL), the solution transferred to an NMR tube and the tube was flame-sealed under vacuum. NMR spectroscopy revealed the selective formation of Na[**6**].

X-ray quality crystals of [Na(dme)$_2$(thf)][**6**] were grown from a DME/THF solution of Na[**6**] at –30 °C.

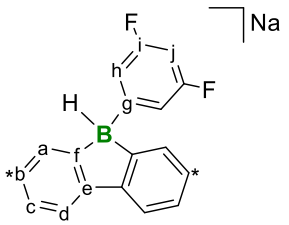

^{1}H NMR (500.2 MHz, THF-d_8): δ = 7.56 (br, 2H; H-a), 7.46 (d, ^{3}J(H,H) = 7.9 Hz, 2H; H-d), 7.04 (dd, ^{3}J(H,H) = 7.9 Hz, ^{4}J(H,H) = 2.0 Hz, 2H; H-c), 6.85 (br, 2H; H-h), 6.20 (tt, ^{3}J(H,F) = 9.4 Hz, ^{4}J(H,H) = 2.5 Hz, 1H; H-j), 2.94 (q, ^{1}J(H,B) = 78 Hz, 1H; B*H*), 1.31 (s, 18H; C(CH_3)$_3$).

^{11}B NMR (160.5 MHz, THF-d_8): δ = –11.8 (d, ^{1}J(B,H) = 78 Hz; *B*H).

^{13}C{^{1}H} NMR (125.8 MHz, THF-d_8): δ = 167.8 (q, ^{1}J(B,C) = 51 Hz; C-g), 164.3 (q, ^{1}J(B,C) = 49 Hz; C-f), 162.8 (br d, ^{1}J(C,F) = 241 Hz; C-i), 147.0 (C-e), 146.6 (C-b), 128.6 (C-a), 121.2 (C-c), 118.1 (C-d), 115.6* (br d, ^{2}J(C,F) = 15 Hz; C-h), 96.9* (t, ^{2}J(C,F) = 26 Hz; C-j), 34.9 (*C*(CH$_3$)$_3$), 32.2 (C(*C*H$_3$)$_3$).

^{19}F NMR (470.6 MHz, THF-d_8): δ = –117.3 (vt, ^{3}J(F,H) = 9 Hz, 2F; F-i).

* These signals gave doublets in an ^{13}C{^{19}F} NMR experiment with a coupling constant ^{1}J(H,C) = 160 Hz (cf. Figure S21).

1.5 Synthesis of Li[7]

Neat hexafluorobenzene (5.6 µL, 0.049 mmol, 1.0 equiv) was added at room temperature *via* syringe to an NMR tube charged with a freshly prepared deep red THF-d_8 solution (0.5 mL) of Li$_2$[**4**] (0.049 mmol). Upon addition, the color of the solution quickly faded. The NMR tube was flame-sealed. NMR spectroscopy revealed the selective formation of Li[**7**].

X-ray quality crystals of [Li(12-c-4)$_2$][**7**] were grown by gas-phase diffusion of *n*-hexane into a THF solution of Li[**7**] in the presence of 12-crown-4.

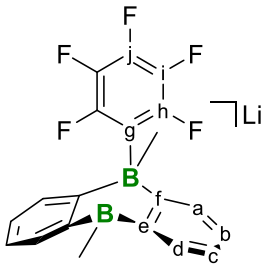

^{1}H NMR (500.2 MHz, THF-d_8): δ = 7.96 (br d, ^{3}J(H,H) = 7.4 Hz, 2H; H-d), 7.27 (br d, ^{3}J(H,H) = 7.4 Hz, 2H; H-a), 7.01 (vtd, ^{3}J(H,H) = 7.4 Hz, ^{4}J(H,H) = 1.4 Hz, 2H; H-b), 6.89 (vtd, ^{3}J(H,H) = 7.4 Hz, ^{4}J(H,H) = 1.3 Hz, 2H; H-c), 1.32 (s, 3H; BCH_3), 0.11 (br s, 3H; Ar^{F}BCH_3).

^{11}B NMR (160.5 MHz, THF-d_8): δ = 64.3 ($h_{1/2}$ ≈ 1030 Hz; *B*CH$_3$), –12.4 (Ar^{F}*B*CH$_3$).

^{13}C{^{1}H} NMR (125.8 MHz, THF-d_8): δ = 178.4 (br; C-f), 150.0 (ddddd, ^{1}J(C,F) = 236 Hz, ^{2}J(C,F) = 20 Hz, ^{3}J(C,F) = 7 Hz, ^{3}J(C,F) = 4 Hz, ^{4}J(C,F) = 4 Hz; C-h), 143.2 (br; C-e), 137.3 (dtt, ^{1}J(C,F) = 240 Hz, ^{2}J(C,F) = 14 Hz, ^{3}J(C,F) = 6 Hz; C-j), 136.7 (dddd, ^{1}J(C,F) = 246 Hz, ^{2}J(C,F) = 23 Hz, ^{2}J(C,F) = 12 Hz, ^{3}J(C,F) = 4 Hz; C-i), 134.5 (C-d), 133.3 (C-a), 129.5 (C-b), 121.7 (C-c), 18.5 (br; Ar^{F}B*C*H$_3$), 5.0 (B*C*H$_3$), n.o. (C-g).

^{19}F NMR (470.6 MHz, THF-d_8): δ = –130.3 (br d, ^{3}J(F,F) = 21 Hz, 2F; F-h), –168.6 (t, ^{3}J(F,F) = 20 Hz, 1F; F-j), –169.4 – (–169.6) (m, 2F; F-i).

1.6 Synthesis of Na[7]

Neat hexafluorobenzene (5.6 µL, 0.049 mmol, 1.0 equiv) was added at room temperature *via* syringe to an NMR tube charged with a freshly prepared deep green THF-d_8 solution (0.5 mL) of Na_2[**4**] (0.049 mmol). Upon addition, the color of the solution quickly faded. The NMR tube was flame-sealed. NMR spectroscopy revealed the selective formation of Na[**7**].

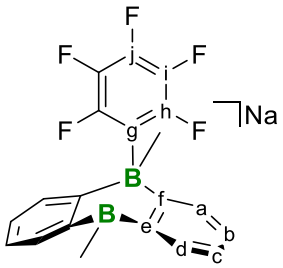

^{1}H NMR (500.2 MHz, THF-d_8): δ = 7.96 (br d, ^3J(H,H) = 7.4 Hz, 2H; H-d), 7.27 (br d, ^3J(H,H) = 7.4 Hz, 2H; H-a), 7.00 (vtd, ^3J(H,H) = 7.4 Hz, ^4J(H,H) = 1.4 Hz, 2H; H-b), 6.88 (vtd, ^3J(H,H) = 7.4 Hz, ^4J(H,H) = 1.4 Hz, 2H; H-c), 1.32 (s, 3H; BCH_3), 0.11 (br s, 3H; Ar^{F}BCH_3).

^{11}B NMR (160.5 MHz, THF-d_8): δ = 63.9 ($h_{1/2}$ ≈ 980 Hz; *B*CH_3), –12.3 (Ar^F*B*CH_3).

^{13}C{^{1}H} NMR (125.8 MHz, THF-d_8): δ = 178.4 (br; C-f), 150.0 (ddddd, ^1J(C,F) = 237 Hz, ^2J(C,F) = 20 Hz, ^3J(C,F) = 8 Hz, ^3J(C,F) = 4 Hz, ^4J(C,F) = 4 Hz; C-h), 143.2 (br; C-e), 137.3 (dtt, ^1J(C,F) = 240 Hz, ^2J(C,F) = 14 Hz, ^3J(C,F) = 6 Hz; C-j), 136.7 (dddd, ^1J(C,F) = 246 Hz, ^2J(C,F) = 23 Hz, ^2J(C,F) = 12 Hz, ^3J(C,F) = 4 Hz; C-i), 134.5 (C-d), 133.3 (C-a), 129.4 (C-b), 121.6 (C-c), 18.5 (br; Ar^{F}B*C*H_3), 5.0 (B*C*H_3), n.o. (C-g).

^{19}F NMR (470.6 MHz, THF-d_8): δ = –130.3 (br d, ^3J(F,F) = 21 Hz, 2F; F-h), –168.6 (t, ^3J(F,F) = 20 Hz, 1F; F-j), –169.5 – (–169.7) (m, 2F; F-i).

1.7 Synthesis of Na[7^{Tol}]

Neat hexafluorobenzene (5.8 µL, 0.050 mmol, 1.0 equiv) was added at room temperature *via* syringe to an NMR tube charged with a freshly prepared deep green THF-d_8 solution (0.5 mL) of Na_2[**4**^{Tol}] (0.050 mmol). Upon addition, the color of the solution quickly faded. The NMR tube was flame-sealed. NMR spectroscopy revealed the selective formation of Na[**7**^{Tol}].

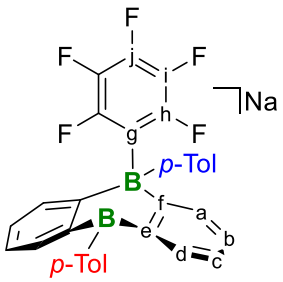

^{1}H NMR (500.2 MHz, THF-d_8): δ = 7.52 (br d, ^3J(H,H) = 7.3 Hz, 2H; H-d), 7.51 (d, ^3J(H,H) = 7.3 Hz, 2H; H-a), 7.38 (d, ^3J(H,H) = 7.7 Hz, 2H; *p*-Tol-H-*o*), 7.16 (d, ^3J(H,H) = 7.7 Hz, 2H; *p*-Tol-H-*m*), 7.02 (td, ^3J(H,H) = 7.3 Hz, ^4J(H,H) = 1.5 Hz, 2H; H-b), 6.97 (d, ^3J(H,H) = 7.7 Hz, 2H; *p*-Tol-H-*o*), 6.80 (td, ^3J(H,H) = 7.3 Hz, ^4J(H,H) = 1.3 Hz, 2H; H-c), 6.56 (d, ^3J(H,H) = 7.7 Hz, 2H; *p*-Tol-H-*m*), 2.39 (s, 3H; *p*-Tol-CH_3), 2.08 (s, 3H; *p*-Tol-CH_3).

^{11}B NMR (160.5 MHz, THF-d_8): δ = 63.4 ($h_{1/2}$ ≈ 1620 Hz; *p*-Tol*B*), –10.0 (*p*-Tol*B*Ar^F).

^{13}C{^{1}H} NMR (125.8 MHz, THF-d_8): δ = 176.4 (br; C-f), 158.8 (br; *p*-Tol-C-*i*), 149.9 (br d, ^1J(C,F) = 240 Hz; C-h), 146.1 (br; *p*-Tol-C-*i*), 143.9 (br; C-e), 138.4 (C-d), 137.8 (br d, ^1J(C,F) = 240 Hz; C-j), 137.1 (br d,

^{1}J(C,F) = 253 Hz; C-i), 135.3 (*p*-Tol-C-*p*), 134.5 (*p*-Tol-C-*o*), 134.0 (C-a), 132.7 (*p*-Tol-C-*o*), 129.8 (*p*-Tol-C-*p*), 129.7 (C-b), 127.6 (*p*-Tol-C-*m*), 126.5 (*p*-Tol-C-*m*), 122.0 (C-c), 21.4 (*p*-Tol-*C*H$_3$), 21.1 (*p*-Tol-*C*H$_3$), n.o. (C-g).

^{19}F NMR (470.6 MHz, THF-d_8): δ = –123.7 – (–123.8) (m, 2F; F-h), –167.9 (t, ^{3}J(F,F) = 20 Hz, 1F; F-j), –169.1 – (–169.2) (m, 2F; F-i).

1.8 Synthesis of Li[8]

Neat 1,3,5-Trifluorobenzene (5.1 µL, 0.049 mmol, 1.0 equiv) was added at room temperature *via* syringe to an NMR tube charged with a freshly prepared deep red THF-d_8 solution (0.5 mL) of Li$_2$[**4**] (0.049 mmol). The NMR tube was flame-sealed. According to NMR spectroscopy, a slow reaction took place at room temperature. After 22 h at 50 °C, the color of the solution had faded and NMR spectroscopy revealed the selective formation of Li[**8**].

X-ray quality crystals of [Li(12-c-4)$_2$][**8**] were grown by gas-phase diffusion of *n*-hexane into a THF solution of Li[**8**] in the presence of 12-crown-4.

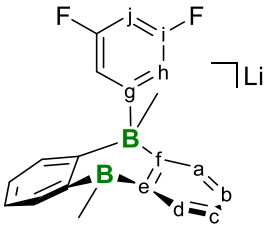

^{1}H NMR (500.2 MHz, THF-d_8): δ = 7.95 (br d, ^{3}J(H,H) = 7.3 Hz, 2H; H-d), 7.34 (br d, ^{3}J(H,H) = 7.3 Hz, 2H; H-a), 6.99 (vtd, ^{3}J(H,H) = 7.3 Hz, ^{4}J(H,H) = 1.5 Hz, 2H; H-b), 6.87 (vtd, ^{3}J(H,H) = 7.3 Hz, ^{4}J(H,H) = 1.4 Hz, 2H; H-c), 6.65 (br d, ^{3}J(H,F) = 9.4 Hz, 2H; H-h), 6.06 (tt, ^{3}J(H,F) = 9.4 Hz, ^{4}J(H,H) = 2.5 Hz, 1H; H-j), 1.33 (s, 3H; BC*H*$_3$), 0.14 (br, 3H; Ar^{F}BC*H*$_3$).

^{11}B NMR (160.5 MHz, THF-d_8): δ = 63.7 ($h_{1/2}$ ≈ 1000 Hz; *B*CH$_3$), –13.2 (Ar^{F}*B*CH$_3$).

^{13}C{^{1}H} NMR (125.8 MHz, THF-d_8): δ = 179.1 (q, ^{1}J(C,B) = 49 Hz; C-f), 175.9 (q, ^{1}J(C,B) = 45 Hz; C-g), 162.4 (br d, ^{1}J(C,F) = 243 Hz; C-i), 144.2 (C-e), 134.4 (C-a), 134.3 (C-d), 129.3 (C-b), 121.5 (C-c), 115.3 (br d, ^{2}J(C,F) = 16 Hz; C-h), 95.8 (t, ^{2}J(C,F) = 26 Hz; C-j), 14.8 (q, ^{1}J(C,B) = 41 Hz; Ar^{F}B*C*H$_3$), 5.0 (br; B*C*H$_3$).

^{19}F NMR (470.6 MHz, THF-d_8): δ = –118.0 (vt, ^{3}J(F,H) = 9 Hz; F-i).

1.9 Synthesis of Na[8]

Neat 1,3,5-trifluorobenzene (5.1 µL, 0.049 mmol, 1.0 equiv) was added at room temperature *via* syringe to an NMR tube charged with a freshly prepared deep green THF-d_8 solution (0.5 mL) of Na$_2$[**4**] (0.049 mmol). The NMR tube was flame-sealed. The color of the solution faded upon storage overnight at room temperature. NMR spectroscopy revealed the selective formation of Na[**8**].

X-ray quality crystals of [Na(thf)$_2$][**8**·py] were grown by gas-phase diffusion of *n*-hexane into a THF solution of Na[**8**] in the presence of 1 equiv. pyridine.

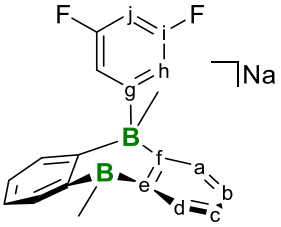

^{1}H NMR (500.2 MHz, THF-d_8): δ = 7.95 (br d, ^{3}J(H,H) = 7.3 Hz, 2H; H-d), 7.32 (br d, ^{3}J(H,H) = 7.3 Hz, 2H; H-a), 6.98 (vtd, ^{3}J(H,H) = 7.3 Hz, ^{4}J(H,H) = 1.4 Hz, 2H; H-b), 6.86 (vtd, ^{3}J(H,H) = 7.3 Hz, ^{4}J(H,H) = 1.3 Hz, 2H; H-c), 6.66 (br d, ^{3}J(H,F) = 9.4 Hz, 2H; H-h), 6.06 (tt, ^{3}J(H,F) = 9.4 Hz, ^{4}J(H,H) = 2.5 Hz, 1H; H-j), 1.33 (s, 3H; BCH_3), 0.14 (br, 3H; Ar^{F}BCH_3).

^{11}B NMR (160.5 MHz, THF-d_8): δ = 64.7 ($h_{1/2}$ ≈ 970 Hz; BCH$_3$), –13.2 (Ar^{F}BCH$_3$).

^{13}C{^{1}H} NMR (125.8 MHz, THF-d_8): δ = 179.1 (q, ^{1}J(C,B) = 49 Hz; C-f), 175.9 (q, ^{1}J(C,B) = 46 Hz; C-g), 162.4 (br d, ^{1}J(C,F) = 241 Hz; C-i), 144.2 (C-e), 134.4 (C-a), 134.3 (C-d), 129.2 (C-b), 121.5 (C-c), 115.4 (br d, ^{2}J(C,F) = 14 Hz; C-h), 95.8 (t, ^{2}J(C,F) = 26 Hz; C-j), 14.8 (q, ^{1}J(C,B) = 41 Hz; Ar^{F}BCH$_3$), 5.0 (br; BCH$_3$).

^{19}F NMR (470.6 MHz, THF-d_8): δ = –118.2 (vt, ^{3}J(F,H) = 9 Hz; F-i).

1.10 Synthesis of Na[8^{Tol}]

Neat 1,3,5-trifluorobenzene (5.2 µL, 0.050 mmol, 1.0 equiv) was added at room temperature *via* syringe to an NMR tube charged with a freshly prepared deep green THF-d_8 solution (0.5 mL) of Na$_2$[**4**^{Tol}] (0.050 mmol). The NMR tube was flame-sealed. According to NMR spectroscopy, no reaction took place at room temperature. After 22 h at 100 °C, the color of the solution had faded and NMR spectroscopy revealed the selective formation of Na[**8**^{Tol}].

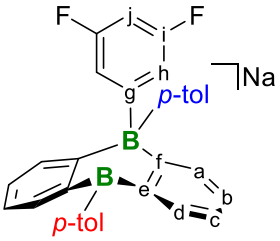

^{1}H NMR (500.2 MHz, THF-d_8): δ = 7.53 (br d, ^{3}J(H,H) = 7.4 Hz, 2H; H-d), 7.43 (br d, ^{3}J(H,H) = 7.4 Hz, 2H; H-a), 7.41 (d, ^{3}J(H,H) = 7.7 Hz, 2H; *p*-Tol-H-*o*), 7.18 (d, ^{3}J(H,H) = 7.7 Hz, 2H; *p*-Tol-H-*m*), 7.08 (br d, ^{3}J(H,H) = 7.2 Hz, 2H; *p*-Tol-H-*o*), 7.00 (vtd, ^{3}J(H,H) = 7.4 Hz, ^{4}J(H,H) = 1.5 Hz, 2H; H-b), 6.79 (vtd, ^{3}J(H,H) = 7.4 Hz, ^{4}J(H,H) = 1.3 Hz, 2H; H-c), 6.76 (br d, ^{3}J(H,F) = 9.4 Hz, 2H; H-h), 6.69 (d, ^{3}J(H,H) = 7.2 Hz, 2H; *p*-Tol-H-*m*), 6.15 (tt, ^{3}J(H,F) = 9.4 Hz, ^{4}J(H,H) = 2.5 Hz, 1H; H-j), 2.40 (s, 3H; *p*-Tol-CH_3), 2.16 (s, 3H; *p*-Tol-CH_3).

^{11}B NMR (160.5 MHz, THF-d_8): δ = 61.7 ($h_{1/2}$ ≈ 1300 Hz; *p*-TolB), –8.5 (*p*-Tol$B$Ar^{F}).

^{13}C{^{1}H} NMR (125.8 MHz, THF-d_8): δ = 178.5 (q, ^{1}J(C,B) = 50 Hz; C-f), 174.1 (q, ^{1}J(C,B) = 46 Hz; C-g), 162.4 (br d, ^{1}J(C,F) = 239 Hz; C-i), 161.3 – 160.0 (m; *p*-Tol-C-*i*), 146.2 (br; *p*-Tol-C-*i*), 144.7 (br; C-e), 138.3 (C-d), 136.1 (*p*-Tol-C-*o*), 135.7 (C-a), 135.3 (*p*-Tol-C-*p*), 132.7 (*p*-Tol-C-*o*), 130.2 (*p*-Tol-C-*p*), 129.5 (C-b), 127.6 (*p*-Tol-C-*m*), 126.9 (*p*-Tol-C-*m*), 121.8 (C-c), 117.2 (d, ^{2}J(C,F) = 15 Hz; C-h), 96.3 (t, ^{2}J(C,F) = 26 Hz; C-j), 21.4 (*p*-Tol-CH$_3$), 21.2 (*p*-Tol-CH$_3$).

^{19}F NMR (470.6 MHz, THF-d_8): δ = –117.8 (vt, ^{3}J(F,H) = 9 Hz; F-i).

1.11 Synthesis of Li$_2$[9]

Neat hexafluorobenzene (17 µL, 0.147 mmol, 1.7 equiv) was added with stirring at room temperature *via* syringe to a deep green solution of [Li$_2$(thf)$_{2.5}$][**3**] (40 mg, 0.085 mmol) in THF (3 mL) to give a solution of Li[**5**] (cf. 1.1). All volatiles were removed *in vacuo*. The solid, off-white residue was dissolved in THF-d_8 (0.5 mL) and [Li$_2$(thf)$_{2.5}$][**3**] (40 mg, 0.085 mmol, 1.0 equiv) was added. The solution was transferred to an NMR tube and the tube was flame-sealed. NMR spectroscopy revealed the selective formation of Li$_2$[**9**]. *Note*: The reaction can also be carried out in one step, but is then less selective (cf. 1.23).

X-ray quality crystals of $[Li(dme)_2][\mathbf{9}]\cdot(THF)_2$ were grown from a DME/THF solution of $Li_2[\mathbf{9}]$ at –30 °C.

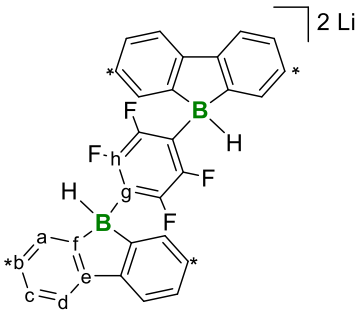

^{1}H NMR (500.2 MHz, THF-d_8): δ = 7.50 (d, ^4J(H,H) = 2.0 Hz, 4H; H-a), 7.34 (d, ^3J(H,H) = 7.9 Hz, 4H; H-d), 6.89 (dd, ^3J(H,H) = 7.9 Hz, ^4J(H,H) = 2.0 Hz, 4H; H-c), 3.18* (2H; B*H*), 1.27 (s, 36H; C(CH_3)$_3$).

^{11}B NMR (160.5 MHz, THF-d_8): δ = –16.9 (d, ^1J(B,H) = 81 Hz; *B*H).

^{13}C{^{1}H} NMR (125.8 MHz, THF-d_8): δ = 167.2 (br, C-f), 149.1** (br d, ^1J(C,F) = 236 Hz; C-h), 147.0 (C-e), 145.1 (C-b), 128.3 (C-a), 119.6 (C-c), 117.0 (C-d), 34.8 (*C*(CH$_3$)$_3$), 32.4 (C(*C*H$_3$)$_3$), n.o. (C-g).

^{19}F NMR (470.6 MHz, THF-d_8): δ = –137.1 (s; F-h).

* This signal was detected in an ^{1}H{^{11}B} NMR experiment (cf. Figure S47).

** This signal gave a singlet in an ^{13}C{^{19}F} NMR experiment (cf. Figure S50).

1.12 Synthesis of Na_2[9]

Neat hexafluorobenzene (1.4 µL, 0.012 mmol, 0.5 equiv) was added with stirring at room temperature *via* syringe to a deep green solution of $[Na_2(thf)_{4.5}][\mathbf{3}]$ (15 mg, 0.023 mmol) in THF-d_8 (0.5 mL). The solution was stirred for 3 d. Afterwards, the solution was transferred to an NMR tube and the tube was flame-sealed. NMR spectroscopy revealed the formation of a product mixture consisting mainly of $Na_2[\mathbf{9}]$ (approx. 50%), $Na_2[\mathbf{3}_2]$, and Na[**3**H] (cf. Figure S2).

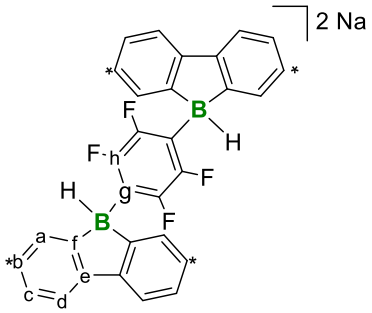

^{1}H NMR (300.0 MHz, THF-d_8): δ = 7.45 (br, 4H; H-a), 7.38 (d, ^3J(H,H) = 7.9 Hz, 4H; H-d), 6.95 (br d, ^3J(H,H) = 7.9 Hz, 4H; H-c), 1.27 (s, 36H; C(CH_3)$_3$), n.o. (B*H*).

^{11}B NMR (96.3 MHz, THF-d_8): δ = –17.2 (d, ^1J(B,H) = 79 Hz; *B*H).

^{19}F NMR (282.3 MHz, THF-d_8): δ = –140.5 (s; F-h).

1.13 Synthesis of Na[10]

Neat hexafluorobenzene (2.0 µL, 0.017 mmol, 1.0 equiv) was added with stirring at room temperature *via* syringe to a deep blue solution of $[Na_2(dme)_{3.75}][\mathbf{2}]$ (16 mg, 0.017 mmol) in THF-d_8 (0.5 mL). The solution turned deep red quickly. The solution was transferred to an NMR tube and the tube was flame-sealed. The deep red color of the solution faded slowly within 6 h. ^{1}H and ^{19}F NMR spectroscopy

revealed the initial conversion of Na_2[**2**] (blue) to Na_2[**2'**] (red)[S1] in the presence of hexafluorobenzene, which afterwards lead to the selective formation of Na[**10**] (cf. Figures S55 and S56).

An independently conducted reaction of Na_2[**2'**] with hexafluorobenzene also furnished selectively Na[**10**].

X-ray quality crystals of [Na(thf)$_3$(dme)][**10**] were grown from a THF solution of Na[**10**] at –30 °C.

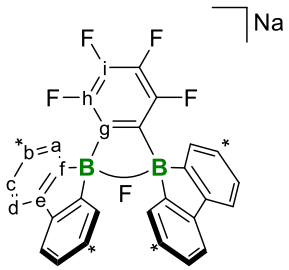

^{1}H NMR (500.2 MHz, THF-d_8): δ = 7.58 (br, 4H; H-a), 7.34 (d, ^3J(H,H) = 7.9 Hz, 4H; H-d), 7.13 (br d, ^3J(H,H) = 7.9 Hz, 4H; H-c), 1.34 (s, 36H; C(CH_3)$_3$).

^{11}B NMR (160.5 MHz, THF-d_8): δ = 19.8 (^1J(B,F) not resolved).

^{13}C{^{1}H} NMR (125.8 MHz, THF-d_8): δ = 152.7* (br d, ^2J(C,F) = 25 Hz; C-f), 148.1 (C-e), 148.0* (br d, ^4J(C,F) = 6 Hz; C-b), 145.8* (br d, ^1J(C,F) = 244 Hz; C-h or C-i), 138.3* (br d, ^1J(C,F) = 244 Hz; C-h or C-i), 136.5 (br, C-g), 128.1 (C-a), 124.5 (C-c), 117.9 (C-d), 35.0 (*C*(CH$_3$)$_3$), 32.3 (C(*C*H$_3$)$_3$).

^{19}F NMR (470.6 MHz, THF-d_8): δ = –139.2 – (–139.3) (m, 2F; F-h or F-i), –165.8 – (–165.8) (m, 2F; F-h or F-i), –186.9 (br, 1F; B(μ-*F*)B).

* These signals gave singlets in an ^{13}C{^{19}F} NMR experiment (see Figure S60).

1.14 Synthesis of 11

Neat hexafluorobenzene (12 μL, 0.104 mmol, 1.1 equiv) was added with stirring at room temperature *via* syringe to a deep green solution of [Li$_2$(thf)$_{2.5}$][**3**] (45 mg, 0.096 mmol) in THF (3 mL) to give a solution of Li[**5**] (cf. 1.1). All volatiles were removed *in vacuo*. The solid, off-white residue was dissolved in THF-d_8 (0.5 mL) and TMSCl (12.5 μL, 0.098 mmol, 1.0 equiv) was added. The solution was transferred to an NMR tube and the tube was flame-sealed. Subsequent heating of the reaction solution to 50 °C for 1 d resulted in only minor conversions (cf. Figures S62 and S63). Upon addition of more TMSCl (0.08 mL, 0.6 mmol, 6 equiv) and upon subsequent heating (50 °C) for an overall period of 3 d, the complete consumption of Li[**5**] was observed (cf. Figures S62 and S63). All volatiles were removed *in vacuo* and the residue was re-dissolved in THF-d_8. **11** was formed with a selectivity of approx. 70% (according to ^{1}H NMR spectroscopy). The other products are unknown.

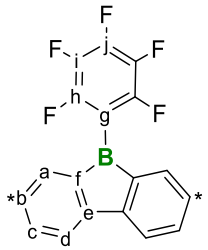

^{1}H NMR (500.2 MHz, THF-d_8): δ = 7.61 (br, 2H; H-a), 7.43 (br d, ^3J(H,H) = 7.6 Hz, 2H; H-d), 7.21 (br d, ^3J(H,H) = 7.6 Hz, 2H; H-c), 1.30 (s, 18H; C(CH_3)$_3$).

^{11}B NMR (96.3 MHz, THF-d_8): δ = 9.3.

^{19}F NMR (282.3 MHz, THF-d_8): δ = –131.3 (br, 2F; F-h or F-i), –161.0 (br, 1F; F-j), –165.8 (br, 2F; F-h or F-i).

Note: Since the measured sample was the crude reaction mixture, no ^{13}C{^{1}H} and 2D NMR spectra were recorded.

1.15 Synthesis of 12

TMSCl (1.0 µL, 0.0079 mmol, 1.1 equiv) was added at room temperature *via* syringe to a solution of [Na(dme)(thf)$_{1.5}$][**10**] (7 mg, 0.007 mmol) in THF-d_8 (0.5 mL). The solution was placed in an NMR tube. The tube was flame-sealed and the sample monitored by ^{1}H and ^{19}F NMR spectroscopy at room temperature (cf. Figures S68 – S72). 2 h after the addition, the formation of a new set of signals, assignable to **12**, was observed. Also, the resonances of TMSF were detected. NMR spectra recorded 10 h after the addition of TMSCl showed the complete consumption of Na[**10**] and the selective formation of **12** (together with TMSF). NMR spectra recorded 4 d later exhibited signal broadening as well as a new set of signals indicating the formation of a minor, unknown new product. The mixture remained essentially unchanged over weeks thereafter.

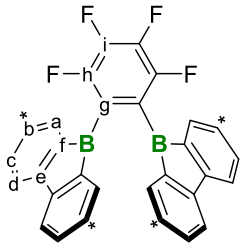

^{1}H NMR (300.0 MHz, THF-d_8): δ = 7.66 (d, ^4J(H,H) = 2.0 Hz, 4H; H-a), 7.39 (d, ^3J(H,H) = 7.9 Hz, 4H; H-d), 7.14 (dd, ^3J(H,H) = 7.9 Hz, ^4J(H,H) = 2.0 Hz, 4H; H-c), 1.35 (s, 36H; C(CH_3)$_3$).

^{11}B NMR (96.3 MHz, THF-d_8): δ = 11.4.

^{19}F NMR (282.3 MHz, THF-d_8): δ = –137.2 – (–137.3) (m, 2F; F-h or F-i), –166.2 – (–166.3) (m, 2F; F-h or F-i).

Note: Since the measured sample was the crude reaction mixture, no ^{13}C{^{1}H} and 2D NMR spectra were recorded.

1.16 Synthesis of LiNa[13]

Methyllithium (1.6 M in Et_2O, 30.5 µL, 0.049 mmol, 1.0 equiv) was added at room temperature *via* syringe to an NMR tube charged with a THF-d_8 solution (0.5 mL) of Na[**4**] (0.049 mmol). All volatiles were removed *in vacuo*, the remaining colorless solid was re-dissolved in THF-d_8, and the NMR tube was flame-sealed. NMR spectroscopy revealed the selective formation of LiNa[**13**].

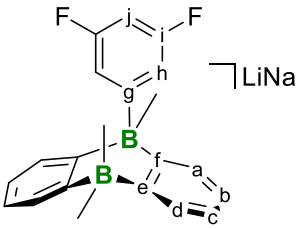

^{1}H NMR (500.2 MHz, THF-d_8): δ = 7.50 (br, 2H; H-d), 7.18 (br d, ^{3}J(H,H) = 7.2 Hz, 2H; H-a), 6.83 (br d, ^{3}J(H,F) = 9.4 Hz, 2H; H-h), 6.72 (vtd, ^{3}J(H,H) = 7.2 Hz, ^{4}J(H,H) = 1.6 Hz, 2H; H-c), 6.63 (vtd, ^{3}J(H,H) = 7.2 Hz, ^{4}J(H,H) = 1.6 Hz, 2H; H-b), 6.01 (tt, ^{3}J(H,F) = 9.4 Hz, ^{4}J(H,H) = 2.5 Hz, 1H; H-j), 0.18 (s, 3H; $Ar^{F}BC\mathit{H}_3$), –0.05 – (–0.11) (m, 6H; $B(C\mathit{H}_3)_2$).

^{11}B NMR (160.5 MHz, THF-d_8): δ = –14.0 ($Ar^{F}\mathit{B}CH_3$), –17.3 ($\mathit{B}(CH_3)_2$).

^{13}C{^{1}H} NMR (125.8 MHz, THF-d_8): δ = 180.4 – 179.1 (m; C-g), 168.0 (q, ^{1}J(C,B) = 48 Hz, C-e), 164.1 (q, ^{1}J(C,B) = 47 Hz; C-f), 162.5 (dd, ^{1}J(C,F) = 244 Hz, ^{3}J(C,F) = 10 Hz; C-i), 133.7 (C-a), 132.5 (C-d), 122.5 (C-c), 122.1 (C-b), 115.2 (dd, ^{2}J(C,F) = 14 Hz, ^{4}J(C,F) = 2 Hz; C-h), 95.2 (t, ^{2}J(C,F) = 26 Hz; C-j), 20.6 (q, ^{1}J(C,B) = 40 Hz; $H_3\mathit{C}BCH_3$), 17.5 (q, ^{1}J(C,B) = 38 Hz; $H_3CB\mathit{C}H_3$), 15.5 (q, ^{1}J(C,B) = 40 Hz; $Ar^{F}B\mathit{C}H_3$).

^{19}F NMR (470.6 MHz, THF-d_8): δ = –118.1 (vt, ^{3}J(F,H) = 9 Hz; F-i).

1.17 Synthesis of LiNa[S1]

A THF-d_8 solution (0.5 mL) of Na[**4**^{Tol}] (0.050 mmol) was added at room temperature *via* syringe to an NMR tube charged with *p*-tolyllithium (5 mg, 0.05 mmol, 1 equiv). The NMR tube was flame-sealed; NMR spectroscopy revealed the selective formation of LiNa[**S1**].

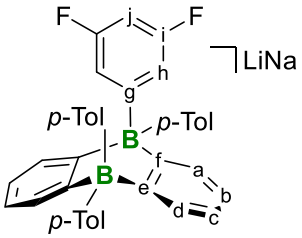

^{1}H NMR (400.3 MHz, THF-d_8): δ = 7.29 – 7.23 (m, 4H; *p*-Tol), 7.18 – 7.15 (m, 2H; H-a or H-d), 7.09 – 7.06 (m, 2H; H-a or H-d), 6.95 (d, ^{3}J(H,H) = 7.5 Hz, 2H; *p*-Tol), 6.71 (d, ^{3}J(H,H) = 7.6 Hz, 2H; *p*-Tol), 6.68 (d, ^{3}J(H,H) = 7.6 Hz, 2H; *p*-Tol), 6.63 – 6.58 (m, 6H; H-b, H-c, and H-h), 6.55 (d, ^{3}J(H,H) = 7.5 Hz, 2H; *p*-Tol), 6.03 (tt, ^{3}J(H,F) = 9.5 Hz, ^{4}J(H,H) = 2.3 Hz, 1H; H-j), 2.13 (s, 3H; *p*-Tol-CH_3), 2.11 (s, 6H; 2x *p*-Tol-CH_3).

^{11}B NMR (128.4 MHz, THF-d_8): δ = –8.5, –8.8.

^{19}F NMR (376.6 MHz, THF-d_8): δ = –118.6 (vt, ^{3}J(F,H) = 10 Hz; F-i).

1.18 Treatment of Na_2[2] with fluorobenzene

Neat fluorobenzene (5.0 μL, 0.053 mmol, 2.4 equiv) was added at room temperature *via* syringe to a deep blue solution of [$Na_2(dme)_{3.75}$][**2**] (21 mg, 0.022 mmol) in THF-d_8 (0.5 mL). The color of the solution remained unchanged. The solution was transferred to an NMR tube. The tube was flame-sealed and the sample monitored by ^{1}H and ^{19}F NMR spectroscopy. No reaction was observed

1.19 Treatment of Na_2[2] with 1,2-difluorobenzene

Neat 1,2-difluorobenzene (5.0 μL, 0.051 mmol, 2.4 equiv) was added at room temperature *via* syringe to a solution of [$Na_2(dme)_{3.75}$][**2**] (20 mg, 0.021 mmol) in THF-d_8 (0.5 mL). The color of the solution remained unchanged. The solution was transferred to an NMR tube. The tube was flame-sealed and the sample monitored by ^{1}H and ^{19}F NMR spectroscopy. No reaction was observed.

1.20 Treatment of Na_2[2] with 1,3,5-trifluorobenzene

Neat 1,3,5-trifluorobezene (2.0 μL, 0.019 mmol, 1.0 equiv) was added at room temperature *via* syringe to a solution of [$Na_2(dme)_{3.75}$][**2**] (18 mg, 0.019 mmol) in THF-d_8 (0.5 mL). The solution was transferred

to an NMR tube. The reaction solution quickly changed its color from deep blue to deep red, indicating the isomerization of Na_2[**2**] to Na_2[**2'**] (cf. 1.13).[S1] The tube was flame-sealed and the sample monitored by ^{1}H and ^{19}F NMR spectroscopy. The quantitative formation of Na_2[**2'**] was observed while 1,3,5-trifluorobezene remained unconsumed. At room temperature or slightly elevated temperatures (up to 50 °C), no further reaction was observed. When the sample was heated to 120 °C, thermal decomposition processes gave a complex reaction mixture.

1.21 Reaction of an excess of Na_2[2] with hexafluorobenzene

Neat hexafluorobenzene (0.5 μL, 0.004 mmol, 0.2 equiv) was added at room temperature *via* syringe to a solution of [Na_2(dme)$_{3.75}$][**2**] (16 mg, 0.017 mmol) in THF-d_8 (0.5 mL). The initially deep blue solution turned deep red quickly. The solution was placed in an NMR tube and the tube was flame-sealed. ^{1}H NMR spectroscopy revealed the selective formation of Na_2[**2'**] and Na[**10**]; no quadruply borylated product was observed (cf. Figure S80).

1.22 Treatment of Li_2[3] with fluorobenzene

Neat fluorobenzene (8.5 μL, 0.090 mmol, 1.0 equiv) was added at room temperature *via* syringe to an NMR tube charged with a freshly prepared solution of Li_2[**3**] (0.090 mmol) in THF-d_8 (0.5 mL). The NMR tube was flame-sealed. According to NMR spectroscopy, a slow reaction took place at room temperature, which yielded multiple products. Among them, Li_2[**3**$_2$] and Li[**3**H] could be identified (cf. Figure S2); other products remained unknown.

1.23 Reaction of an excess of Li_2[3] with hexafluorobenzene

Neat hexafluorobenzene (2.4 μL, 0.21 mmol, 0.5 equiv) was added at room temperature *via* syringe to a solution of [Li_2(thf)$_{2.5}$][**3**] (20 mg, 0.043 mmol) in THF-d_8 (0.5 mL). The solution was transferred to an NMR tube and the tube was flame-sealed. The sample was monitored by ^{1}H and ^{19}F NMR spectroscopy at room temperature (cf. Figures S81 and S82). 2 h after mixing, hexafluorobenzene was fully consumed and the solution consisted mainly of Li_2[**3**], Li[**5**], and Li_2[**9**]. After 2 d, also most of the Li_2[**3**] was consumed and the solution consisted mainly of Li_2[**9**].

1.24 Reaction of Li_2[4^H] with hexafluorobenzene

Neat hexafluorobenzene (5.9 μL, 0.051 mmol, 1.0 equiv) was added at room temperature *via* syringe to an NMR tube charged with a freshly prepared deep green THF-d_8 solution (0.5 mL) of Li_2[**4^H**] (0.051 mmol). Upon addition, the color of the solution quickly faded. The NMR tube was flame-sealed. NMR spectroscopy revealed the formation of Li[**7^H**] (cf. Figures S83 – S85).

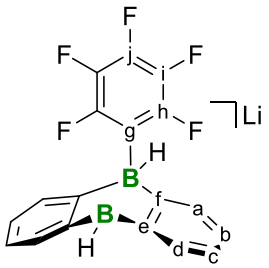

^{1}H NMR (300.0 MHz, THF-d_8): δ = 7.81 (br d, ^3J(H,H) = 7.2 Hz, 2H; H-d), 7.25 (br d, ^3J(H,H) = 7.2 Hz, 2H; H-a), 7.05 (br vt, ^3J(H,H) = 7.2 Hz, 2H; H-b), 6.94 (br vt, ^3J(H,H) = 7.2 Hz, 2H; H-c), 3.59 (q, ^1J(H,B) = 79 Hz, 1H; Ar^{F}B*H*), n.o. (B*H*).

^{11}B NMR (96.3 MHz, THF-d_8): δ = 64.9 ($h_{1/2}$ = 1000 Hz, *B*H), –17.7 (d, ^1J(B,H) = 79 Hz, Ar^F*B*H).

^{19}F NMR (282.3 MHz, THF-d_8): δ = –130.6 (br d, ^3J(F,F) = 25 Hz, 2F, F-h), –167.8 (t, ^3J(F,F) = 20 Hz, 1F, F-j), –168.8 – (–169.0) (m, 2F, F-i).

Note: The assignment of the resonances is based on that of Li[**7**] (cf. 1.5).

1.25 Reaction of 11 with LiH

A sample of **11** (0.04 mmol), obtained from Li[**5**] and TMSCl (cf. 1.19), was taken from the reaction solution. All volatiles were removed *in vacuo*. The solid, yellowish residue was dissolved in THF-d_8 (0.5 mL) and LiH (2 mg, 0.3 mmol, 8 equiv) was added at room temperature. The mixture was placed in an NMR tube, which was flame-sealed under vacuum. The signals of Li[**5**] were detected again by NMR spectroscopy (cf. Figures S86 – S88).

2. Plots of the NMR spectra

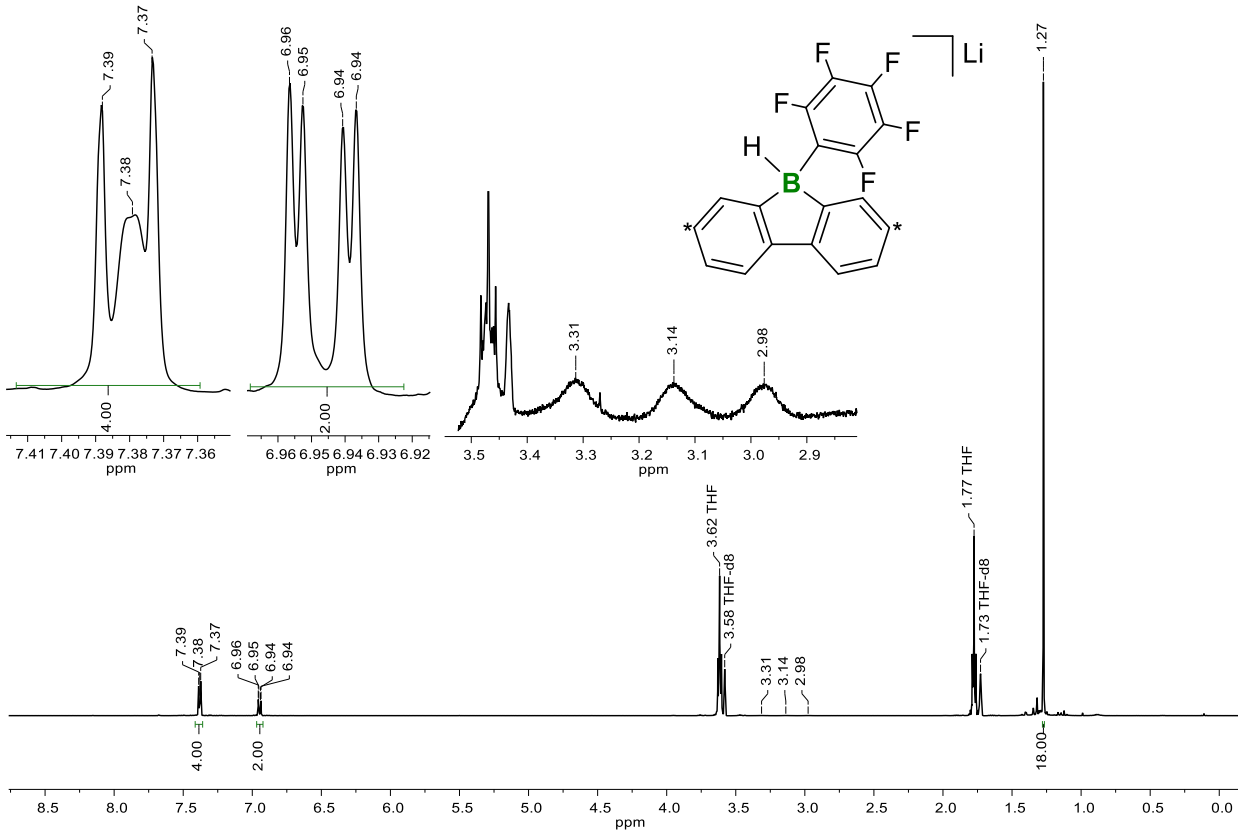

Figure S3. ^{1}H NMR spectrum (500.2 MHz, THF-d_8) of Li[**5**].

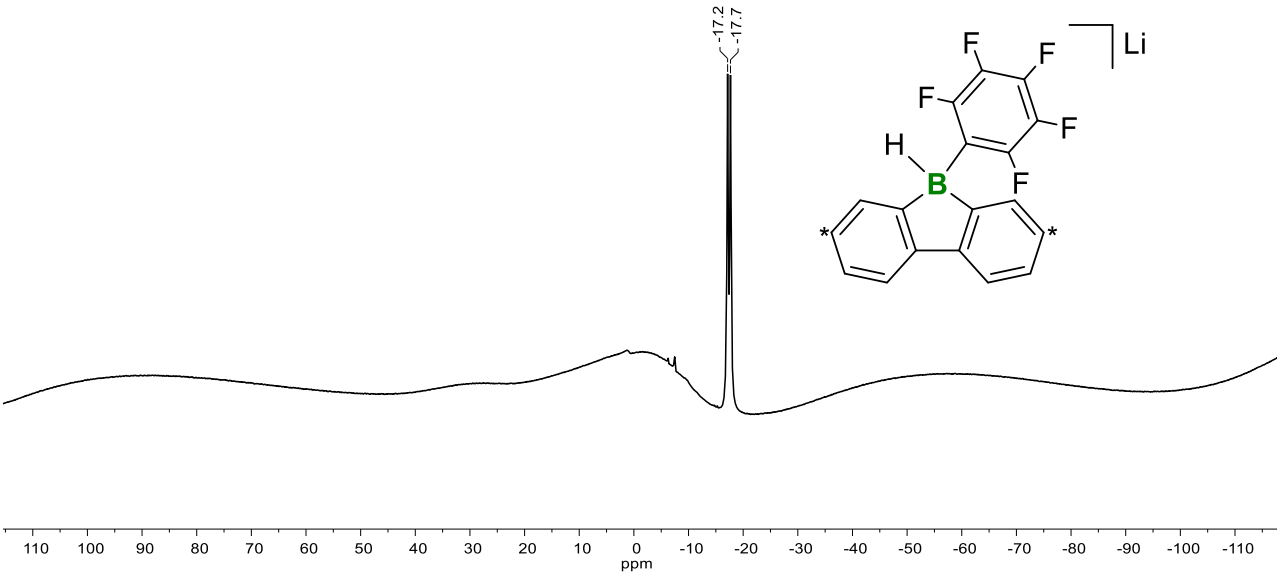

Figure S4. ^{11}B NMR spectrum (160.5 MHz, THF-d_8) of Li[**5**].

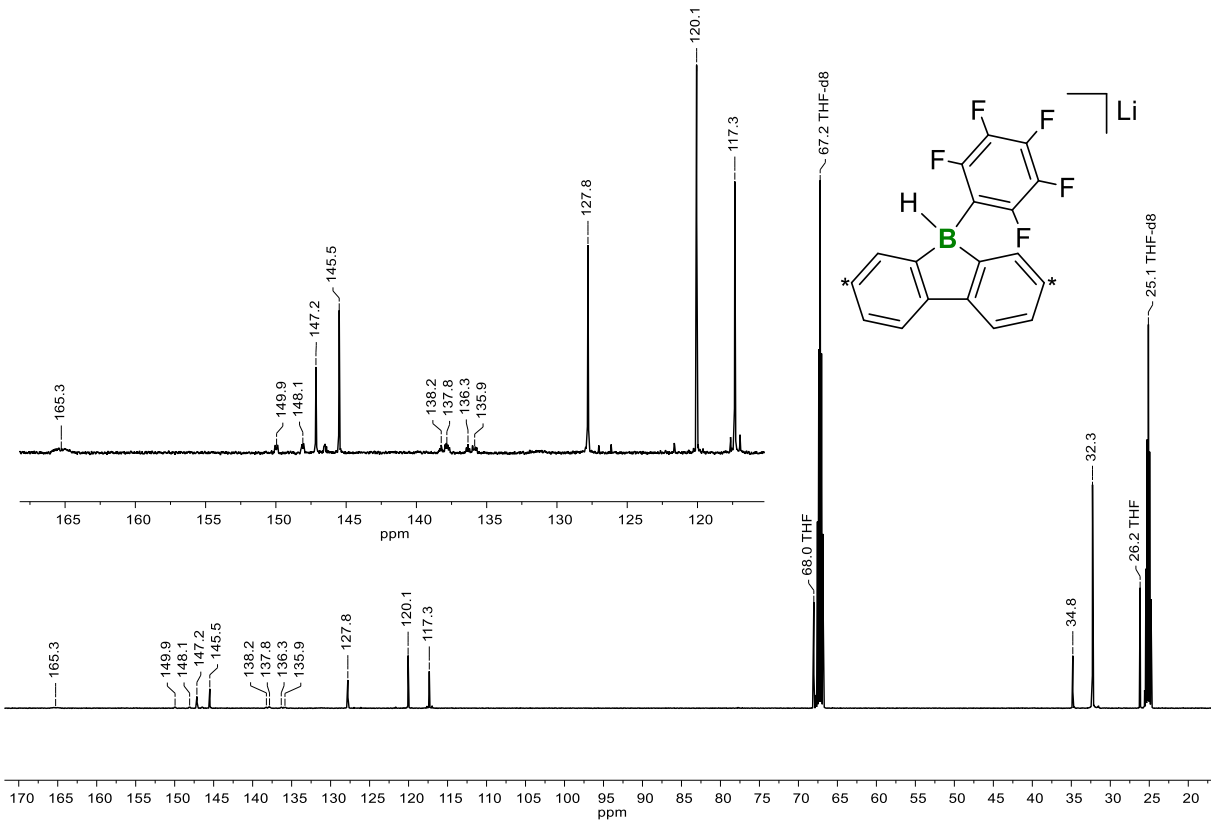

Figure S5. $^{13}C\{^{1}H\}$ NMR spectrum (125.8 MHz, THF-d_8) of Li[**5**].

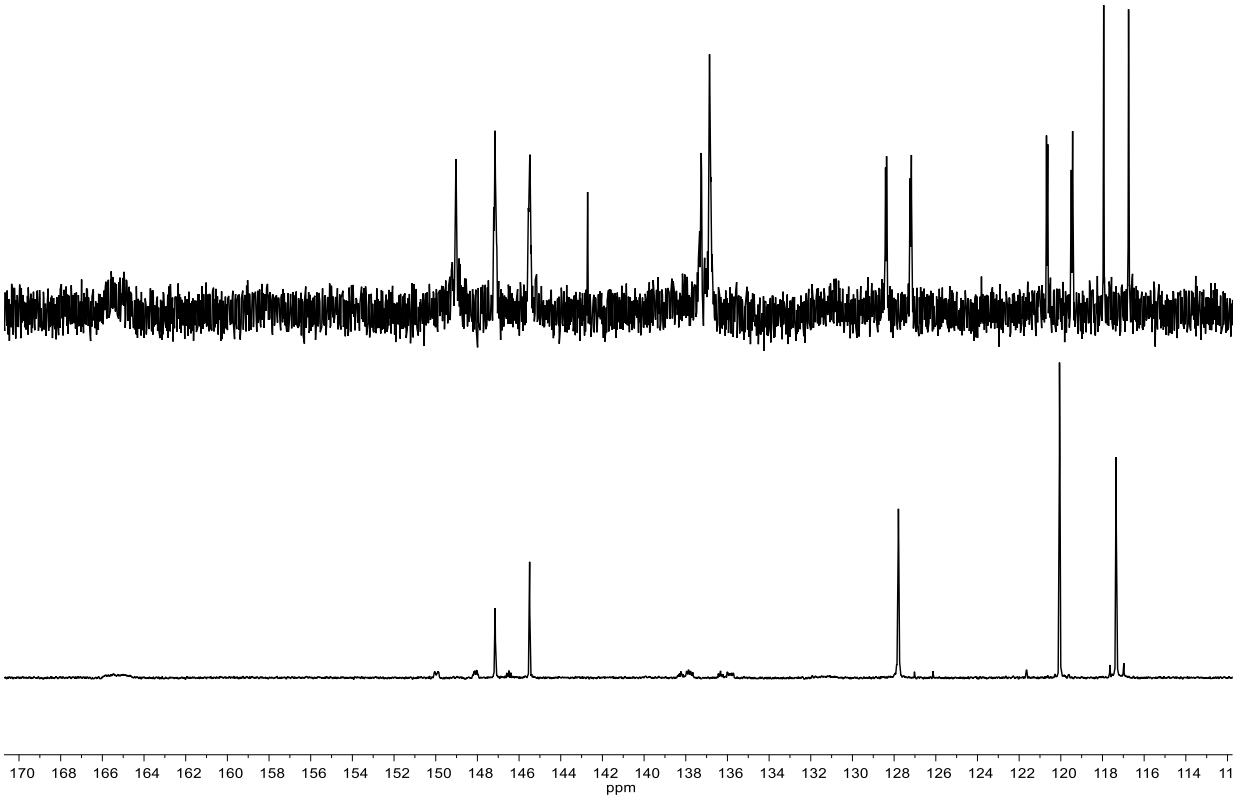

Figure S6. Aromatic regions of the $^{13}C\{^{19}F\}$ (125.8 MHz, THF-d_8; top) and $^{13}C\{^{1}H\}$ NMR spectra (125.8 MHz, THF-d_8; bottom) of Li[**5**].

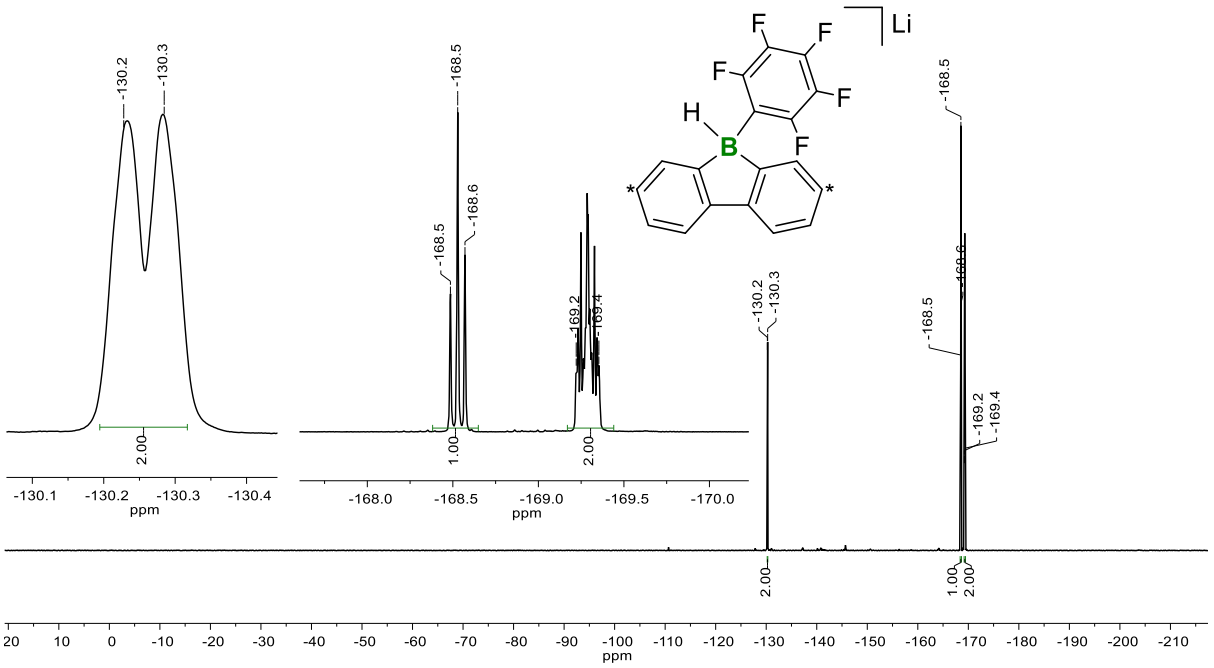

Figure S7. ^{19}F NMR spectrum (470.6 MHz, THF-d_8) of Li[**5**].

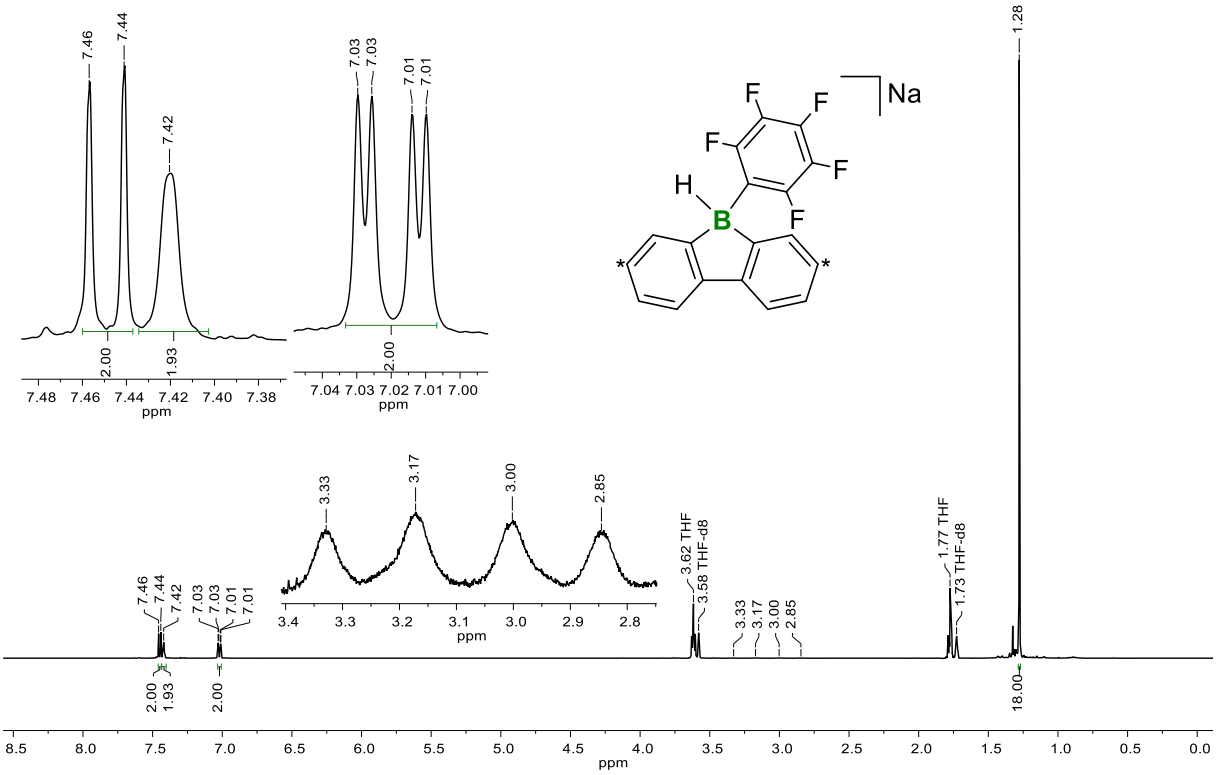

Figure S8. ^{1}H NMR spectrum (500.2 MHz, THF-d_8) of Na[**5**].

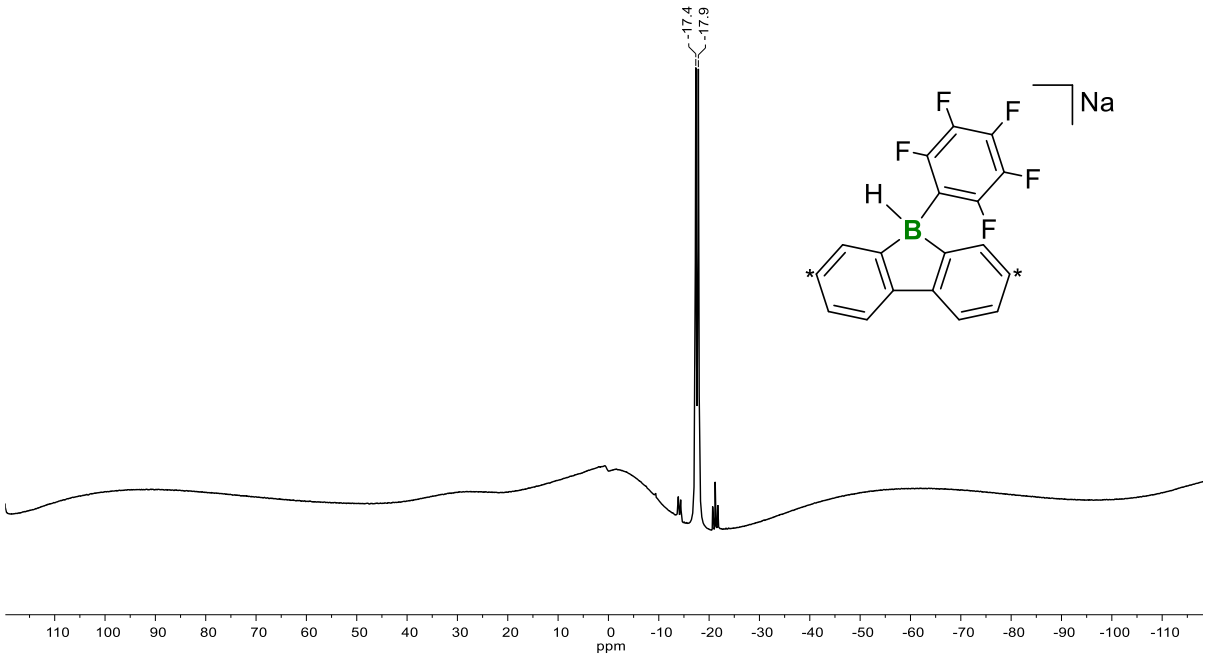

Figure S9. ^{11}B NMR spectrum (160.5 MHz, THF-d_8) of Na[**5**].

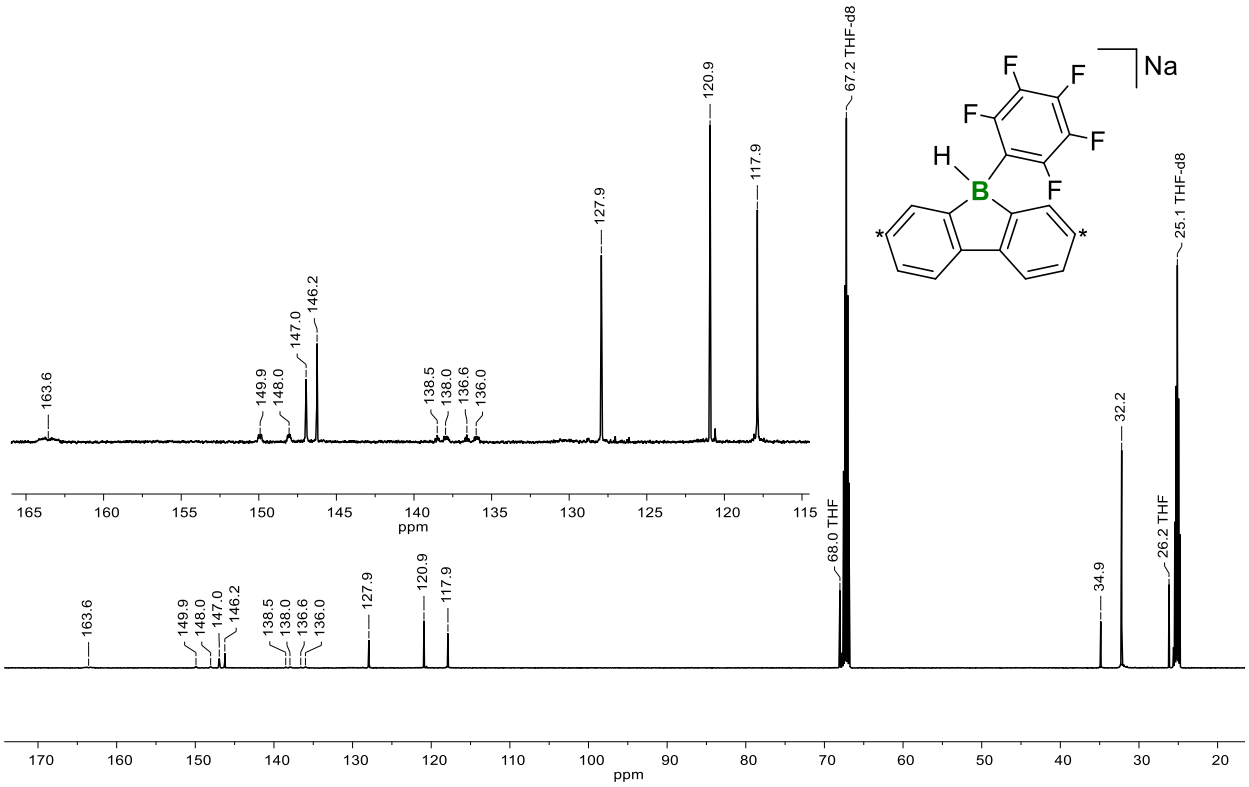

Figure S10. ^{13}C{^{1}H} NMR spectrum (125.8 MHz, THF-d_8) of Na[**5**].

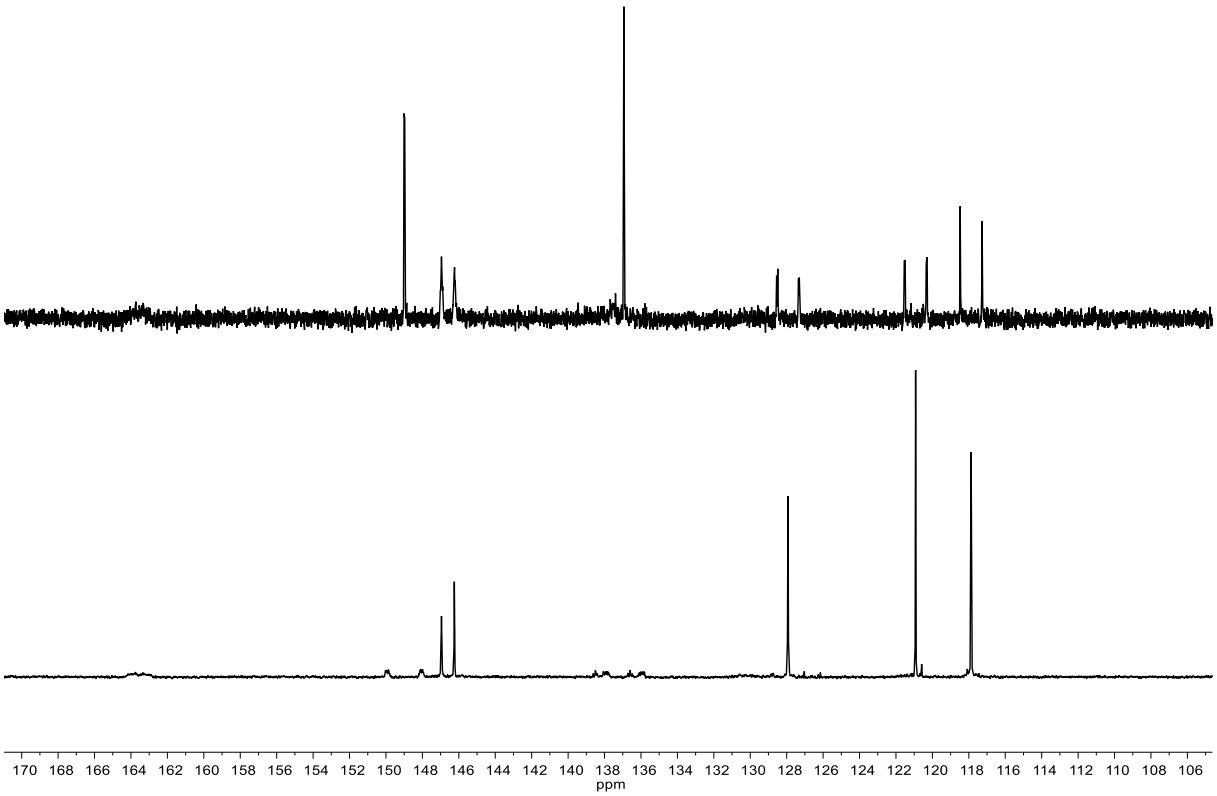

Figure S11. Aromatic regions of the $^{13}C\{^{19}F\}$ (125.8 MHz, THF-d_8; top) and $^{13}C\{^{1}H\}$ NMR spectra (125.8 MHz, THF-d_8; bottom) of Na[**5**].

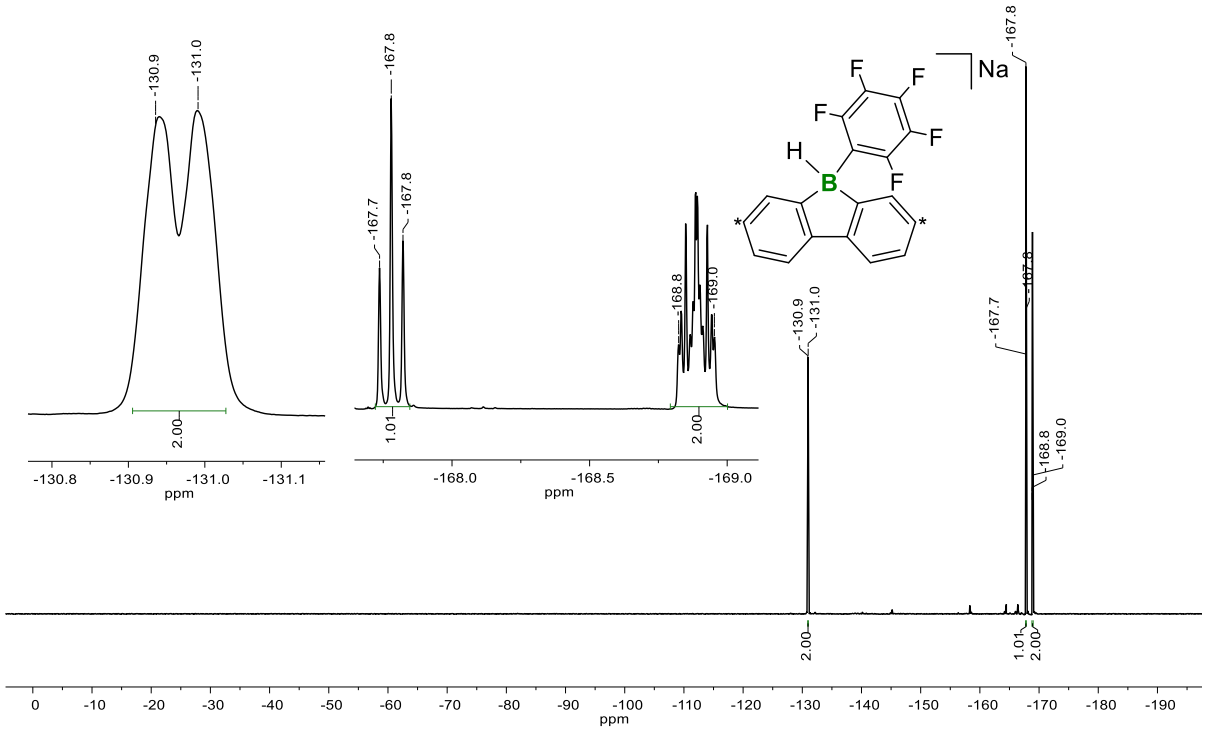

Figure S12. ^{19}F NMR spectrum (470.6 MHz, THF-d_8) of Na[**5**].

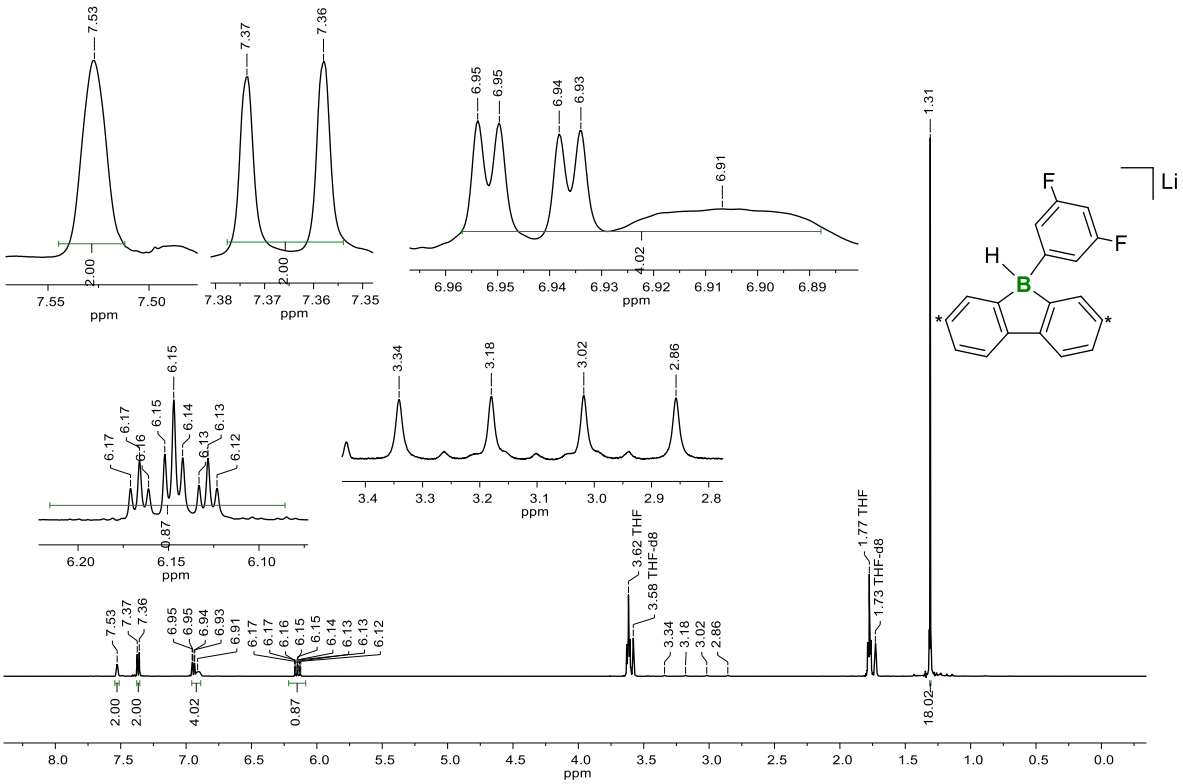

Figure S13. ^{1}H NMR spectrum (500.2 MHz, THF-d_8) of Li[**6**].

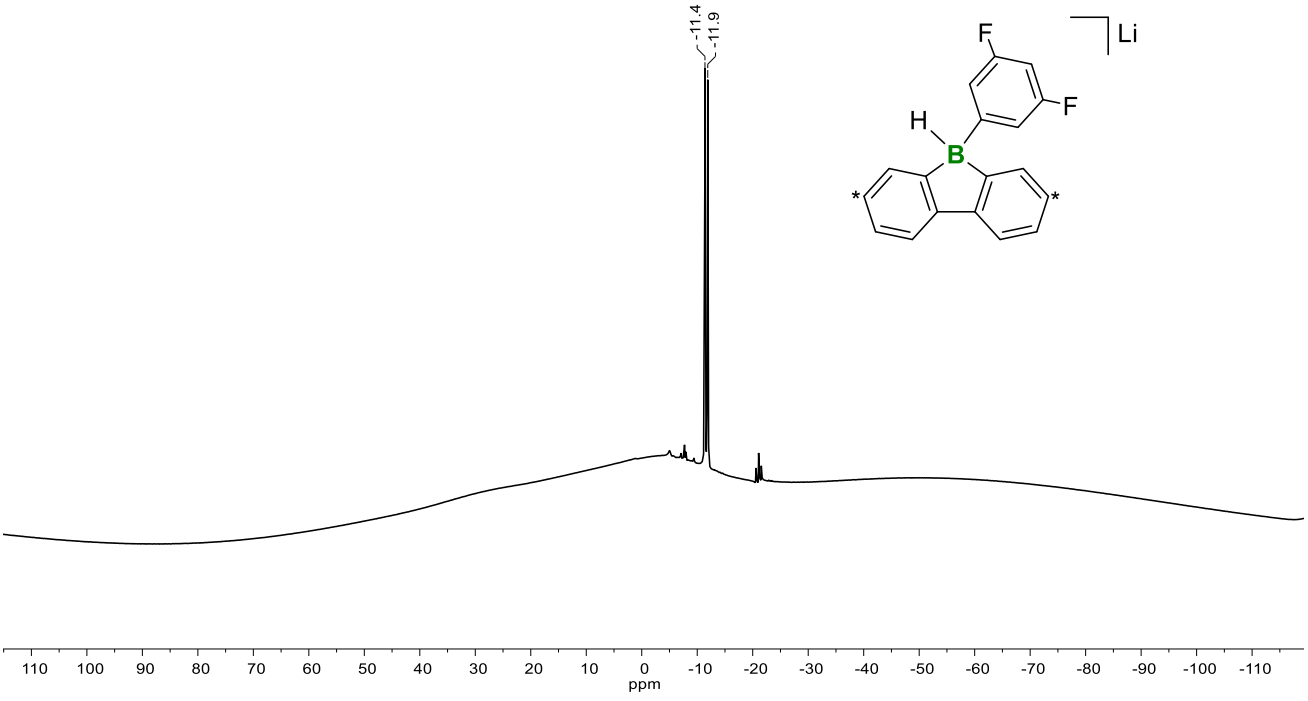

Figure S14. ^{11}B NMR spectrum (160.5 MHz, THF-d_8) of Li[**6**].

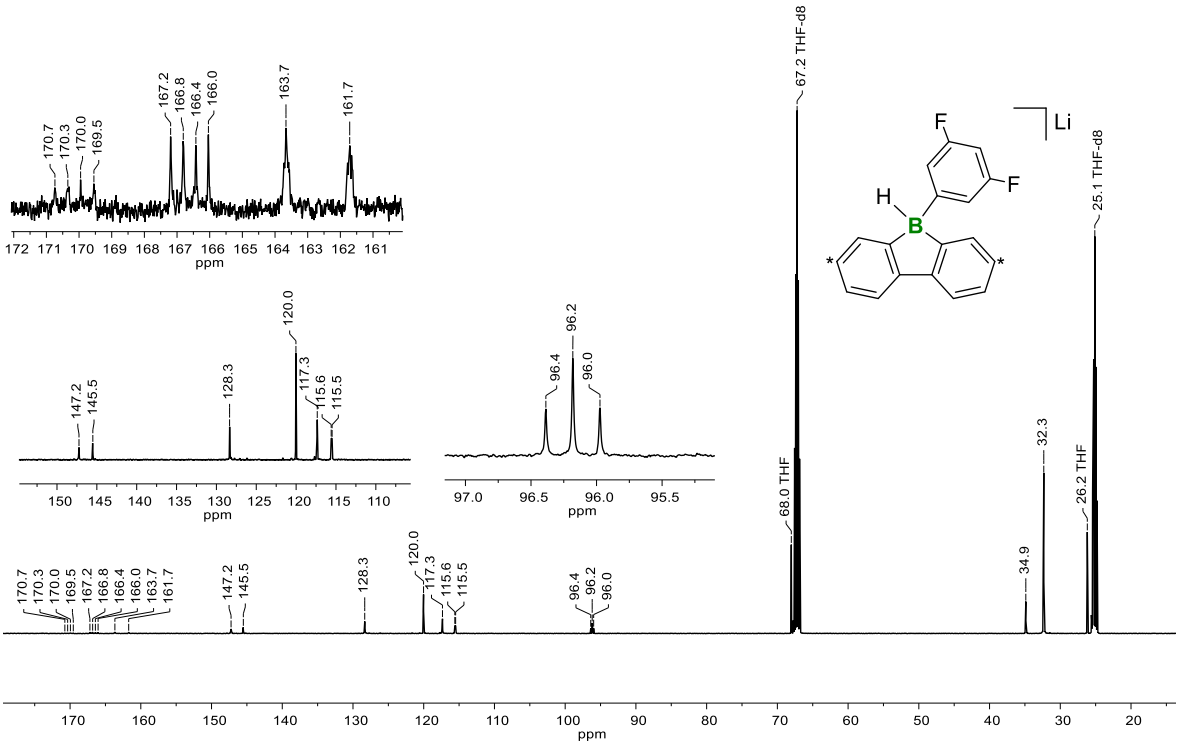

Figure S15. $^{13}C\{^{1}H\}$ NMR spectrum (125.8 MHz, THF-d_8) of Li[**6**].

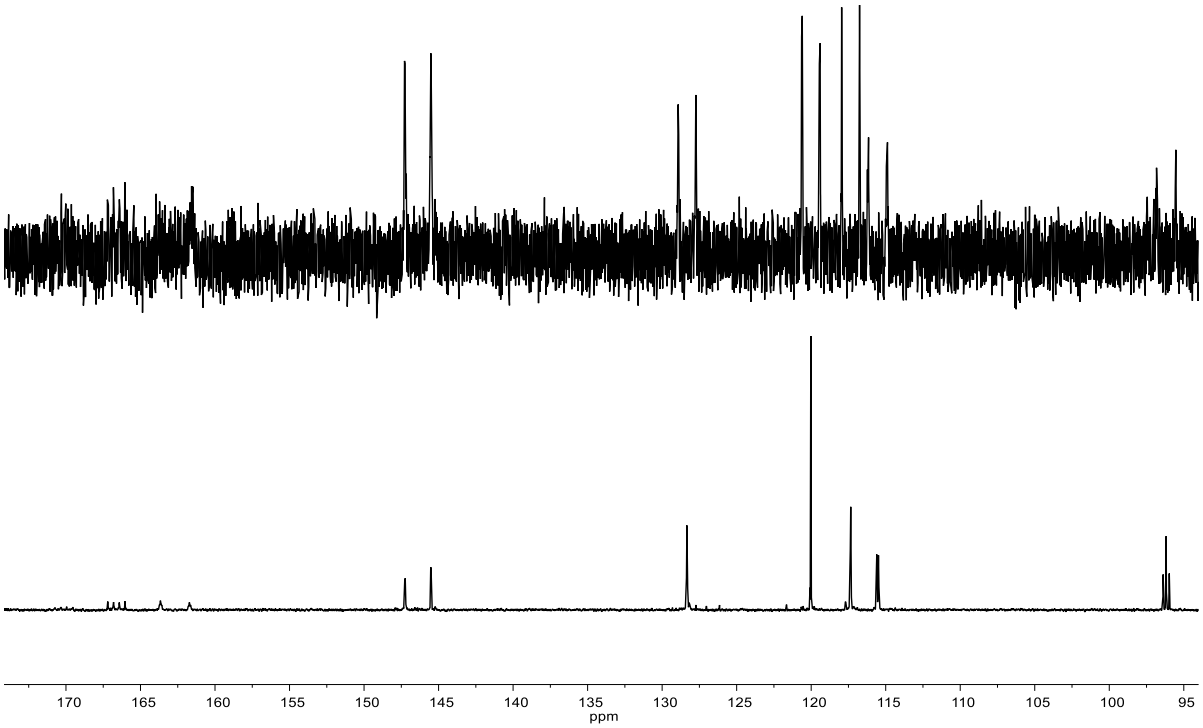

Figure S16. Aromatic regions of the $^{13}C\{^{19}F\}$ NMR (125.8 MHz, THF-d_8; top) and $^{13}C\{^{1}H\}$ NMR spectra (125.8 MHz, THF-d_8; bottom) of Li[**6**].

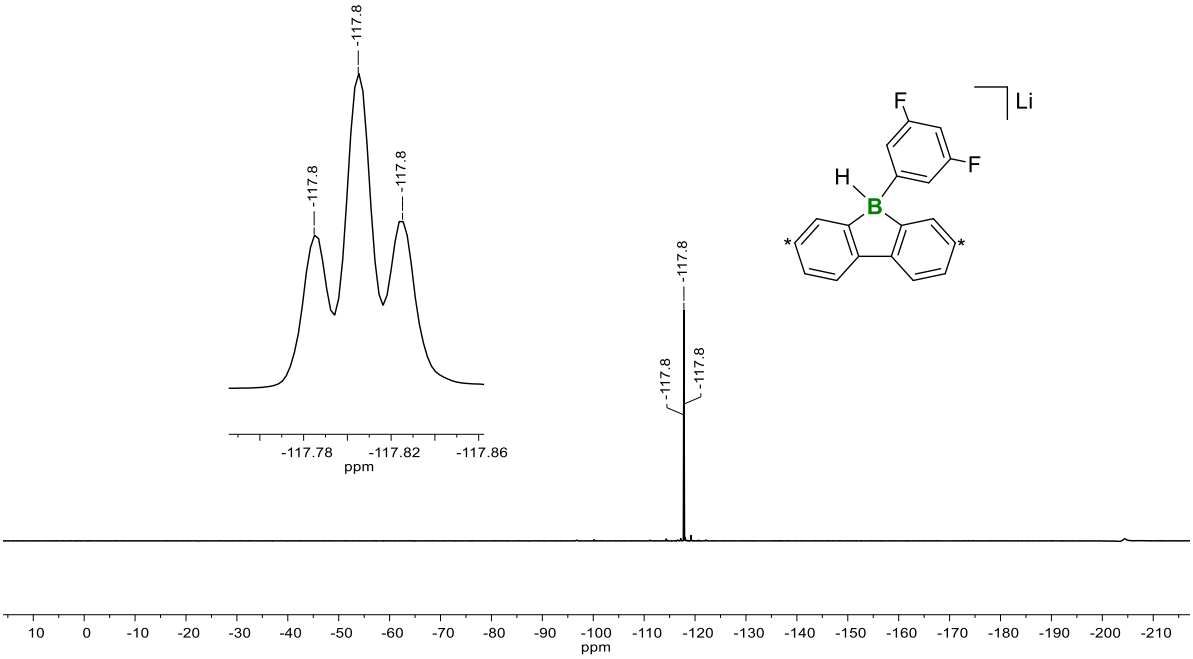

Figure S17. ^{19}F NMR spectrum (470.6 MHz, THF-d_8) of Li[**6**].

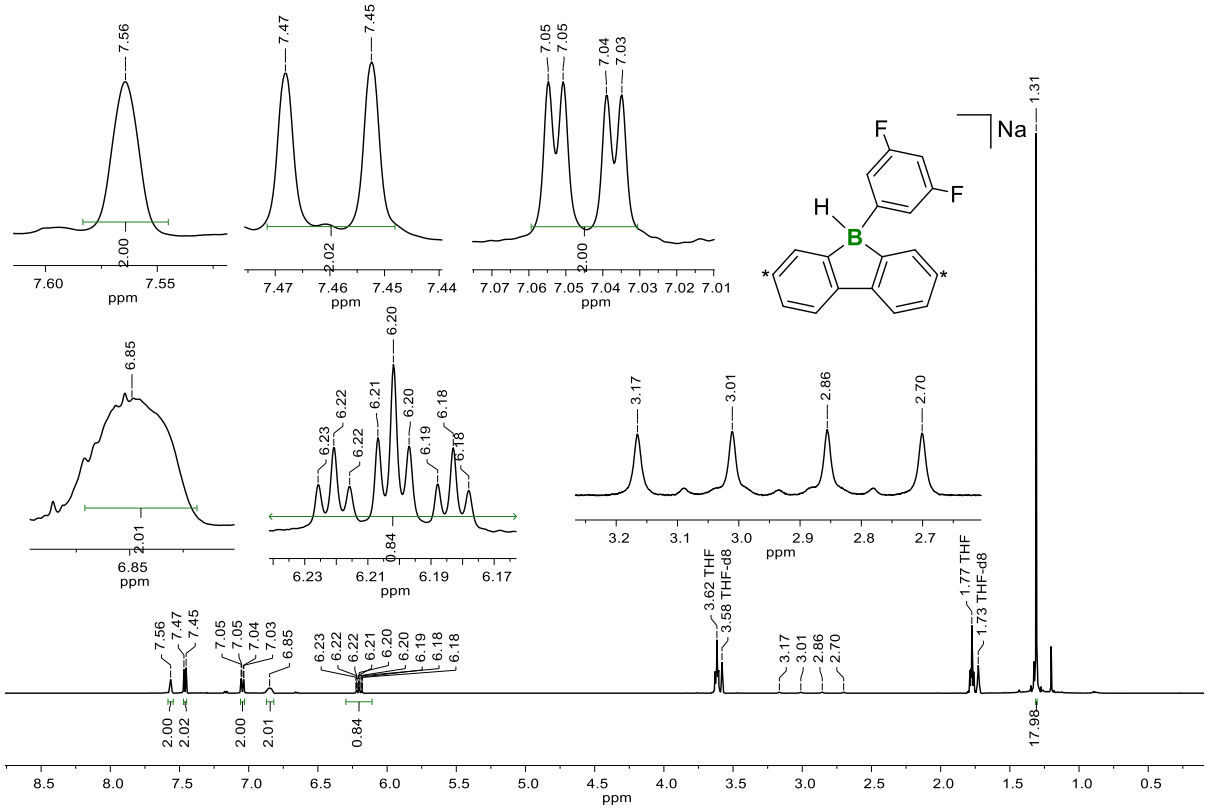

Figure S18. ^{1}H NMR spectrum (500.2 MHz, THF-d_8) of Na[**6**].

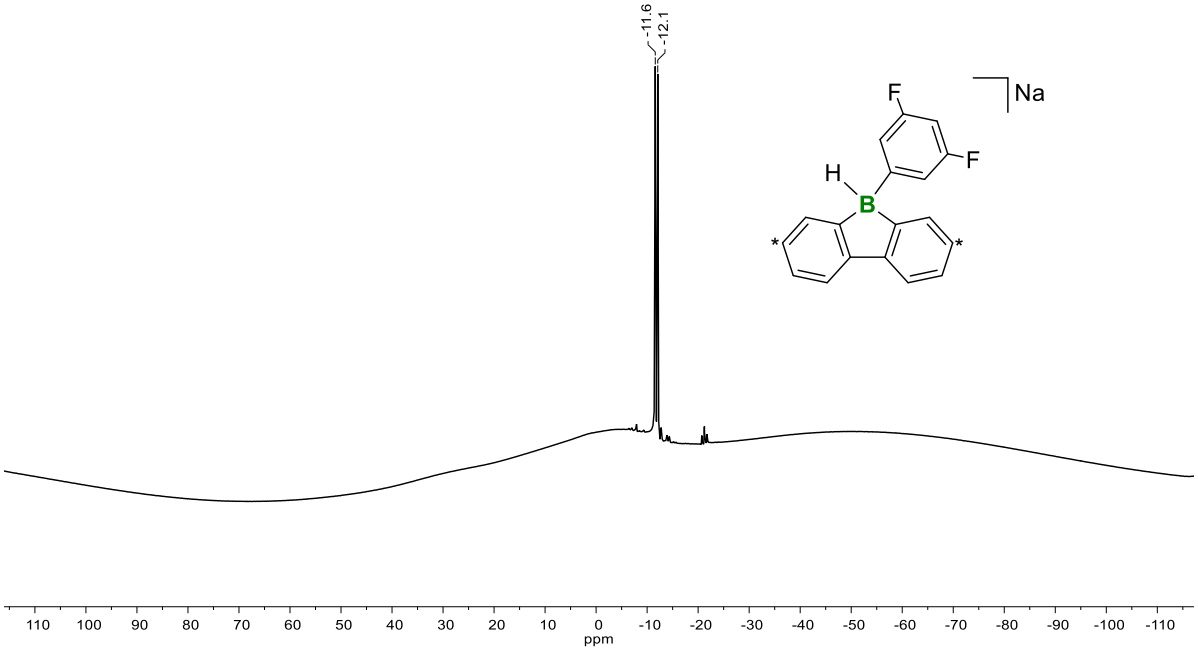

Figure S19. ^{11}B NMR spectrum (160.5 MHz, THF-d_8) of Na[**6**].

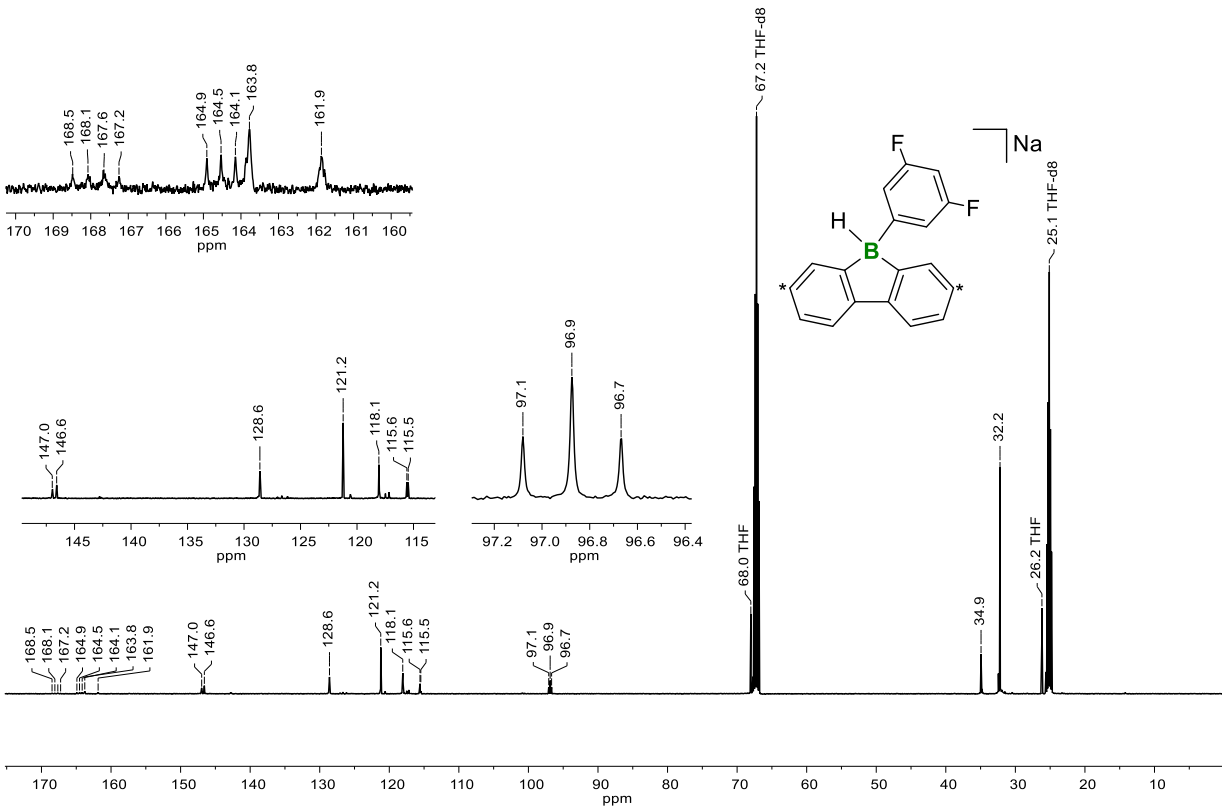

Figure S20. ^{13}C{^{1}H} NMR spectrum (125.8 MHz, THF-d_8) of Na[**6**].

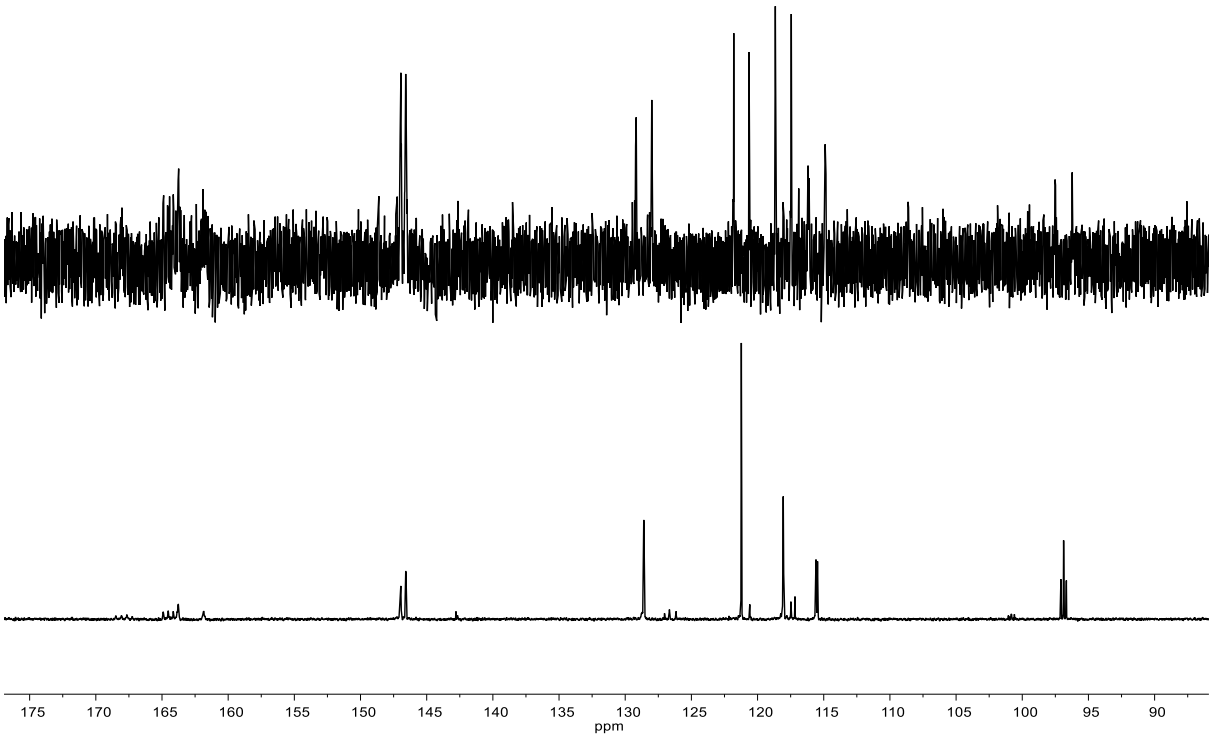

Figure S21. Aromatic regions of the $^{13}C\{^{19}F\}$ NMR (125.8 MHz, THF-d_8; top) and $^{13}C\{^{1}H\}$ NMR spectra (125.8 MHz, THF-d_8; bottom) of Na[**6**].

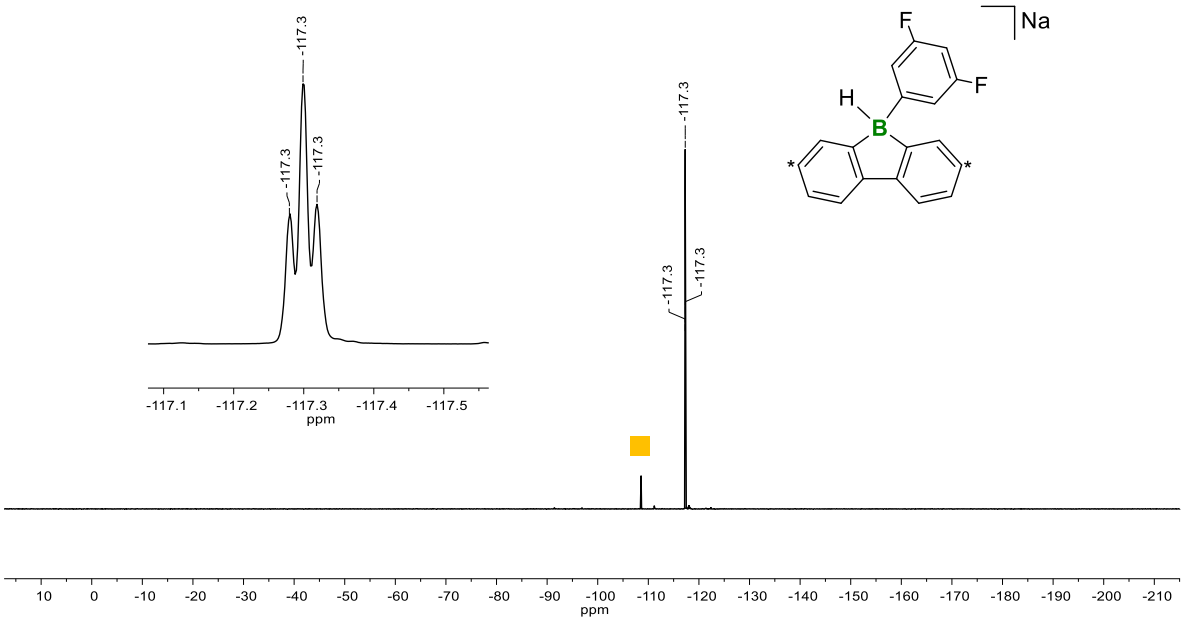

Figure S22. ^{19}F NMR spectrum (470.6 MHz, THF-d_8) of Na[**6**]. Marked component: 1,3,5-trifluorobenzene (■).

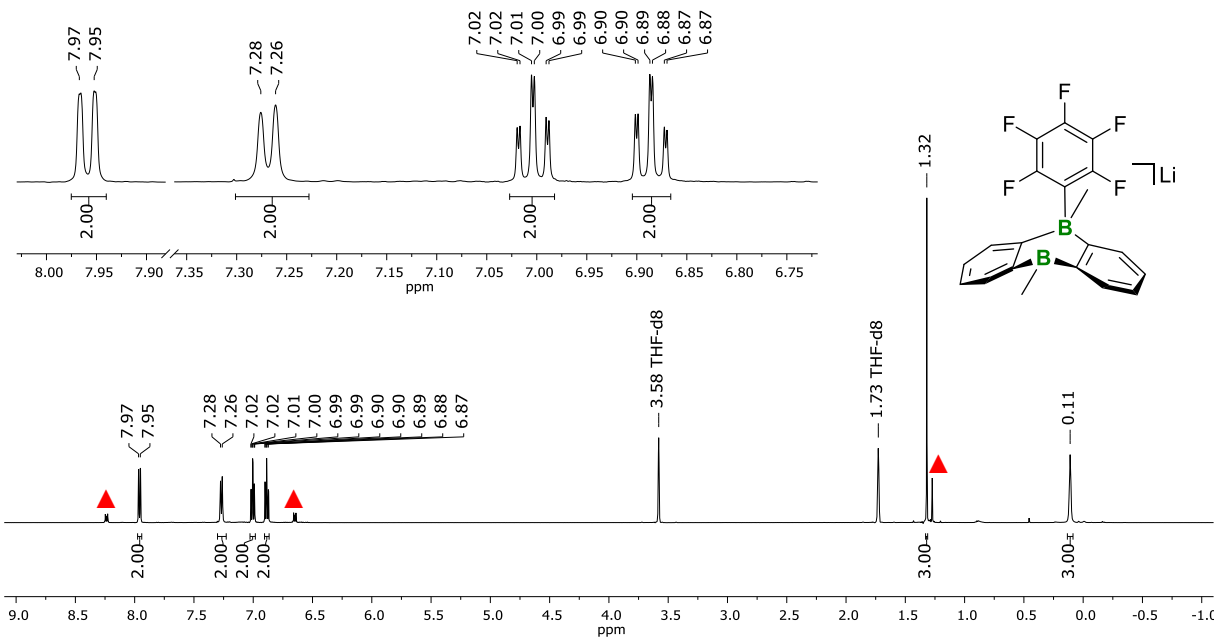

Figure S23. ^{1}H NMR spectrum (500.2 MHz, THF-d_8) of Li[**7**]. Marked component: Li_2[**4**] (▲).

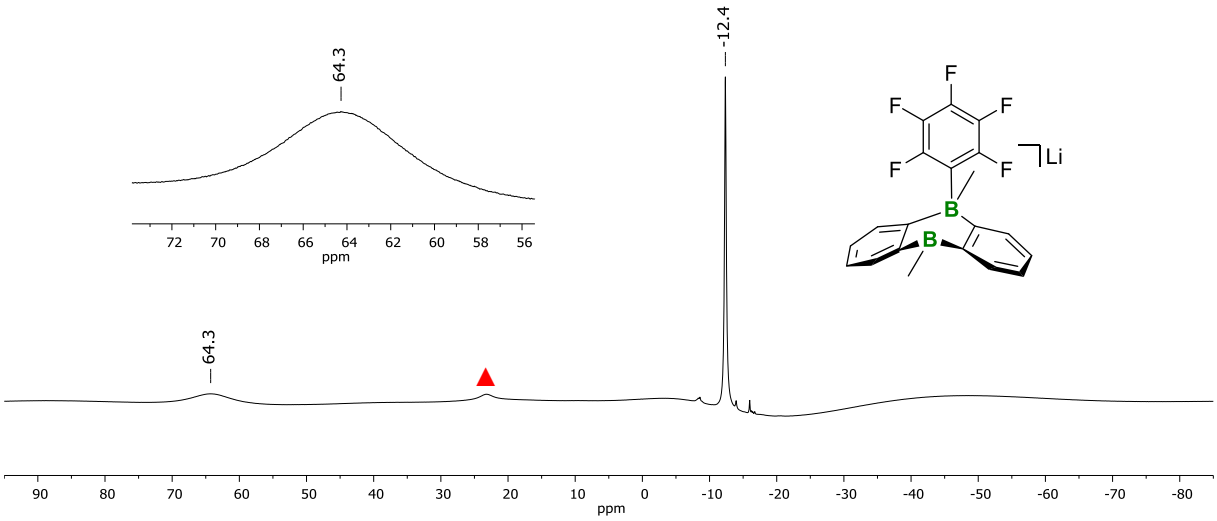

Figure S24. ^{11}B NMR spectrum (160.5 MHz, THF-d_8) of Li[**7**]. Marked component: Li_2[**4**] (▲).

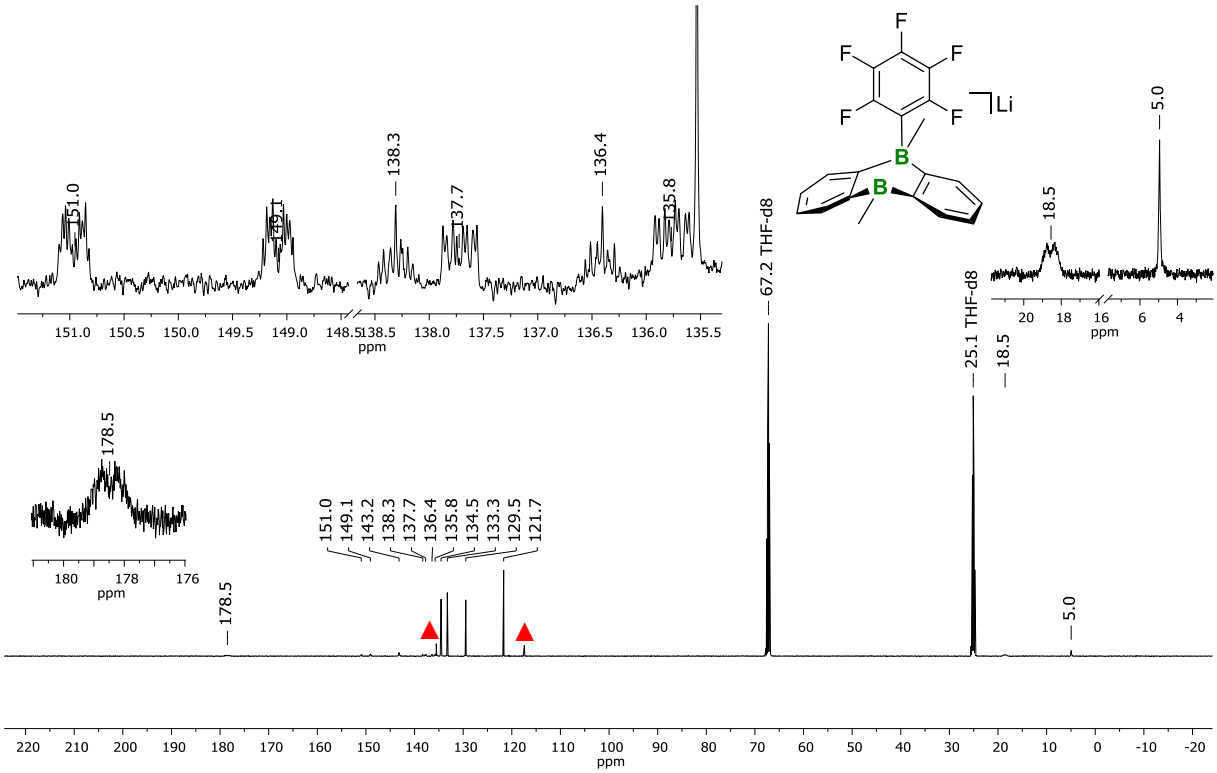

Figure S25. $^{13}C\{^{1}H\}$ NMR spectrum (125.8 MHz, THF-d_8) of Li[**7**]. Marked component: Li_2[**4**] (▲).

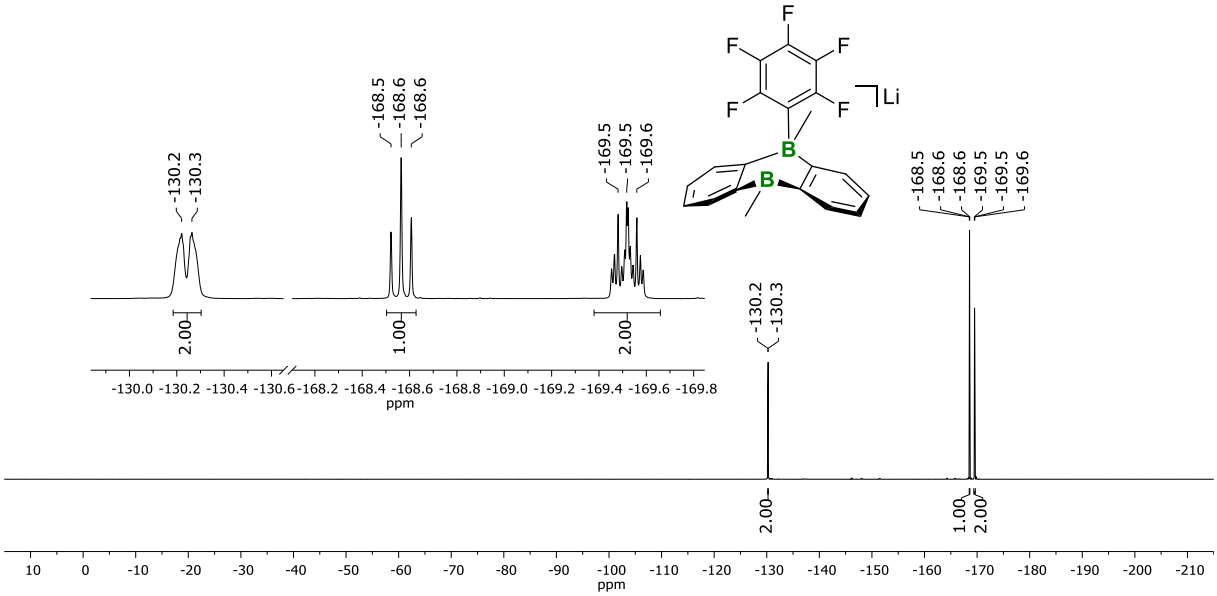

Figure S26. ^{19}F NMR spectrum (470.6 MHz, THF-d_8) of Li[**7**].

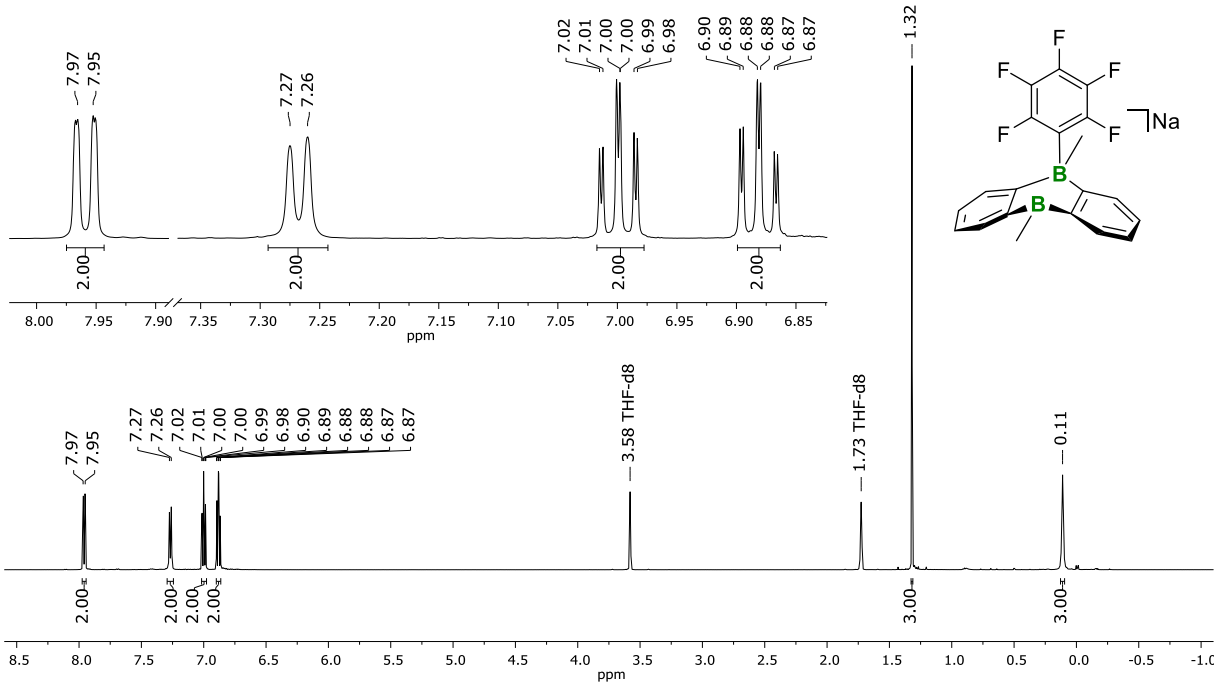

Figure S27. ^{1}H NMR spectrum (500.2 MHz, THF-d_8) of Na[**7**].

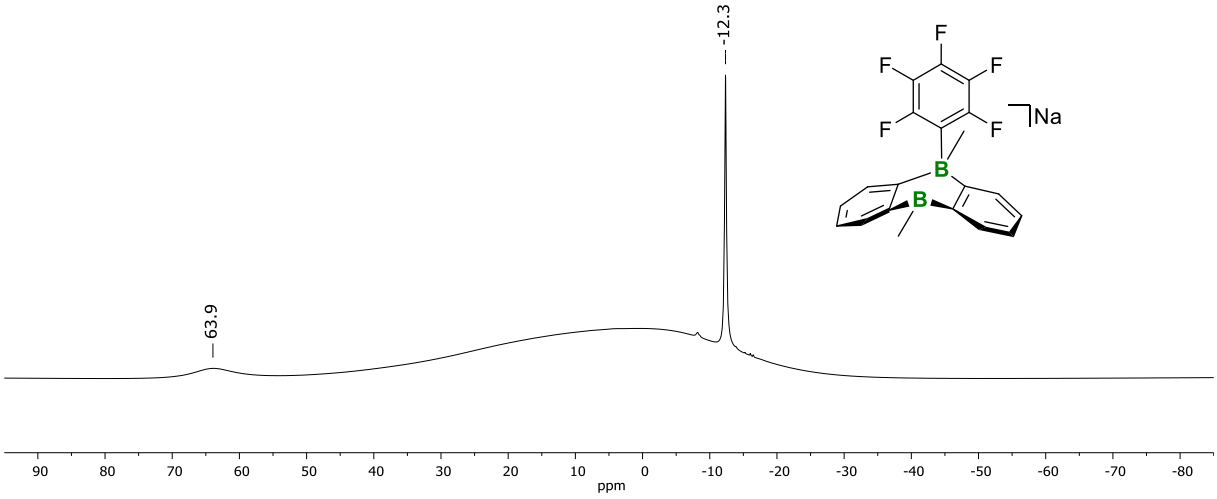

Figure S28. ^{11}B NMR spectrum (160.5 MHz, THF-d_8) of Na[**7**].

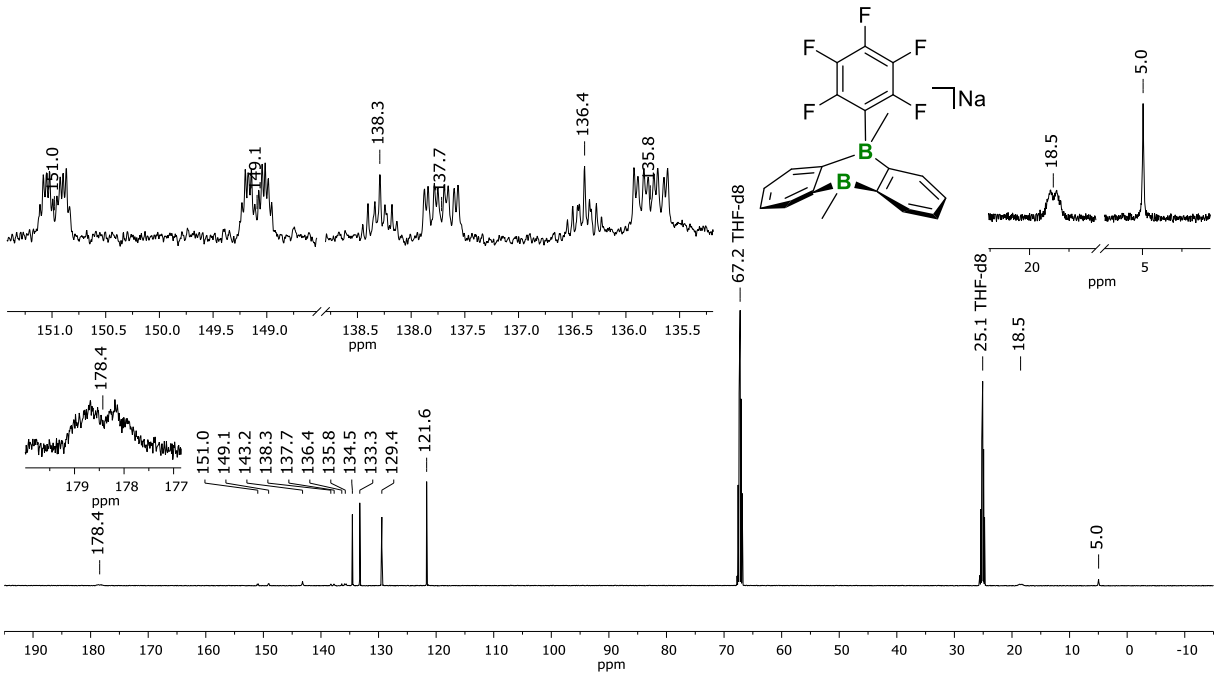

Figure S29. $^{13}C\{^{1}H\}$ NMR spectrum (125.8 MHz, THF-d_8) of Na[**7**].

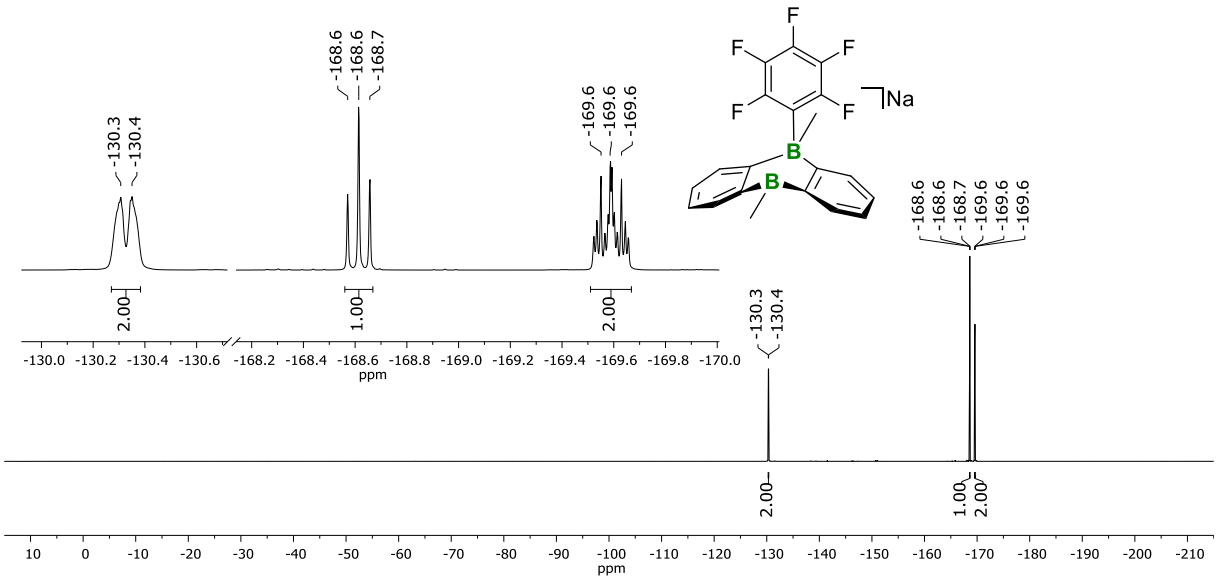

Figure S30. ^{19}F NMR spectrum (470.6 MHz, THF-d_8) of Na[**7**].

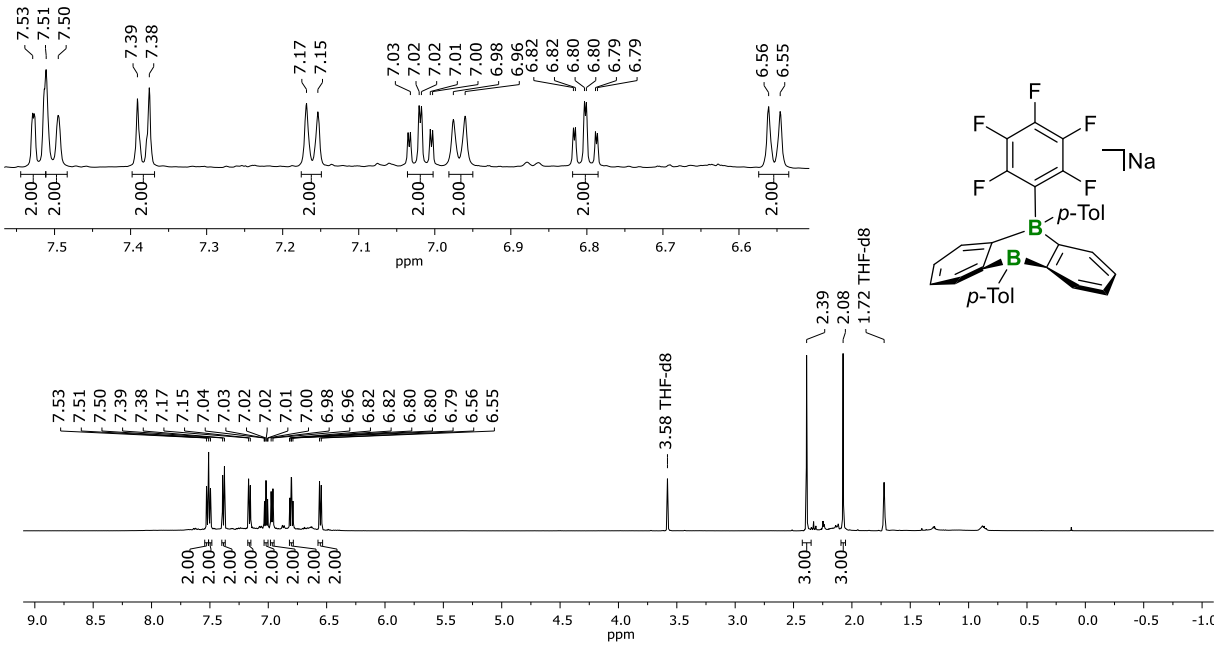

Figure S31. ^{1}H NMR spectrum (500.2 MHz, THF-d_8) of Na[**7^{Tol}**].

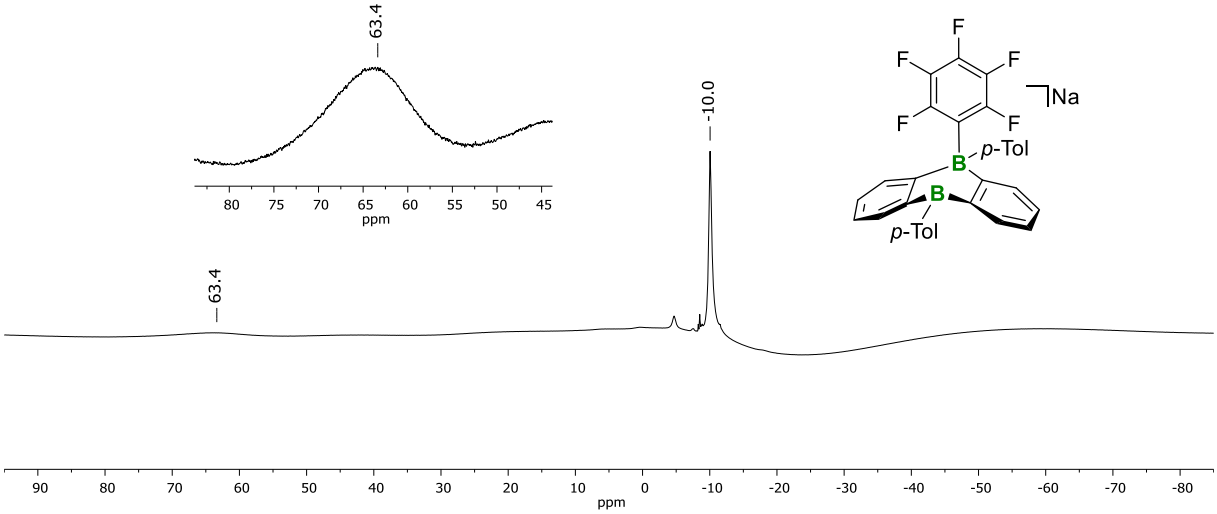

Figure S32.^{11}B NMR spectrum (160.5 MHz, THF-d_8) of Na[**7^{Tol}**].

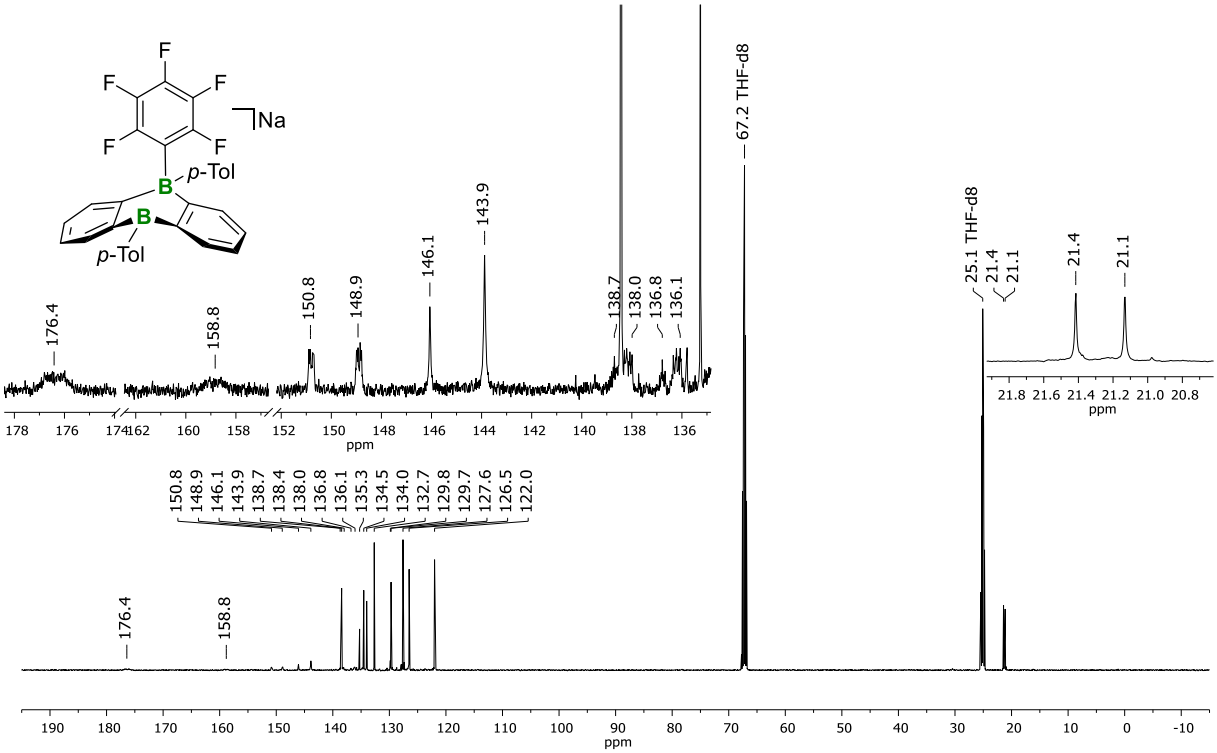

Figure S33. $^{13}C\{^{1}H\}$ NMR spectrum (125.8 MHz, THF-d_8) of Na[**7**^{Tol}].

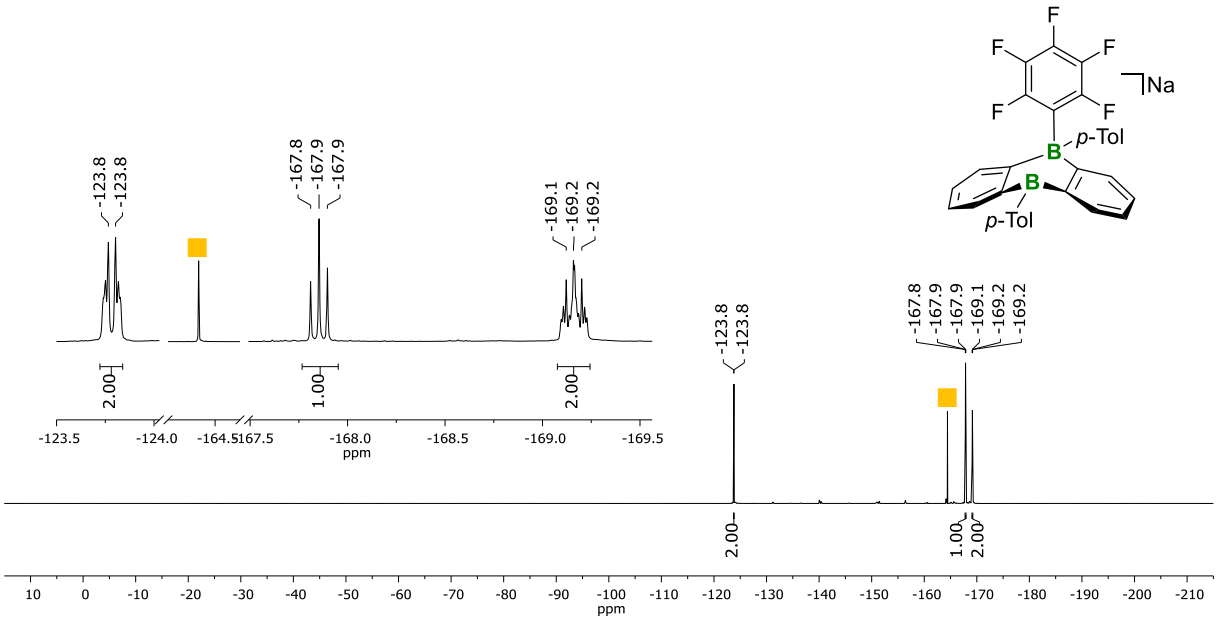

Figure S34. ^{19}F NMR spectrum (470.6 MHz, THF-d_8) of Na[**7**^{Tol}]. Marked component: hexafluorobenzene (■).

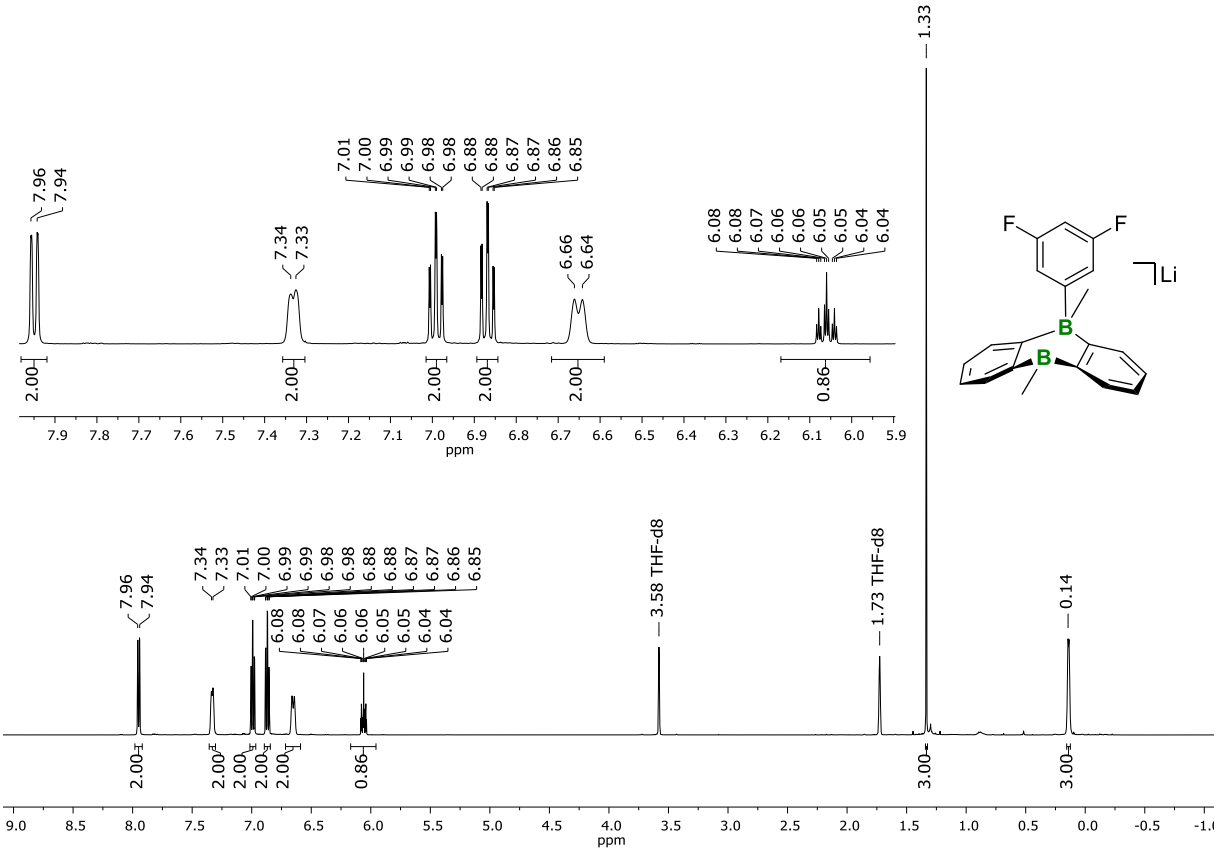

Figure S35. ^{1}H NMR spectrum (500.2 MHz, THF-d_8) of Li[**8**].

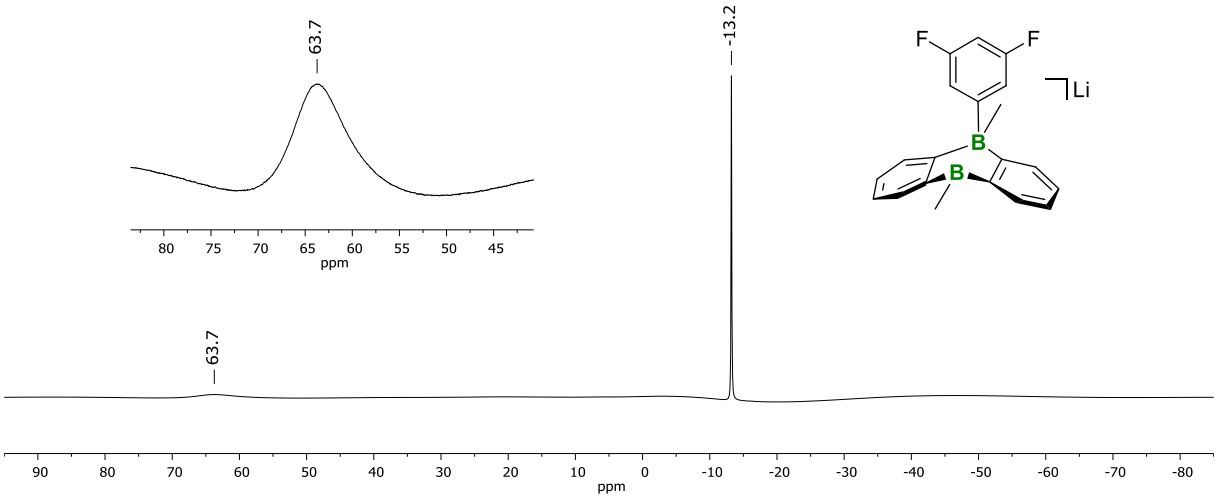

Figure S36. ^{11}B NMR spectrum (160.5 MHz, THF-d_8) of Li[**8**].

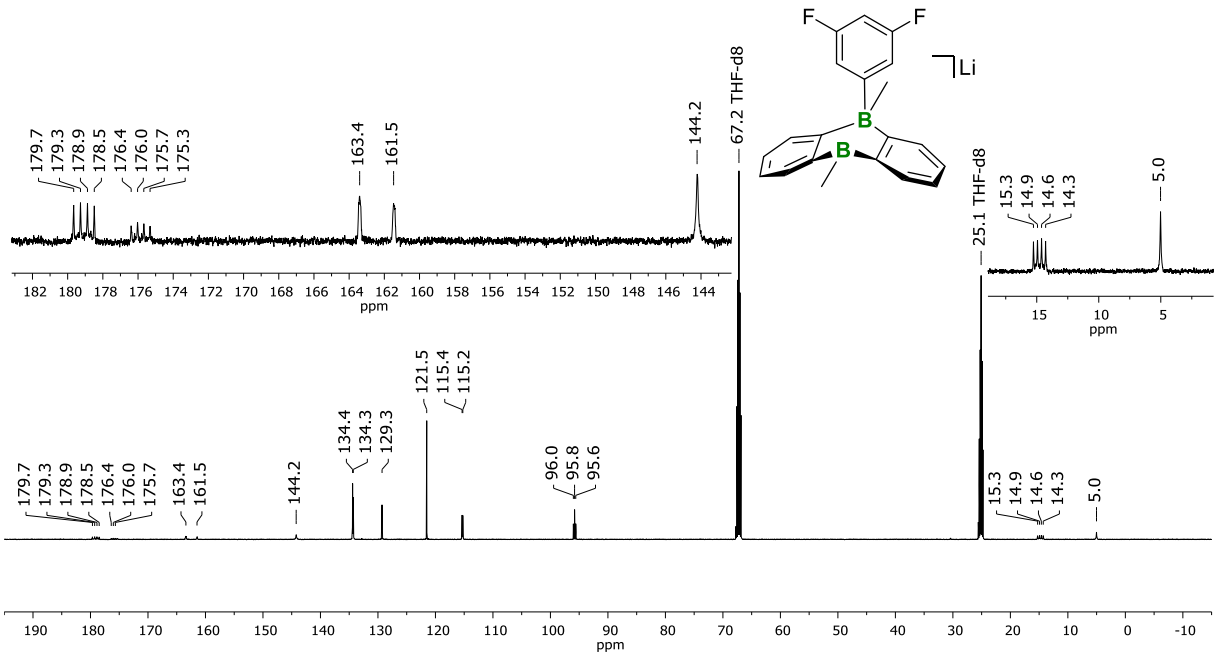

Figure S37. $^{13}C\{^{1}H\}$ NMR spectrum (125.8 MHz, THF-d_8) of Li[**8**].

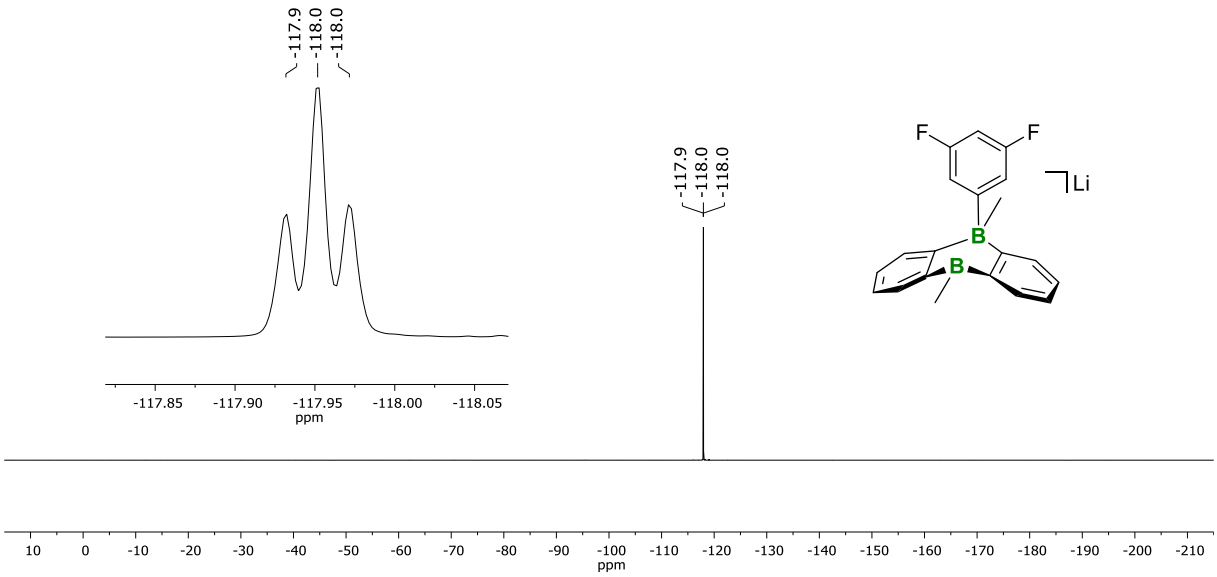

Figure S38. ^{19}F NMR spectrum (470.6 MHz, THF-d_8) of Li[**8**].

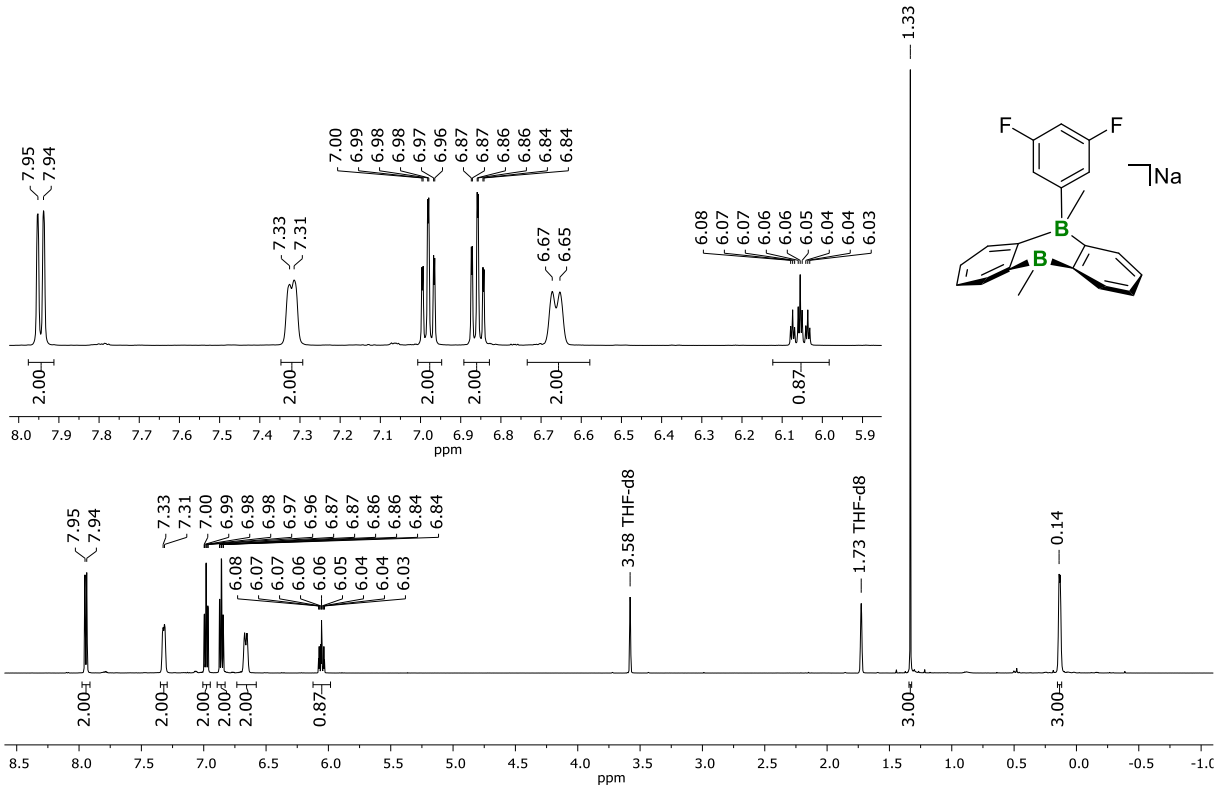

Figure S39. ^{1}H NMR spectrum (500.2 MHz, THF-d_8) of Na[**8**].

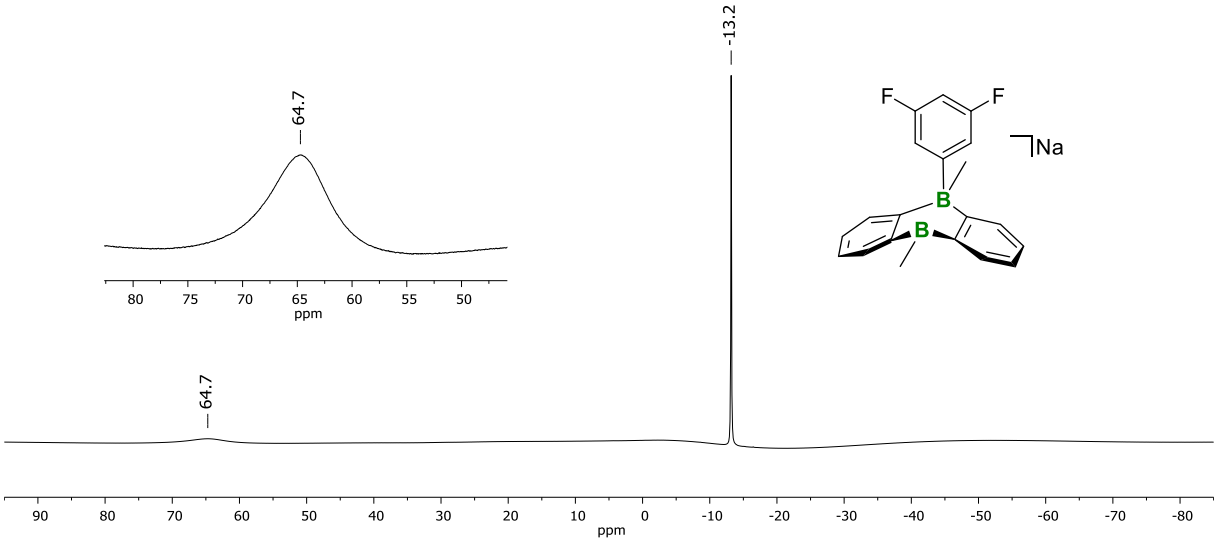

Figure S40. ^{11}B NMR spectrum (160.5 MHz, THF-d_8) of Na[**8**].

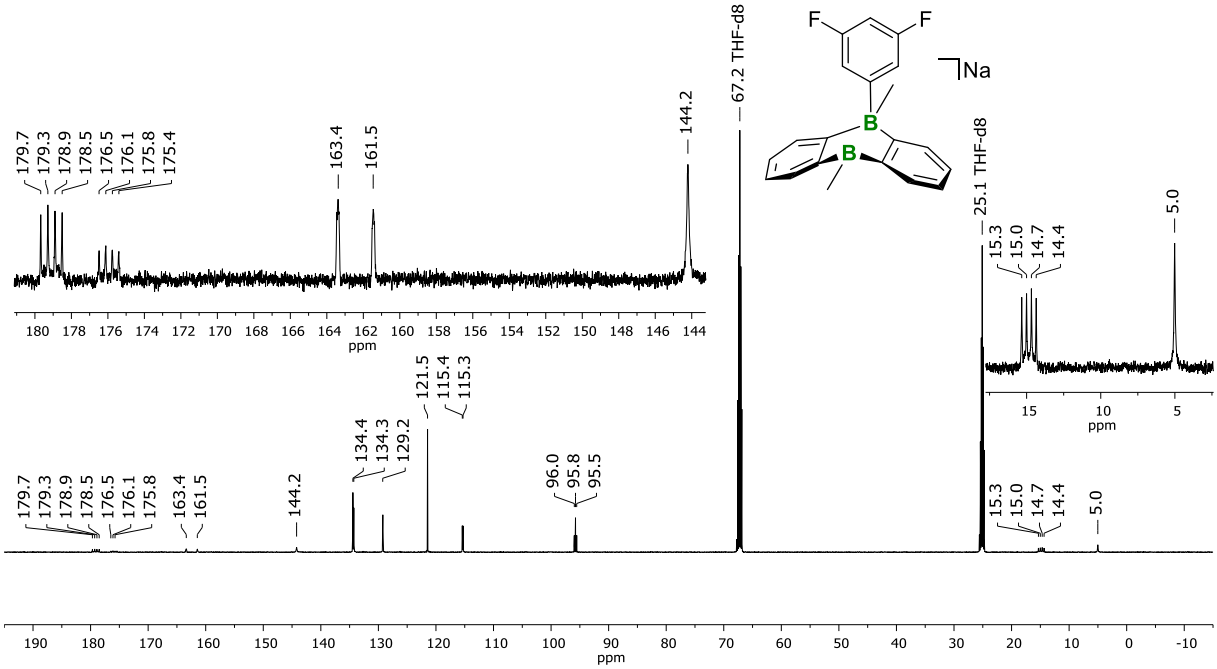

Figure S41. $^{13}C\{^{1}H\}$ NMR spectrum (125.8 MHz, THF-d_8) of Na[**8**].

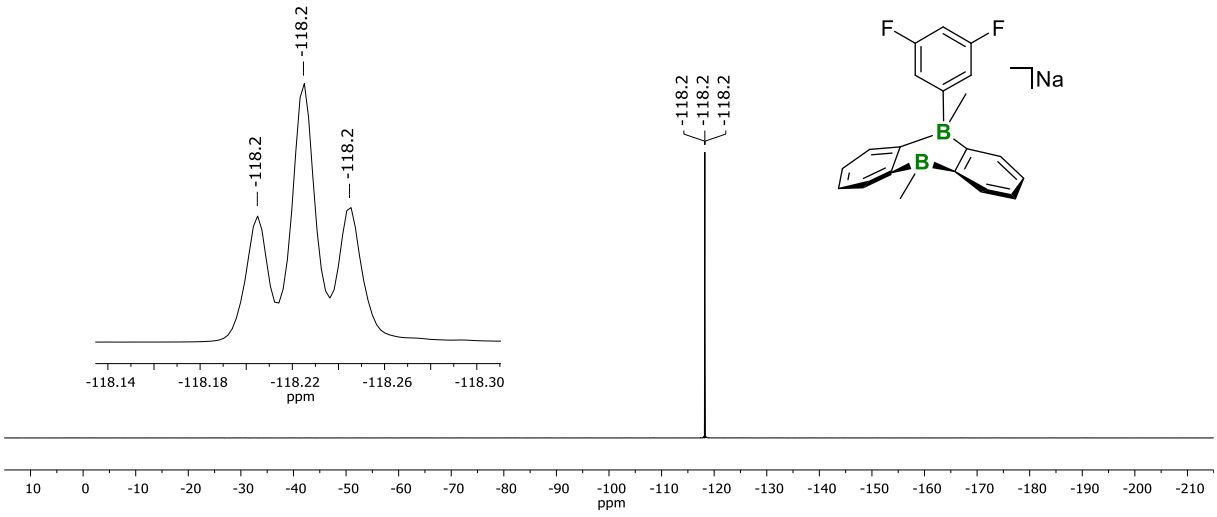

Figure S42. ^{19}F NMR spectrum (470.6 MHz, THF-d_8) of Na[**8**].

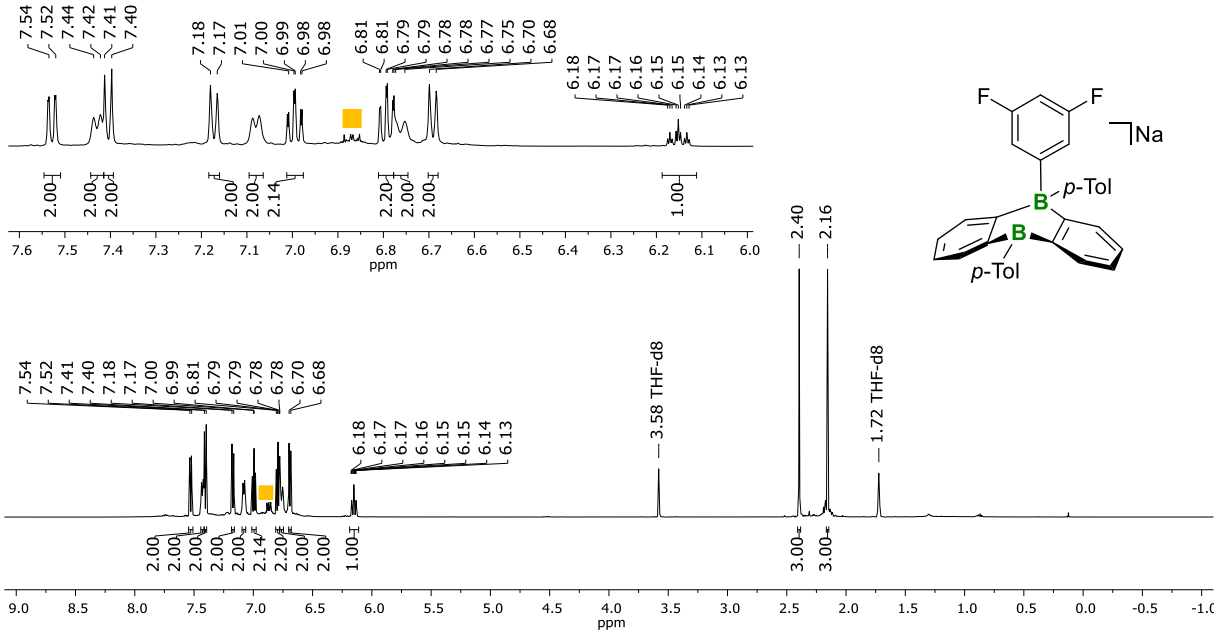

Figure S43. ^{1}H NMR spectrum (500.2 MHz, THF-d_8) recorded on the crude reaction mixture of Na_2[**4**^{Tol}] and 1,3,5-trifluorobenzene after 22 h at 100 °C. Marked component: 1,3,5-trifluorobenzene (■).

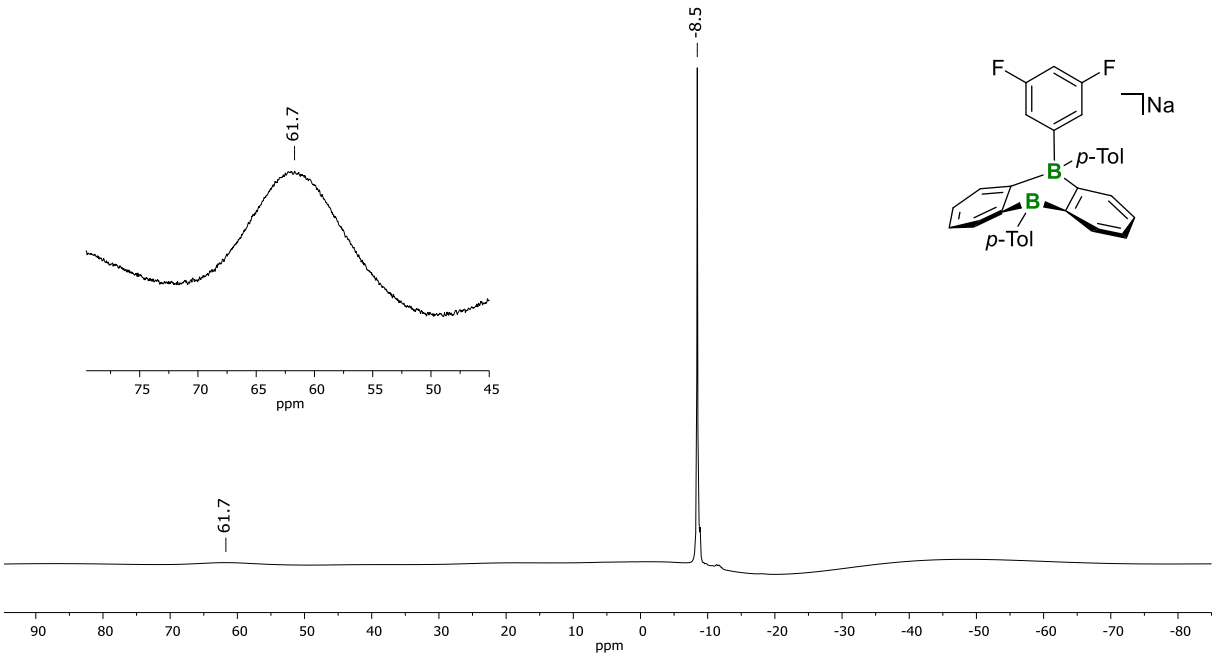

Figure S44. ^{11}B NMR spectrum (160.5 MHz, THF-d_8) recorded on the crude reaction mixture of Na_2[**4**^{Tol}] and 1,3,5-trifluorobenzene after 22 h at 100 °C.

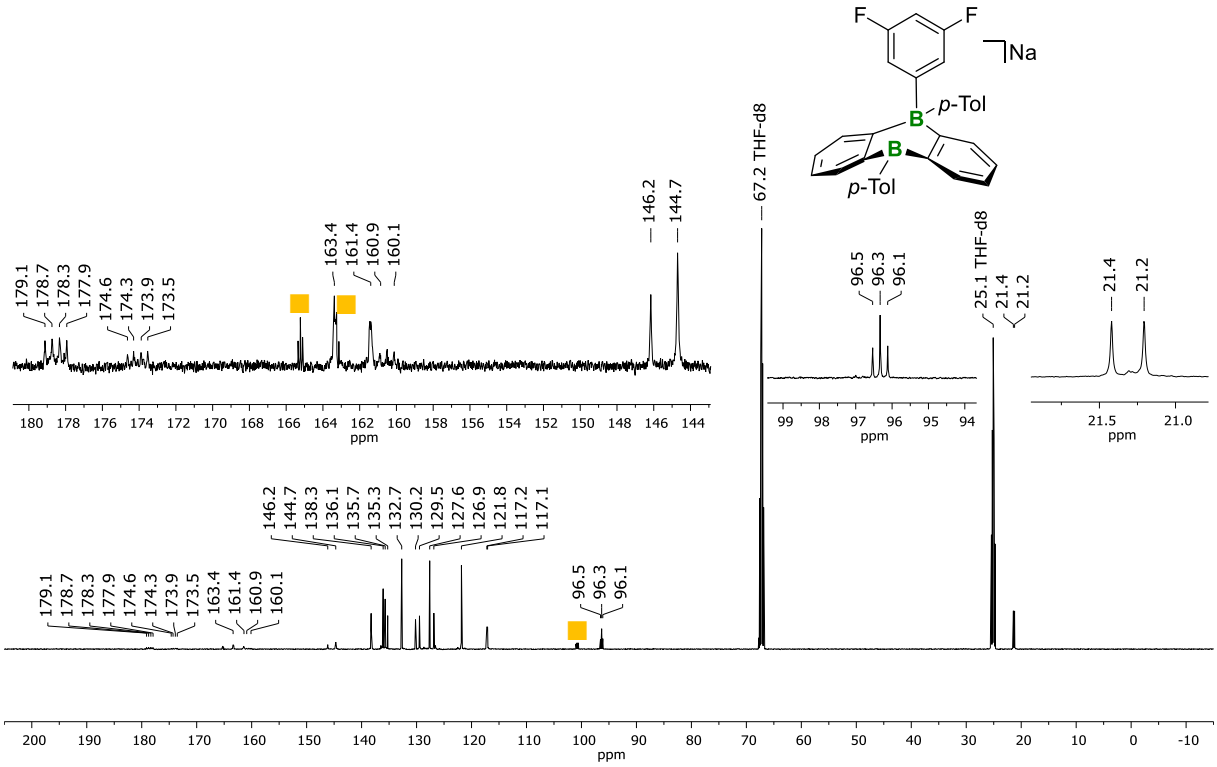

Figure S45. $^{13}C\{^{1}H\}$ NMR spectrum (125.8 MHz, THF-d_8) recorded on the crude reaction mixture of Na_2[**4**^{Tol}] and 1,3,5-trifluorobenzene after 22 h at 100 °C. Marked component: 1,3,5-trifluorobenzene (■).

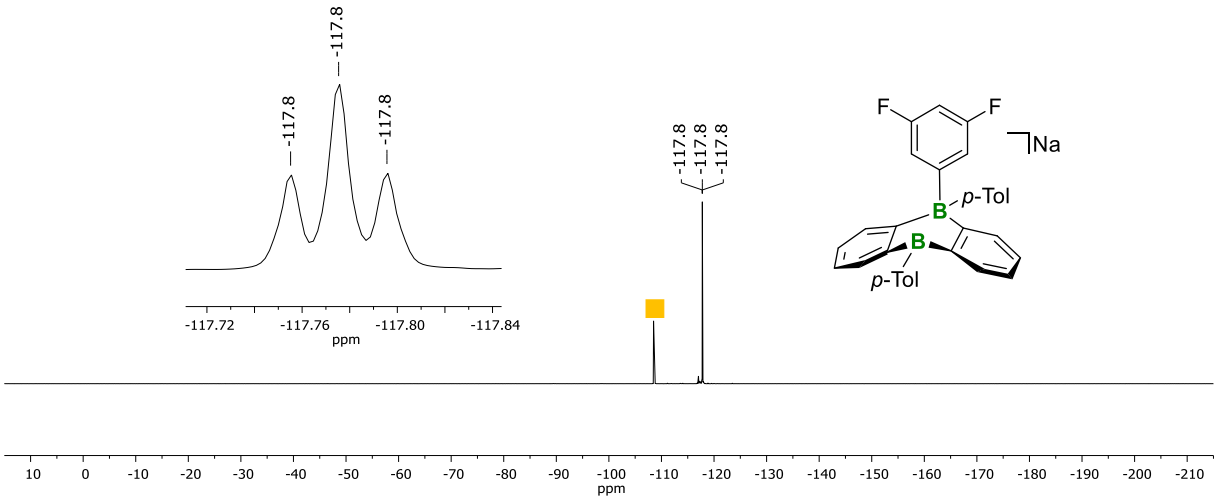

Figure S46. ^{19}F NMR spectrum (470.6 MHz, THF-d_8) recorded on the crude reaction mixture of Na_2[**4**^{Tol}] and 1,3,5-trifluorobenzene after 22 h at 100 °C. Marked component: 1,3,5-trifluorobenzene (■).

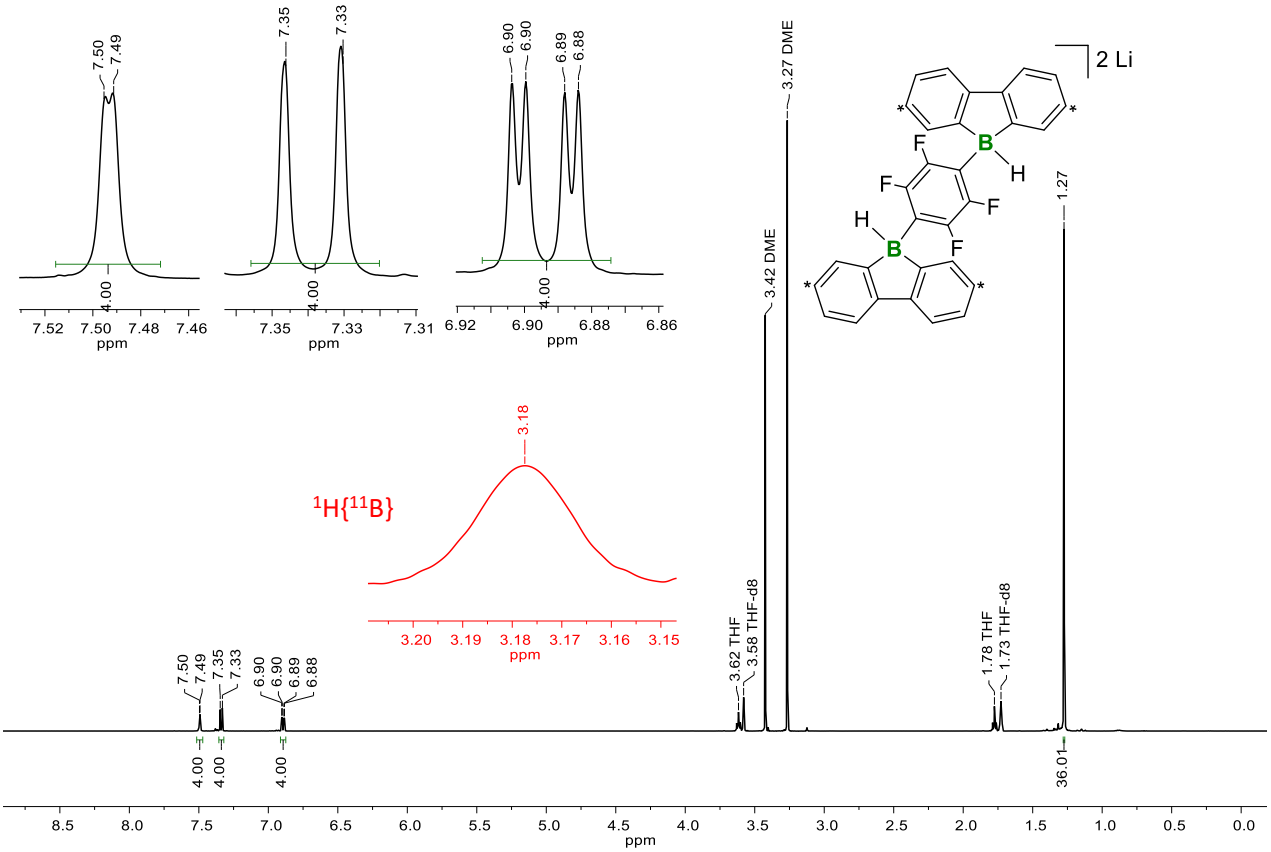

Figure S47. ^{1}H NMR spectrum (500.2 MHz, THF-d_8) of Li_2[**9**].

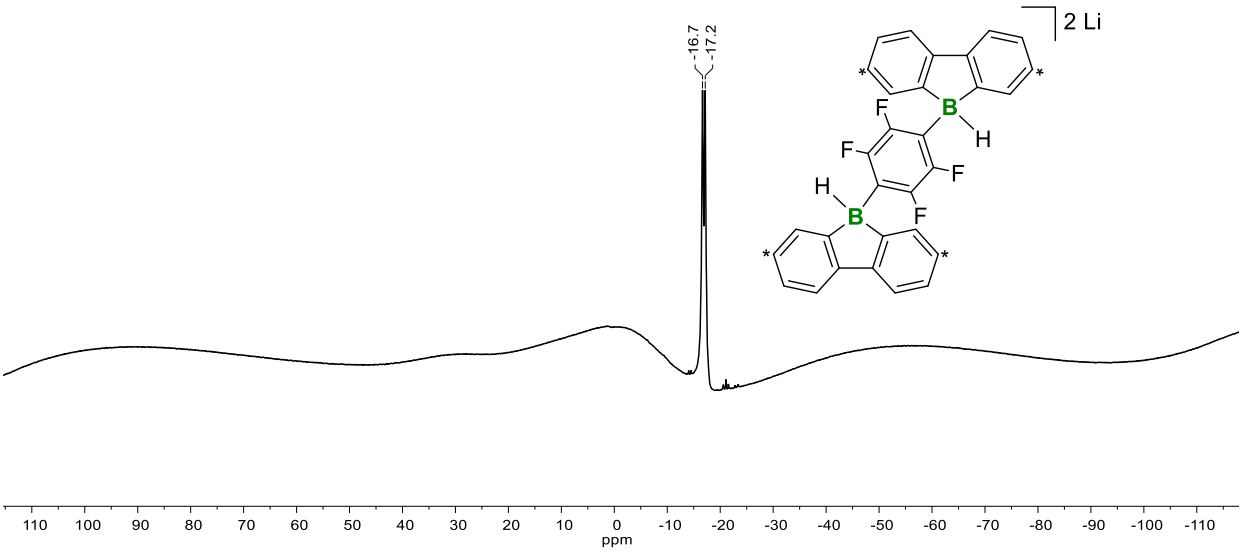

Figure S48. ^{11}B NMR spectrum (160.5 MHz, THF-d_8) of Li_2[**9**].

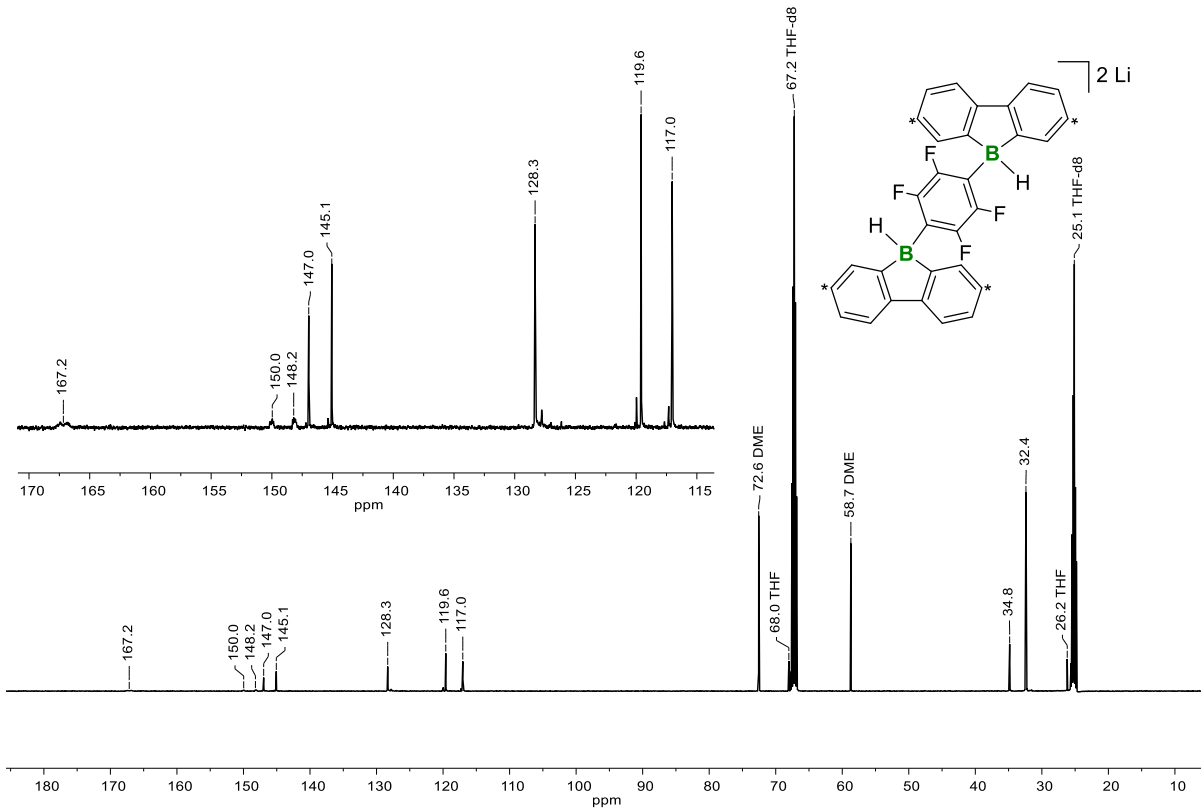

Figure S49. $^{13}C\{^{1}H\}$ NMR spectrum (125.8 MHz, THF-d_8) of Li_2[**9**].

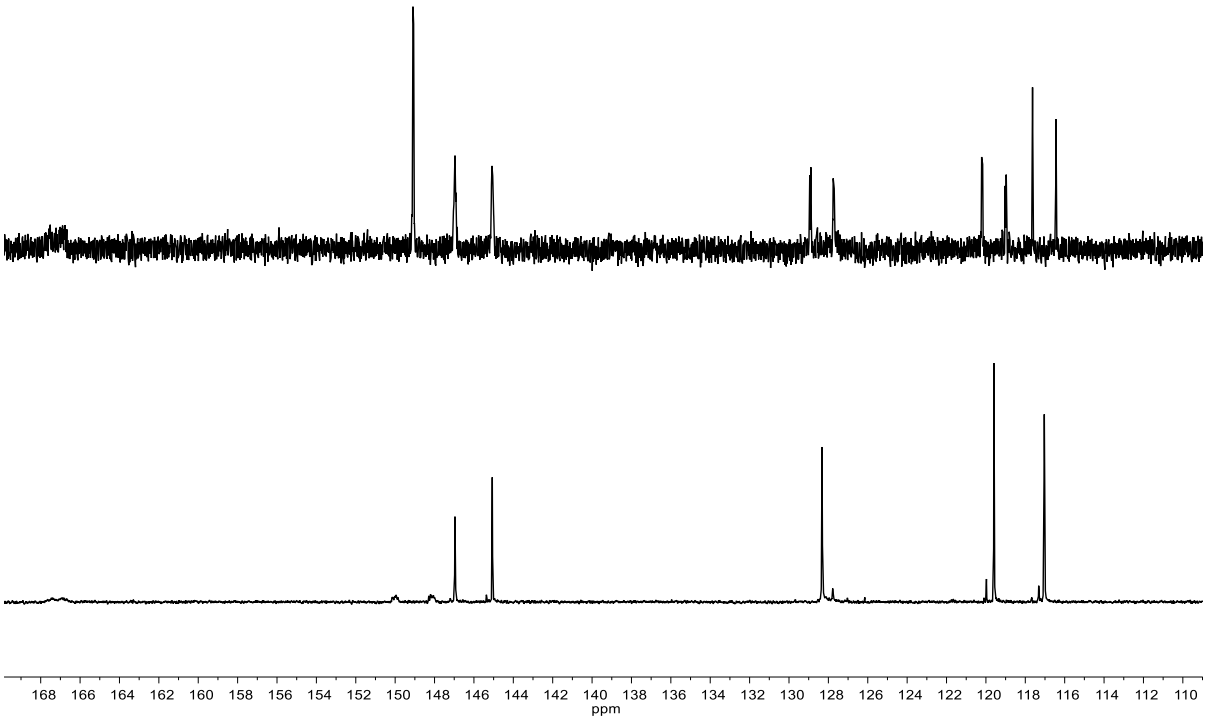

Figure S50. Aromatic regions of the $^{13}C\{^{19}F\}$ (125.8 MHz, THF-d_8; top) and $^{13}C\{^{1}H\}$ NMR spectra (125.8 MHz, THF-d_8; bottom) of Li_2[**9**].

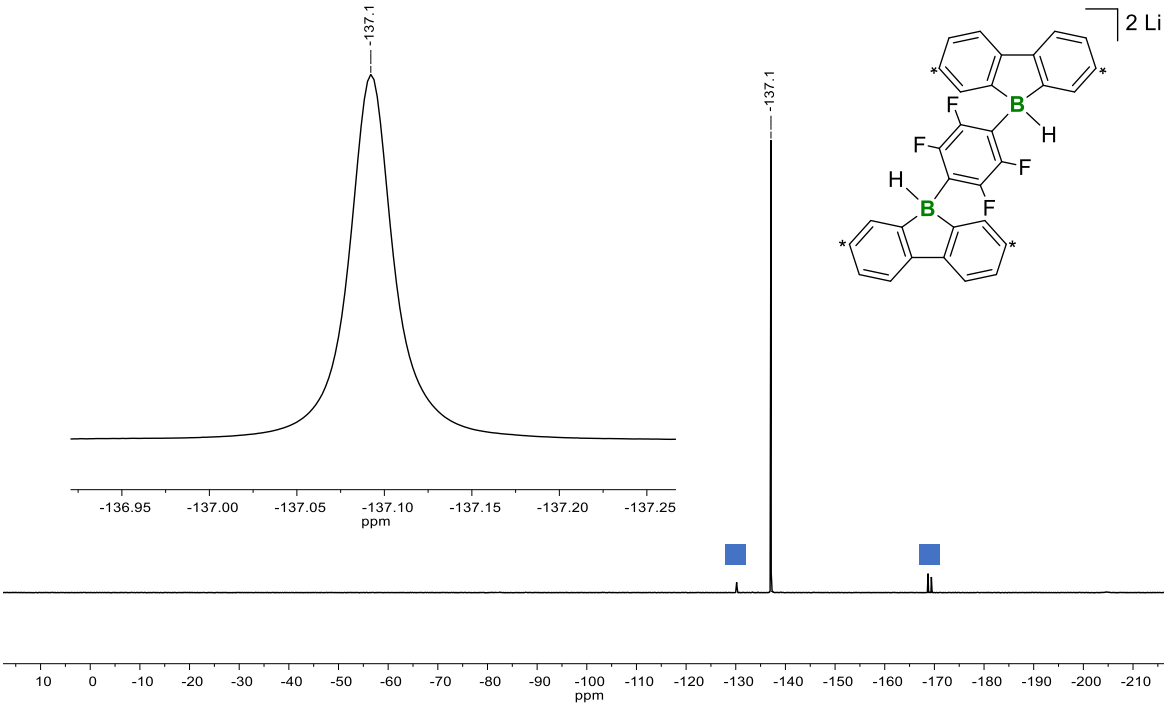

Figure S51.[19]F NMR spectrum (470.6 MHz, THF-d_8) of Li_2[**9**]. Marked component: Li[**5**] (■).

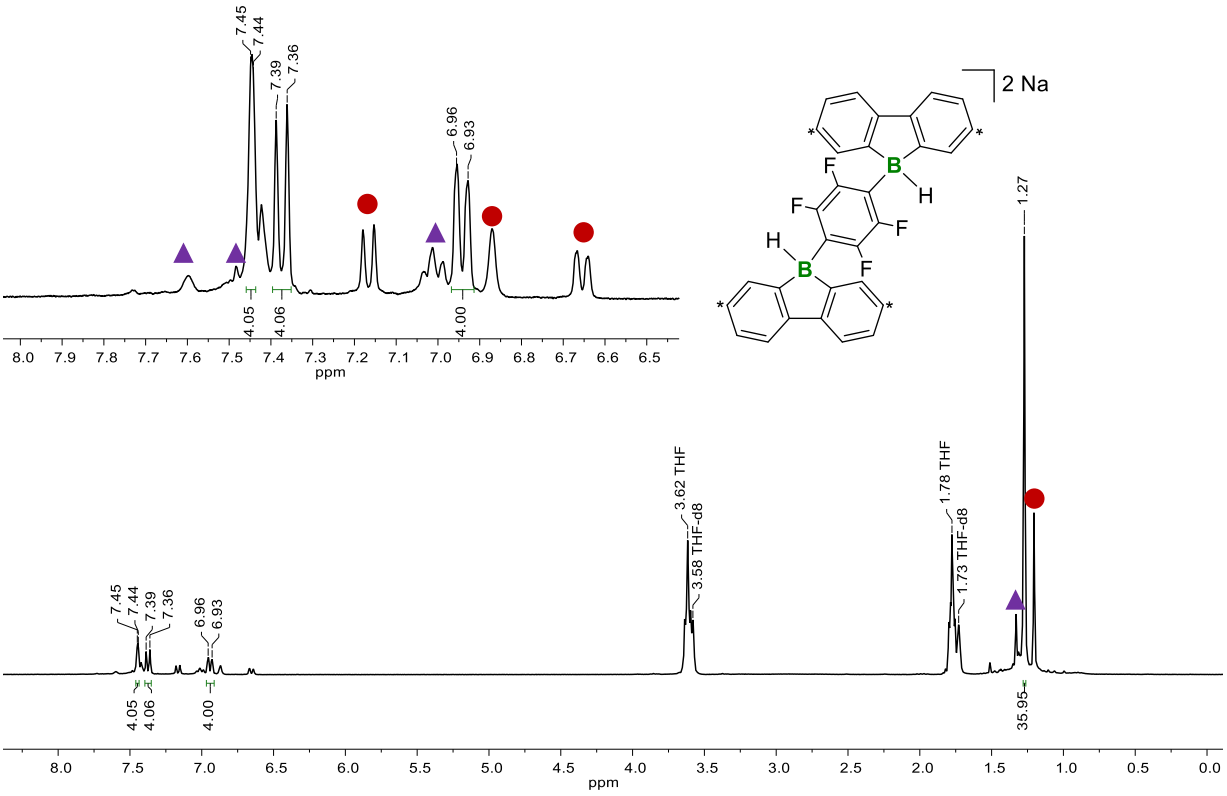

Figure S52.[1]H NMR spectrum (300.0 MHz, THF-d_8) of Na_2[**9**]. Marked components: Na[**3**H] (▲) and Na[$\mathbf{3}_2$] (●).

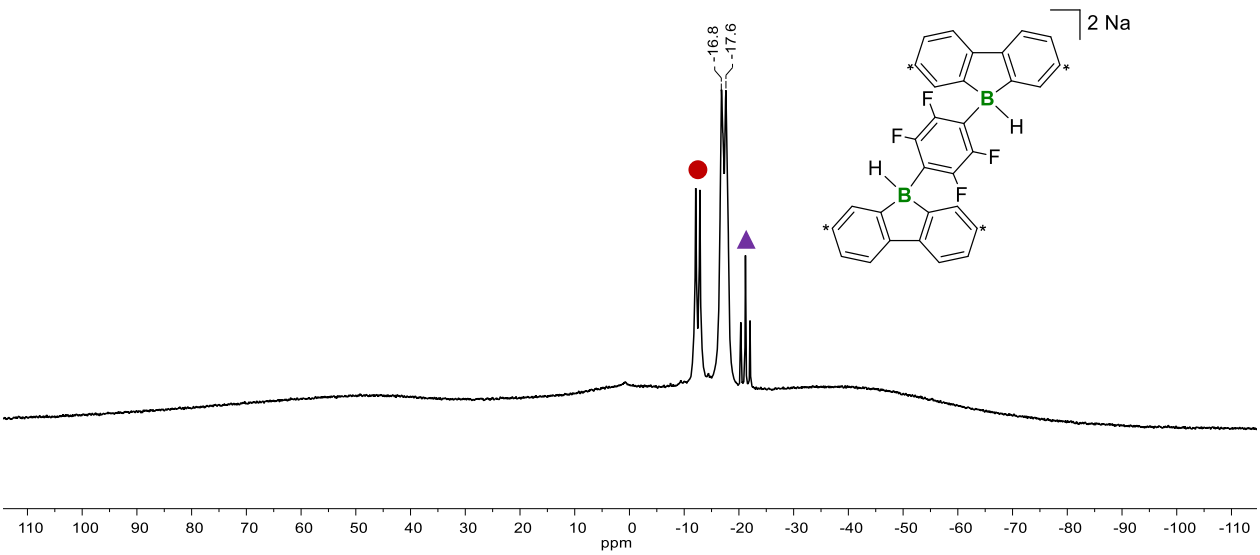

Figure S53. ^{11}B NMR spectrum (96.3 MHz, THF-d_8) of Na_2[**9**]. Marked components: Na[**3**H] (▲) and Na[$\mathbf{3}_2$] (●).

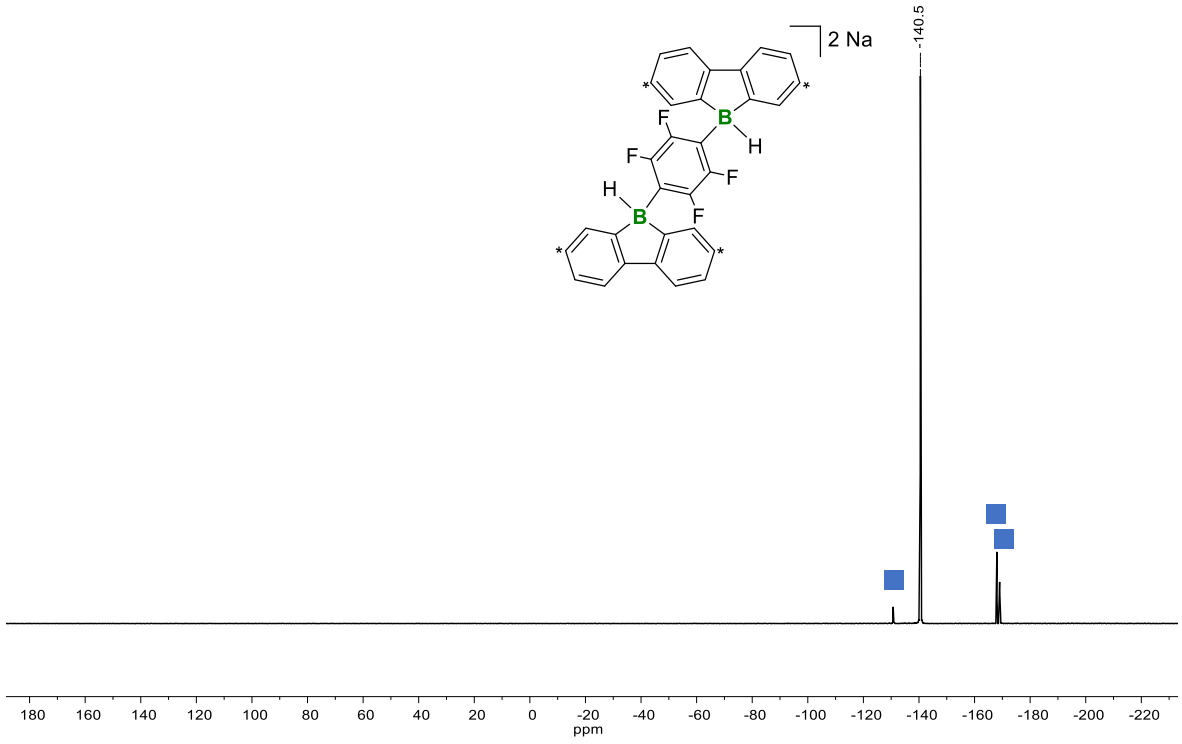

Figure S54. ^{19}F NMR spectrum (282.3 MHz, THF-d_8, THF-d_8) of Na_2[**9**]. Marked component: Na[**5**] (■).

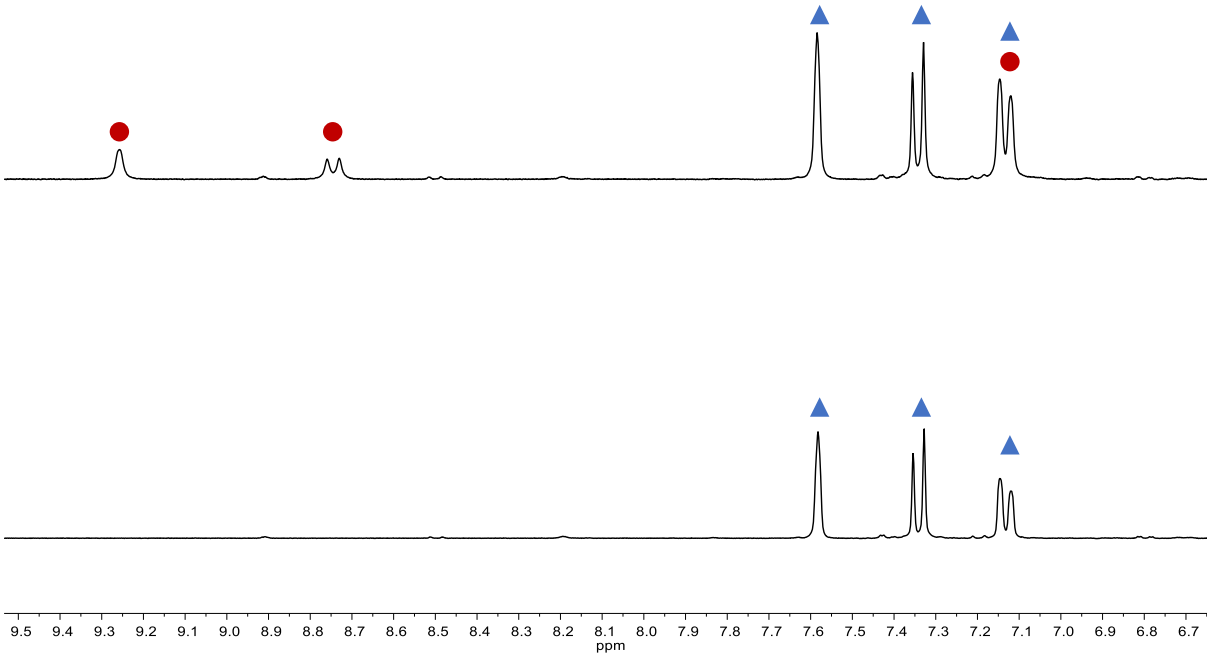

Figure S55. Aromatic regions of the ^{1}H NMR spectra (300.0 MHz, THF-d_8) corresponding to different stages of the reaction between Na_2[**2**] and hexafluorobenzene (cf. 1.13; top: after 1 h, bottom: after 6 h). Marked components: Na_2[**2'**] (●), Na[**10**](▲).

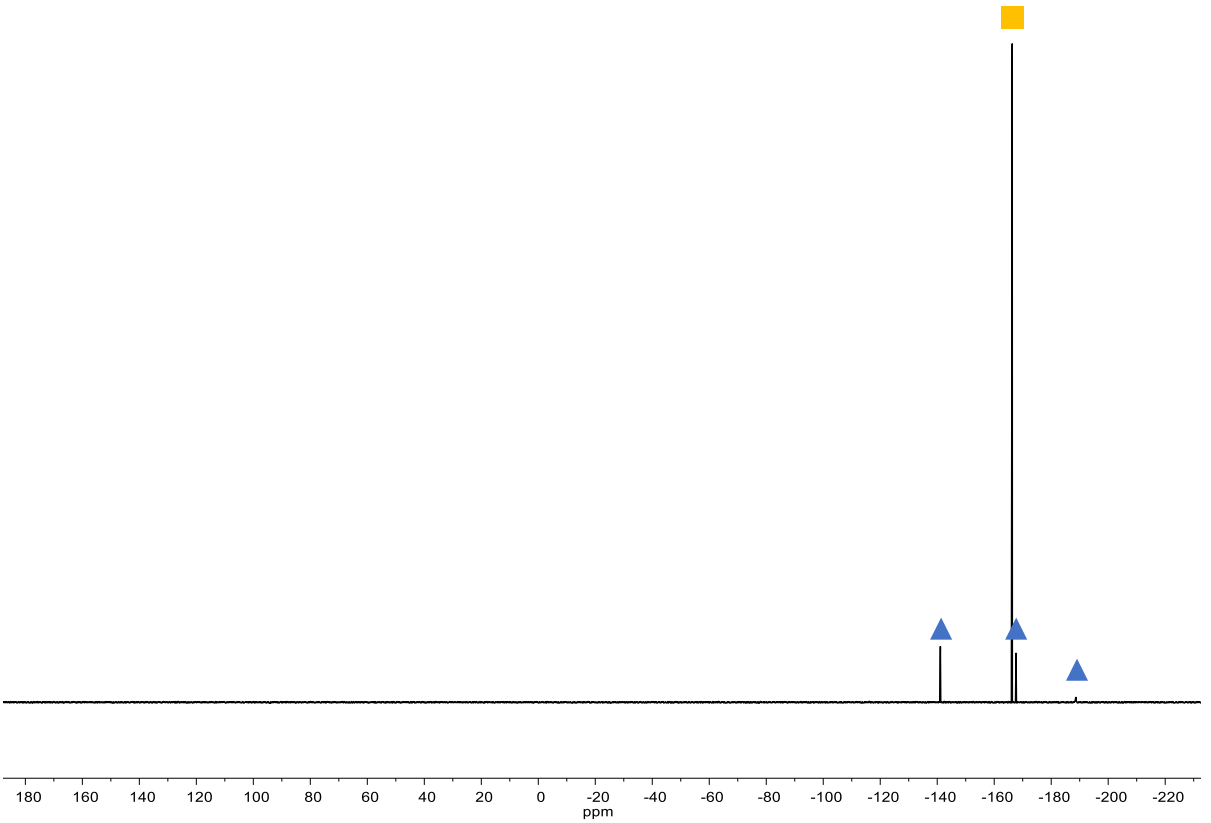

Figure S56. ^{19}F NMR spectrum (282.3 MHz, THF-d_8) recorded on the reaction mixture of Na_2[**2**] and hexafluorobenzene (cf. 1.13) after 1 h (cf. Figure S55). Marked components: Na[**10**](▲), hexafluorobenzene (■).

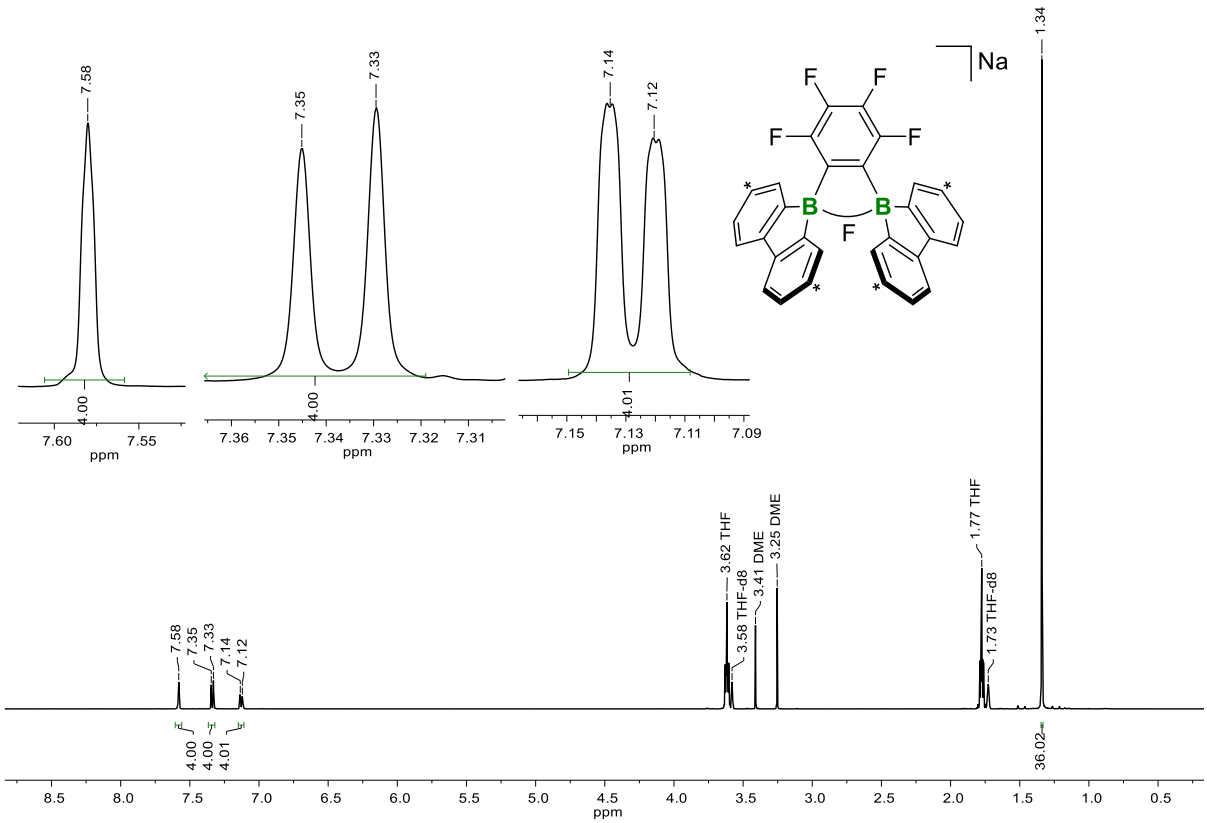

Figure S57. ^{1}H NMR spectrum (500.2 MHz, THF-d_8) of Na[**10**].

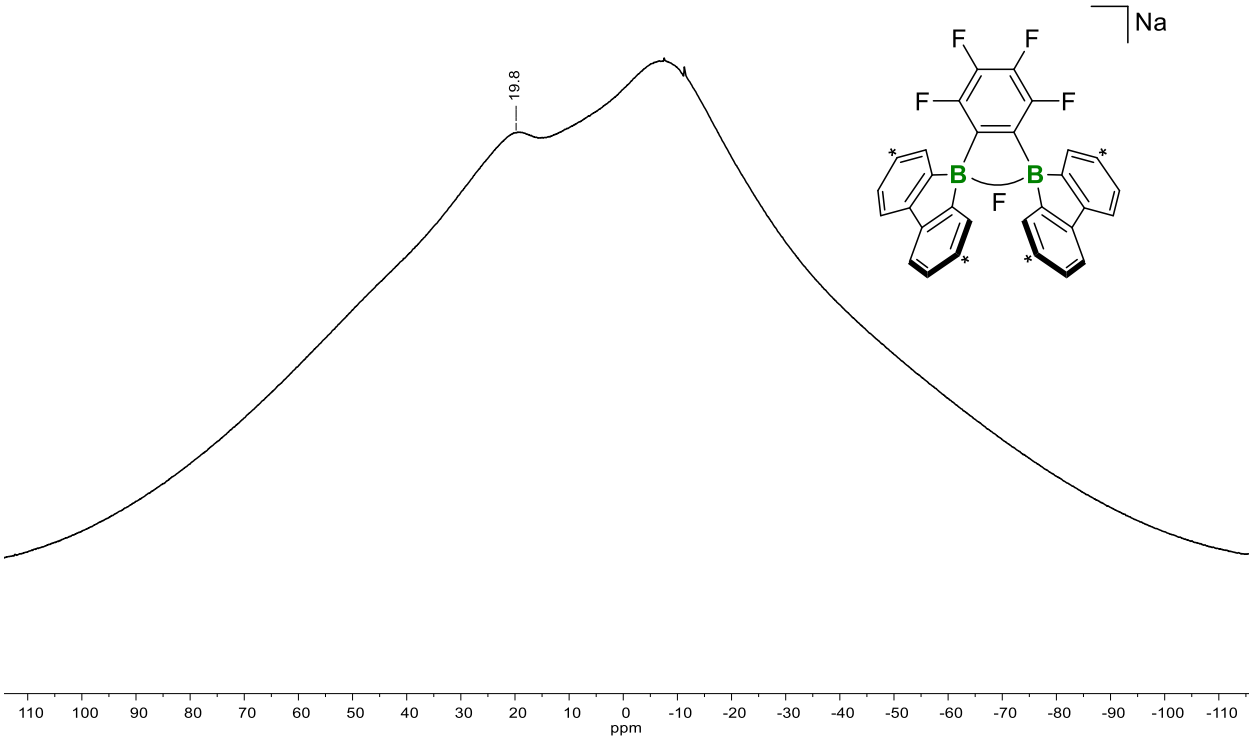

Figure S58. ^{11}B NMR spectrum (160.5 MHz, THF-d_8) of Na[**10**].

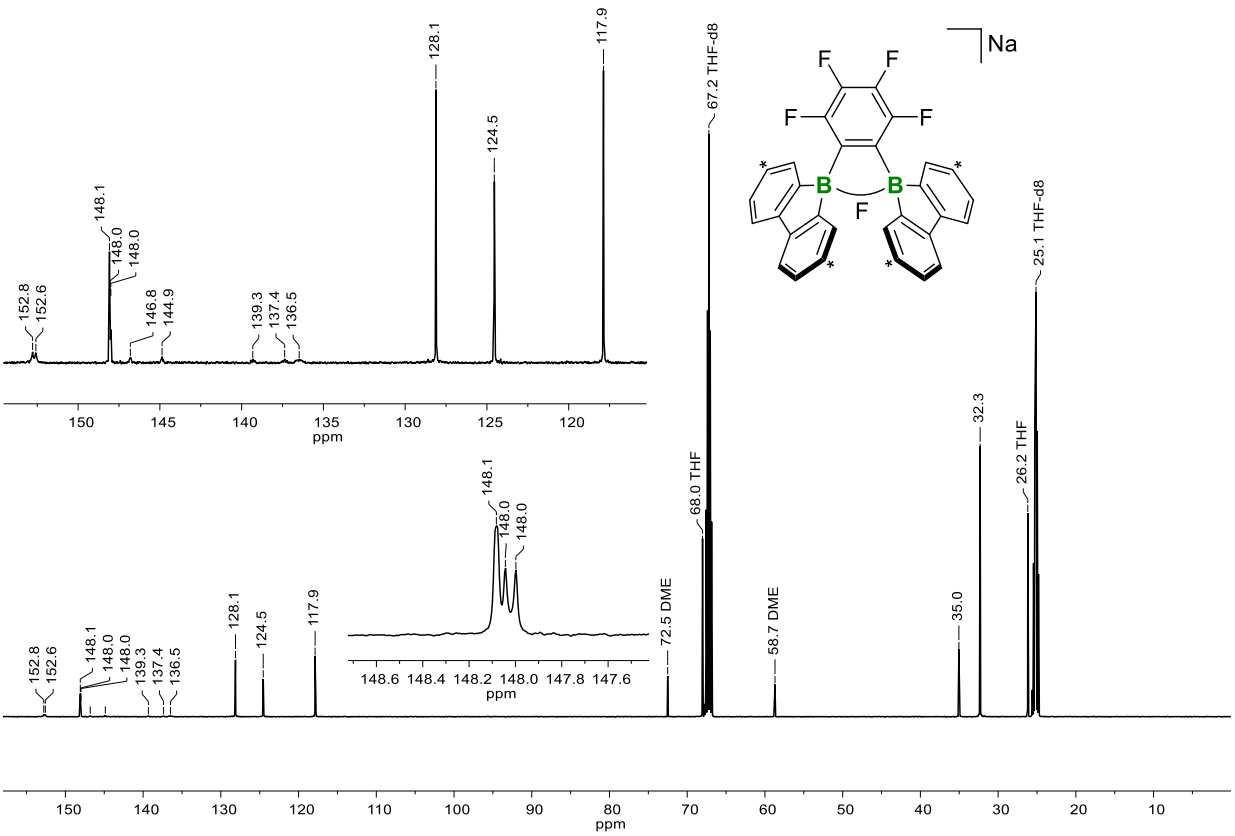

Figure S59. $^{13}C\{^{1}H\}$ NMR spectrum (125.8 MHz, THF-d_8) of Na[**10**].

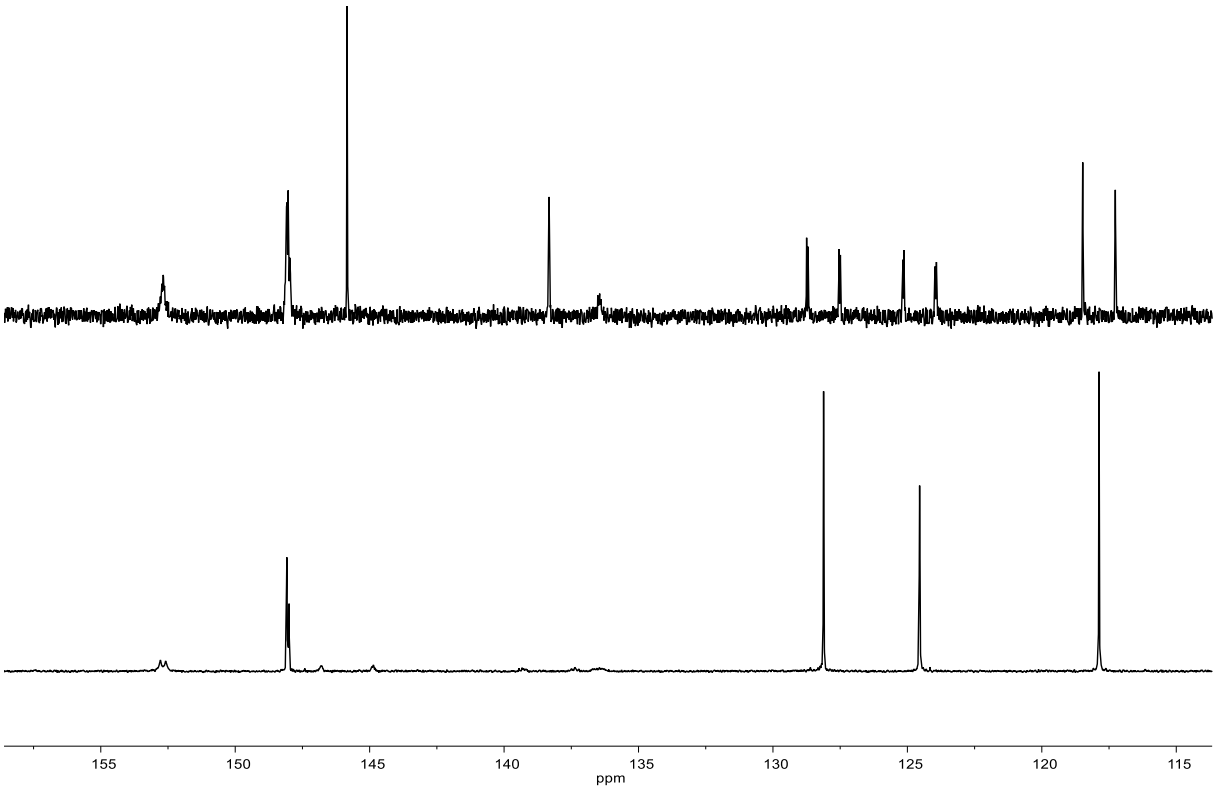

Figure S60. Aromatic regions of the $^{13}C\{^{19}F\}$ (125.8 MHz, THF-d_8; top) and $^{13}C\{^{1}H\}$ NMR spectra (125.8 MHz, THF-d_8; bottom) of Na[**10**].

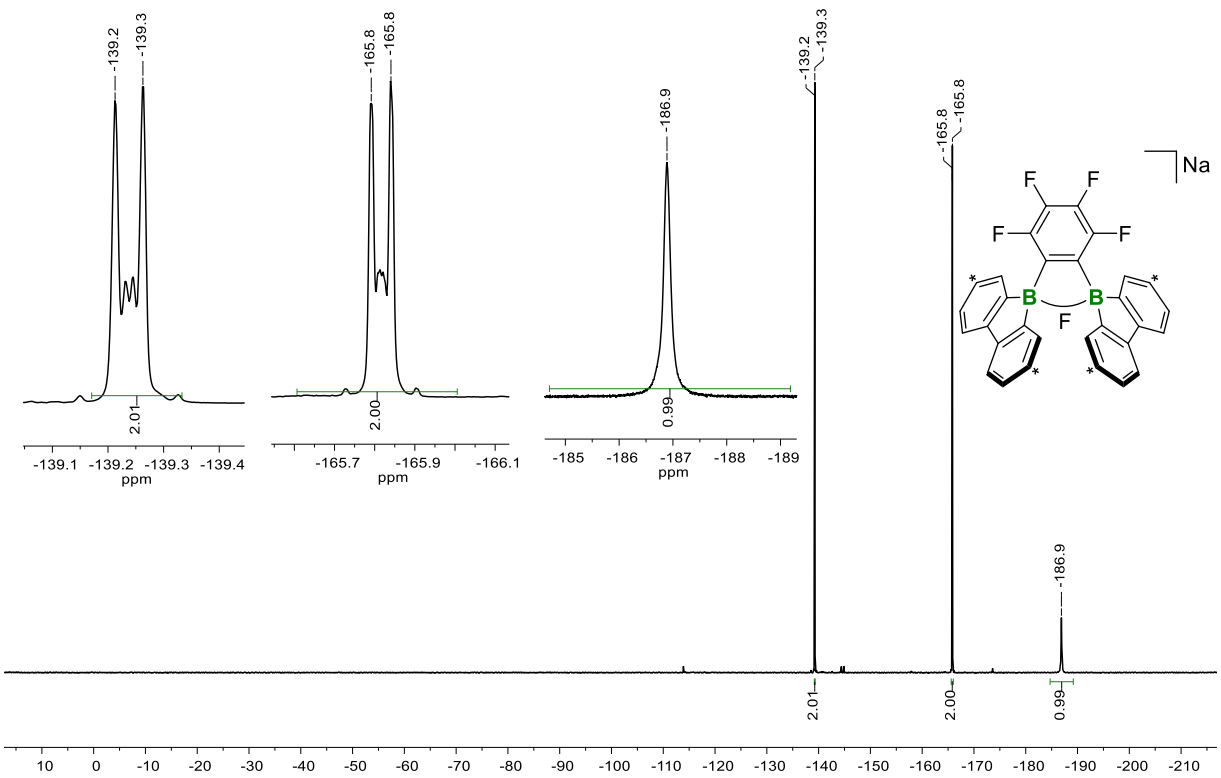

Figure S61. ^{19}F NMR spectrum (470.6 MHz, THF-d_8) of Na[**10**].

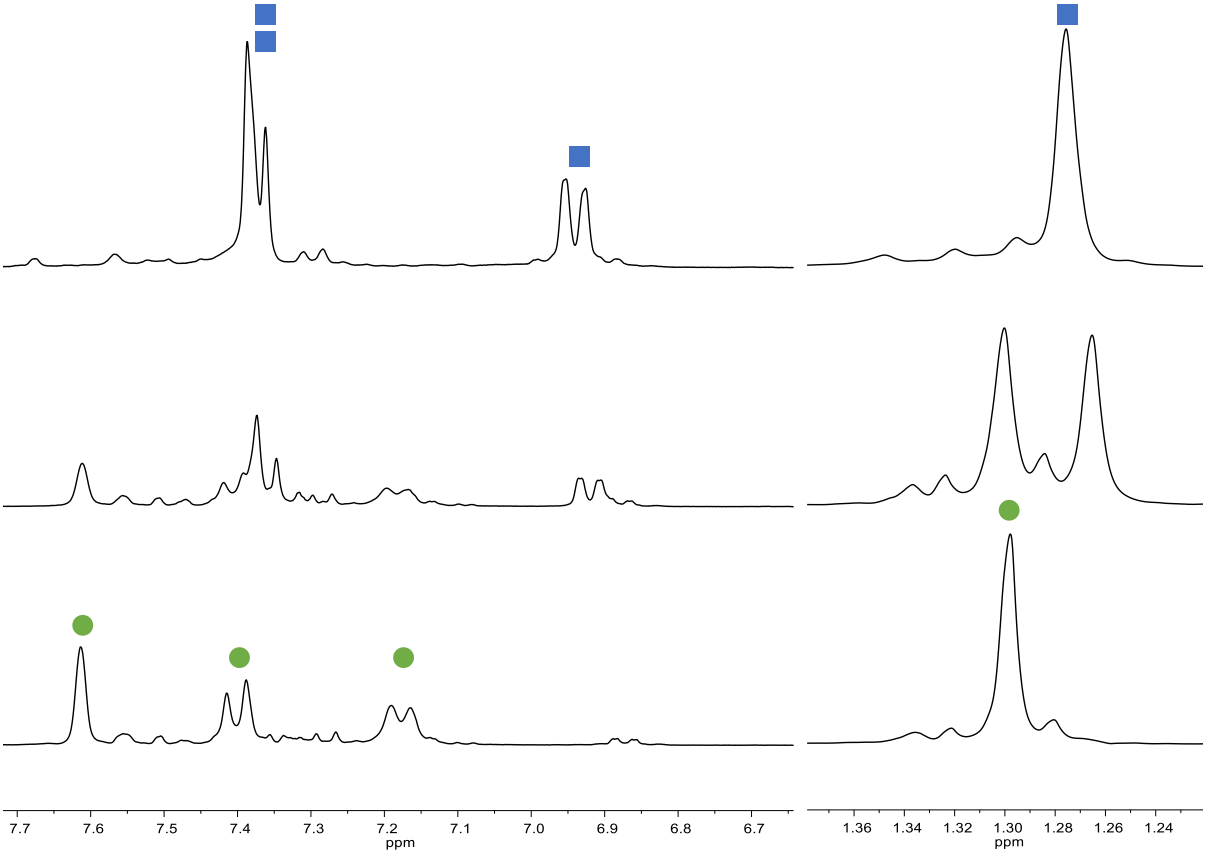

Figure S62. Aryl as well as alkyl regions of the ^{1}H NMR spectra (300.0 MHz, THF-d_8) corresponding to different stages of the reaction between Li[**5**] and TMSCl (cf. 1.14; top: after addition of 1 equiv TMSCl and heating for 1d at 50 °C, middle: after addition of another 6 equiv TMSCl and heating at 50 °C for 1d, bottom: after heating at 50 °C for another 2d). Marked components: Li[**5**] (■), **11** (●). The aromatic and alkyl regions are scaled differently.

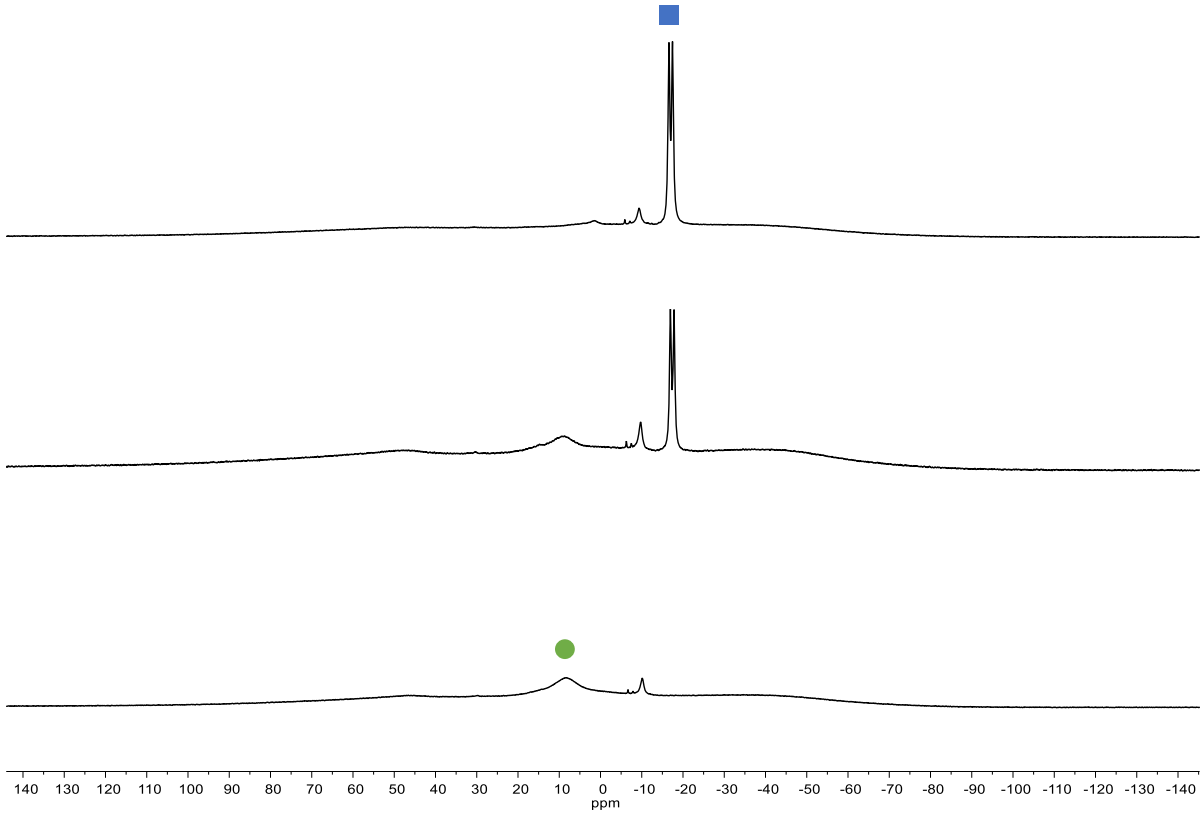

Figure S63. ^{11}B NMR spectra (96.3 MHz, THF-d_8) corresponding to different stages of the reaction between Li[**5**] and TMSCl (cf. 1.14; top: after addition of 1 equiv TMSCl and heating for 1d at 50 °C, middle: after addition of another 6 equiv TMSCl and heating at 50 °C for 1d, bottom: after heating at 50 °C for another 2d). Marked components: Li[**5**] (■) and **11** (●).

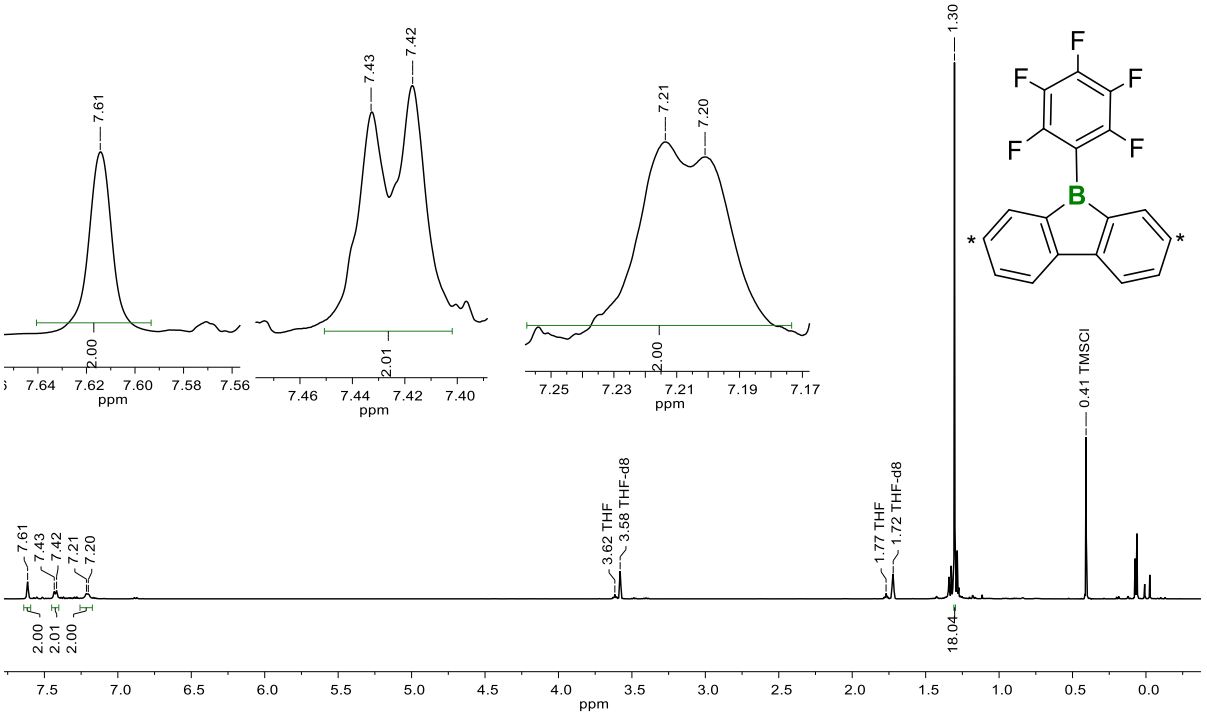

Figure S64. ^{1}H NMR spectrum (500.2 MHz, THF-d_8) of **11**.

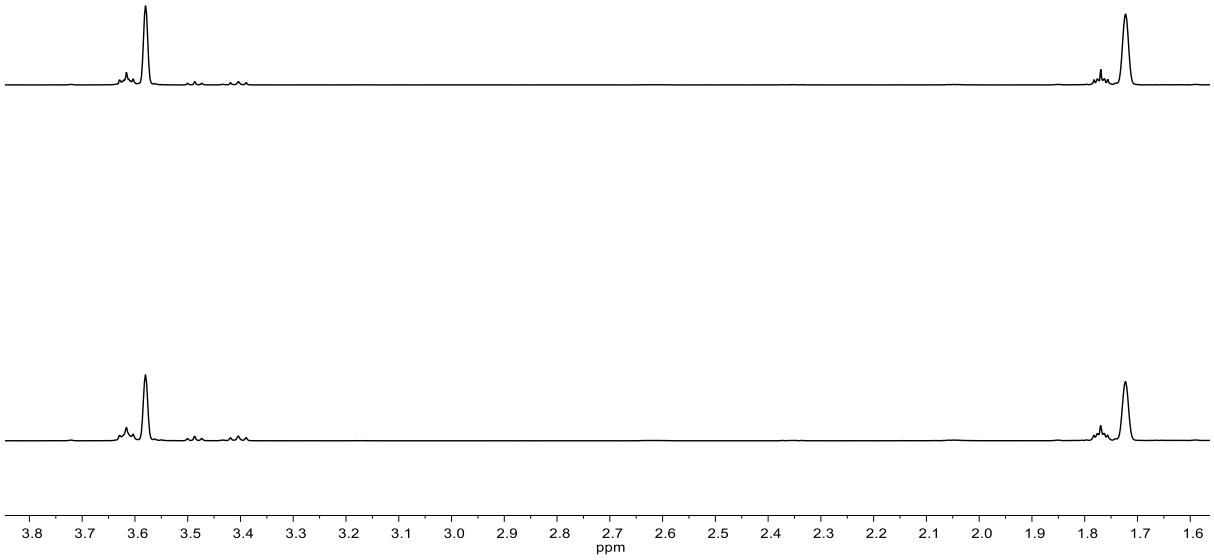

Figure S65. Cutouts from the ^{1}H NMR (500.2 MHz, THF-d_8; top) and ^{1}H{^{11}B} NMR spectrum (500.2 MHz, THF-d_8; bottom;) of **11**.

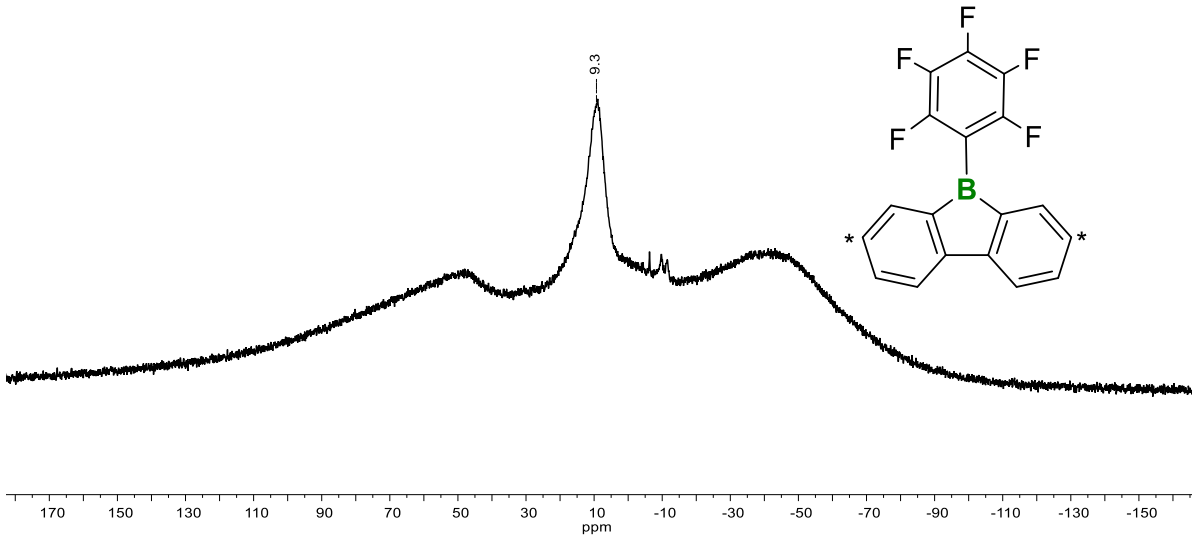

Figure S66. ^{11}B NMR spectrum (96.3 MHz, THF-d_8) of **11**.

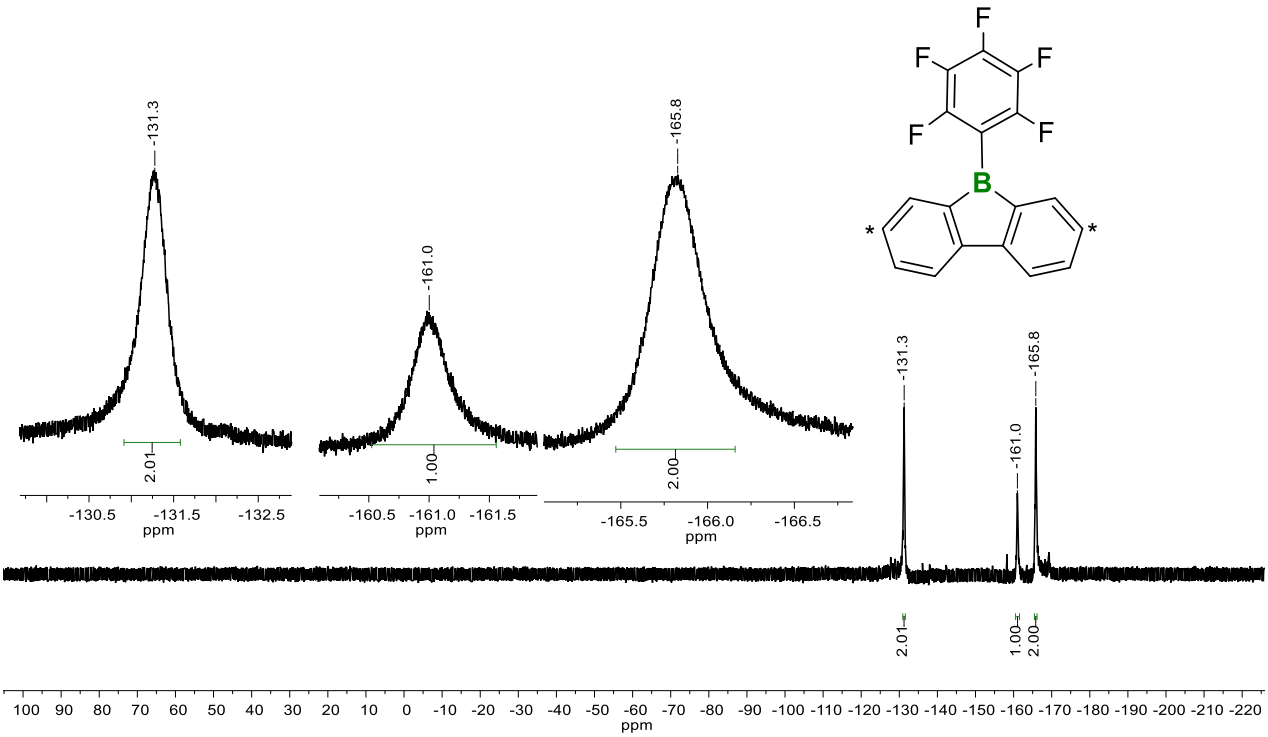

Figure S67. ^{19}F NMR spectrum (282.3 MHz, THF-d_8) of **11**.

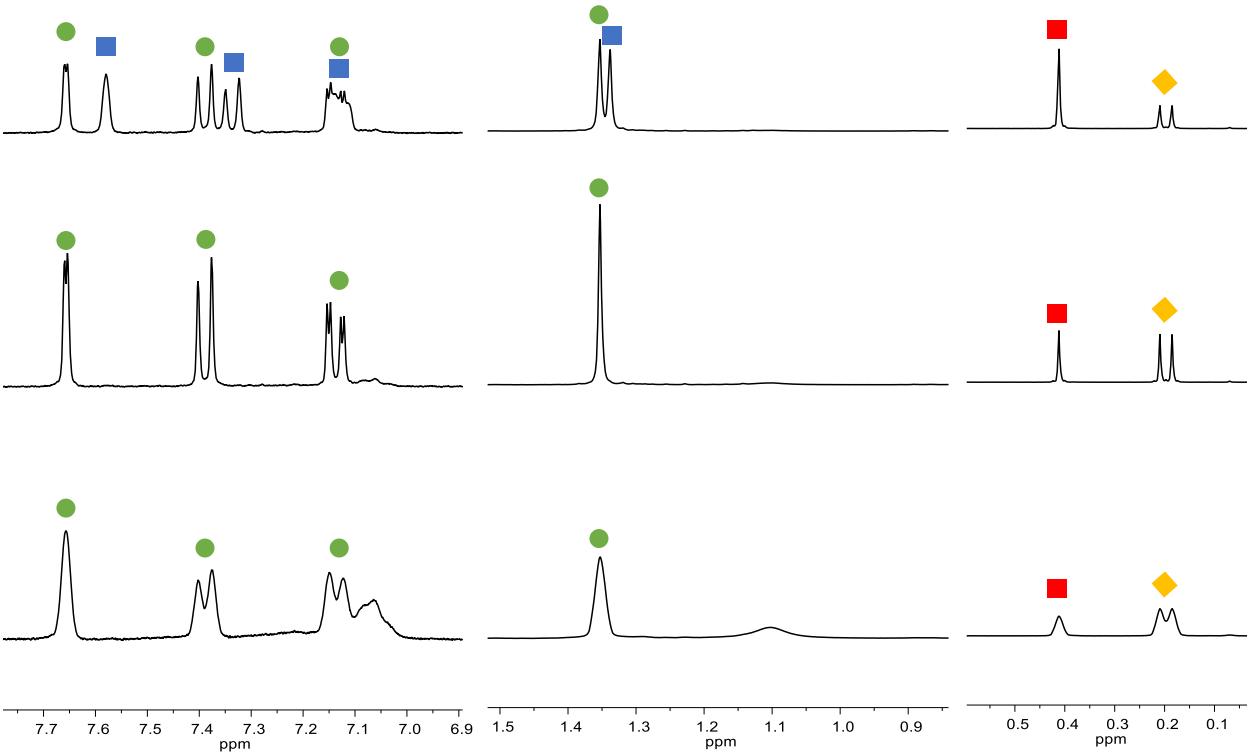

Figure S68. Aryl and alkyl regions of the ^{1}H NMR spectra (300.0 MHz, THF-d_8) recorded on the reaction mixture of Na[**10**] and TMSCl (top: after 2 h, middle: after 10 h, bottom: after 4 d; cf. 1.15). Marked components: Na[**10**] (■), **12** (●), TMSCl (■), TMSF (◆). The aromatic and alkyl regions are each scaled differently.

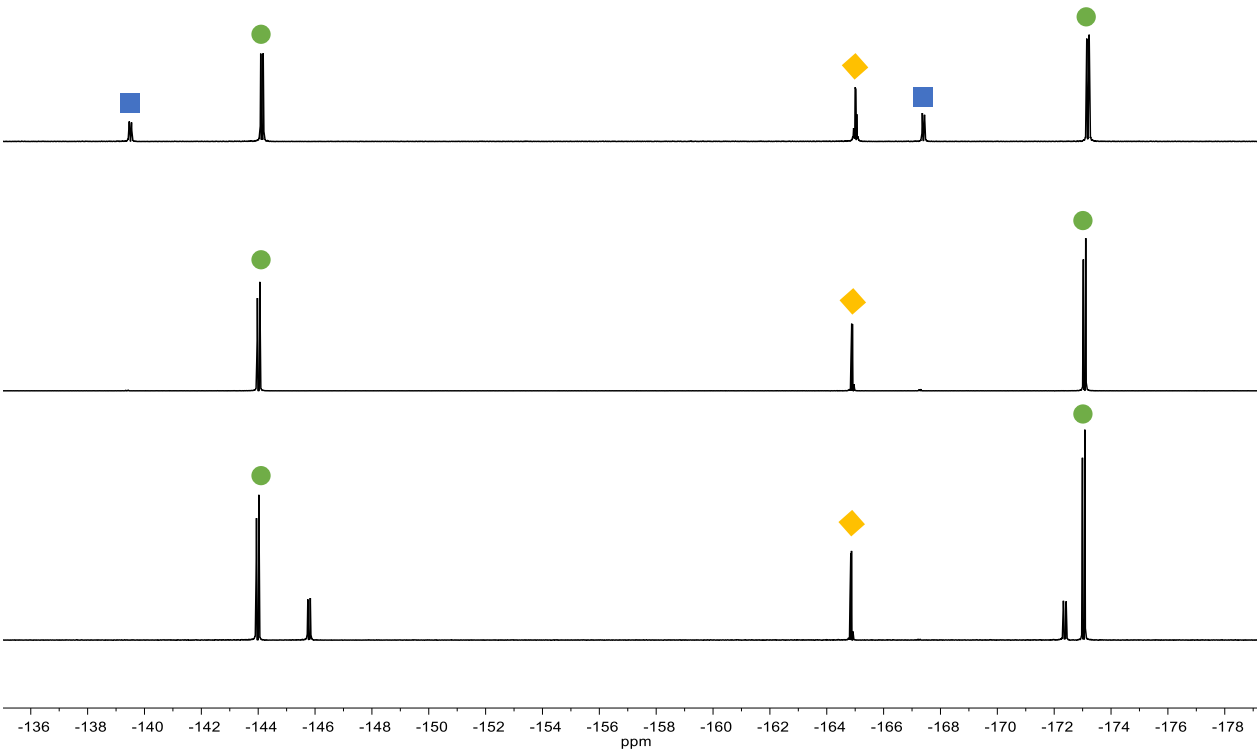

Figure S69. ^{19}F NMR spectra (282.3 MHz, THF-d_8) recorded on the reaction mixture of Na[**10**] and TMSCl (top: after 2 h, middle: after 10 h, bottom: after 4 d; cf. 1.15). Marked components: Na[**10**] (■), **12** (●),TMSF (◆).

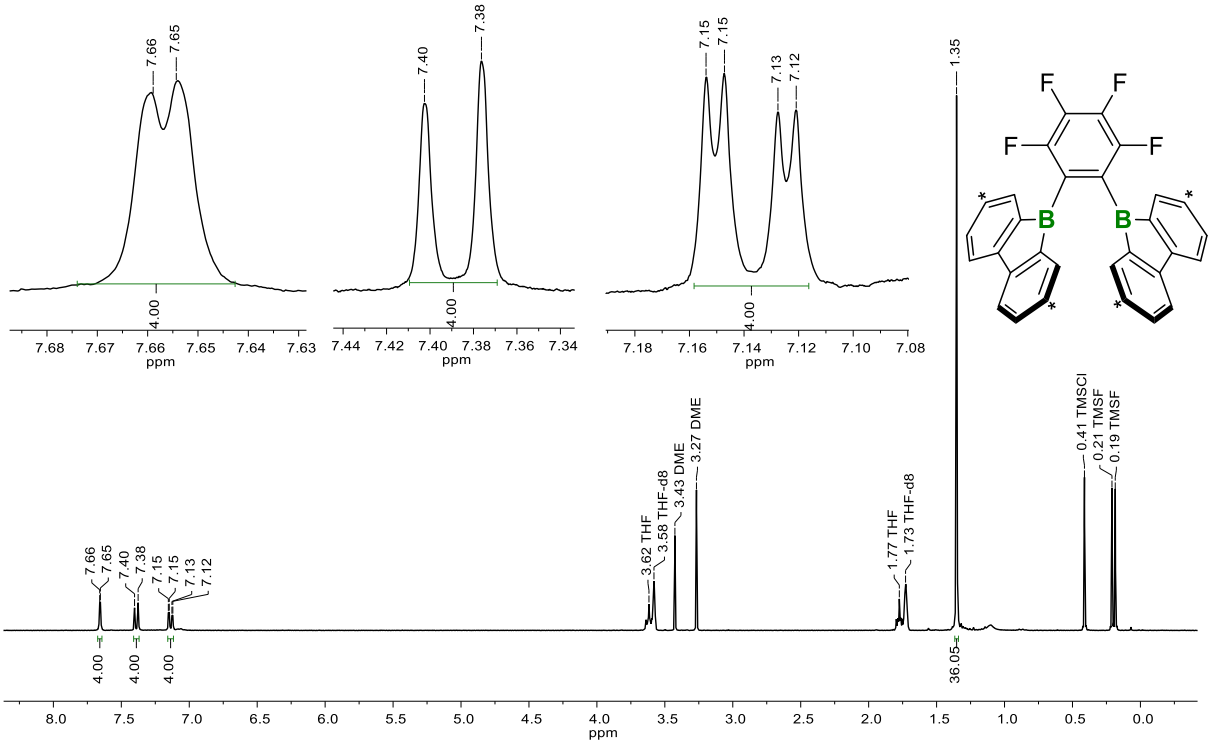

Figure S70. ^{1}H NMR spectrum (300.0 MHz, THF-d_8) of **12** recorded on the reaction mixture of Na[**10**] and TMSCl after 10 h (cf. 1.15).

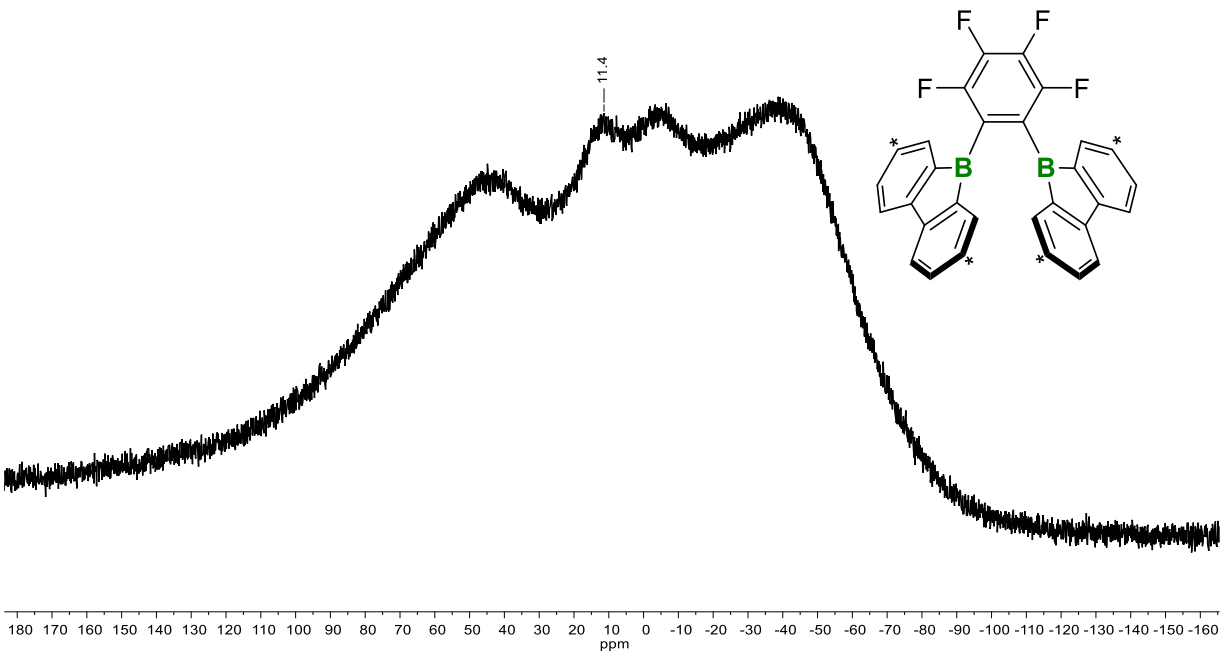

Figure S71. ^{11}B NMR spectrum (96.3 MHz, THF-d_8) of **12** recorded on the reaction mixture of Na[**10**] and TMSCl after 10 h (cf. 1.15).

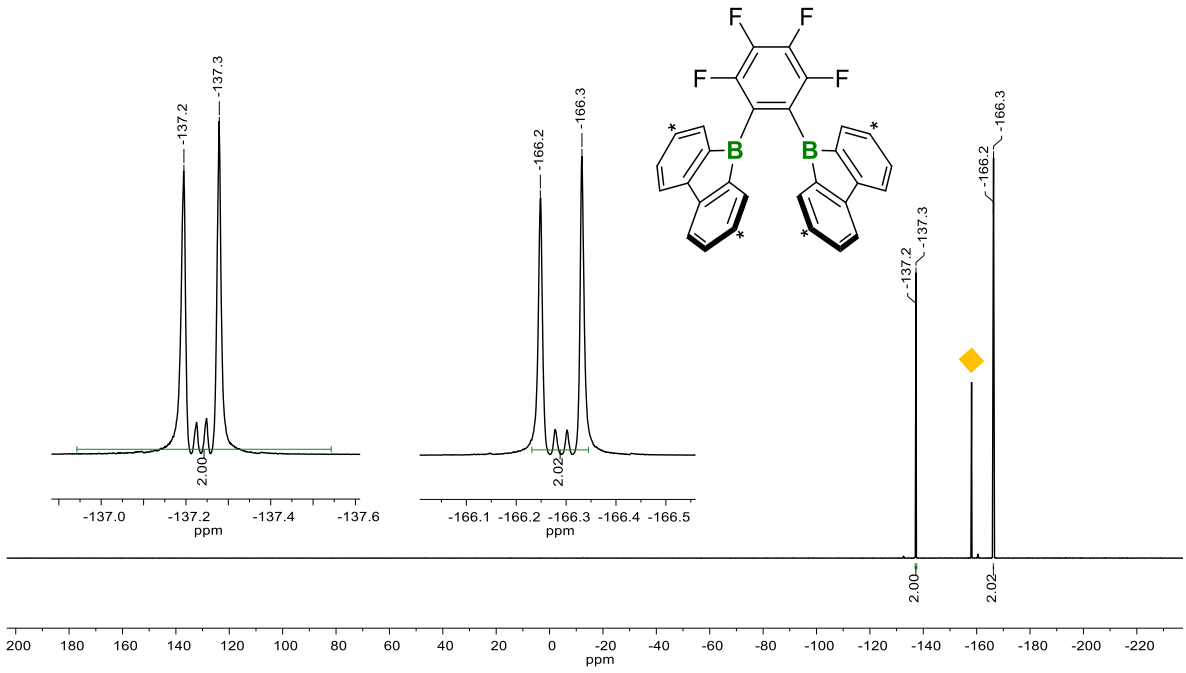

Figure S72. ^{19}F NMR spectrum (282.3 MHz, THF-d_8) of **12** recorded on the reaction mixture of Na[**10**] and TMSCl after 10 h (cf. 1.15). Marked component: TMSF (◆).

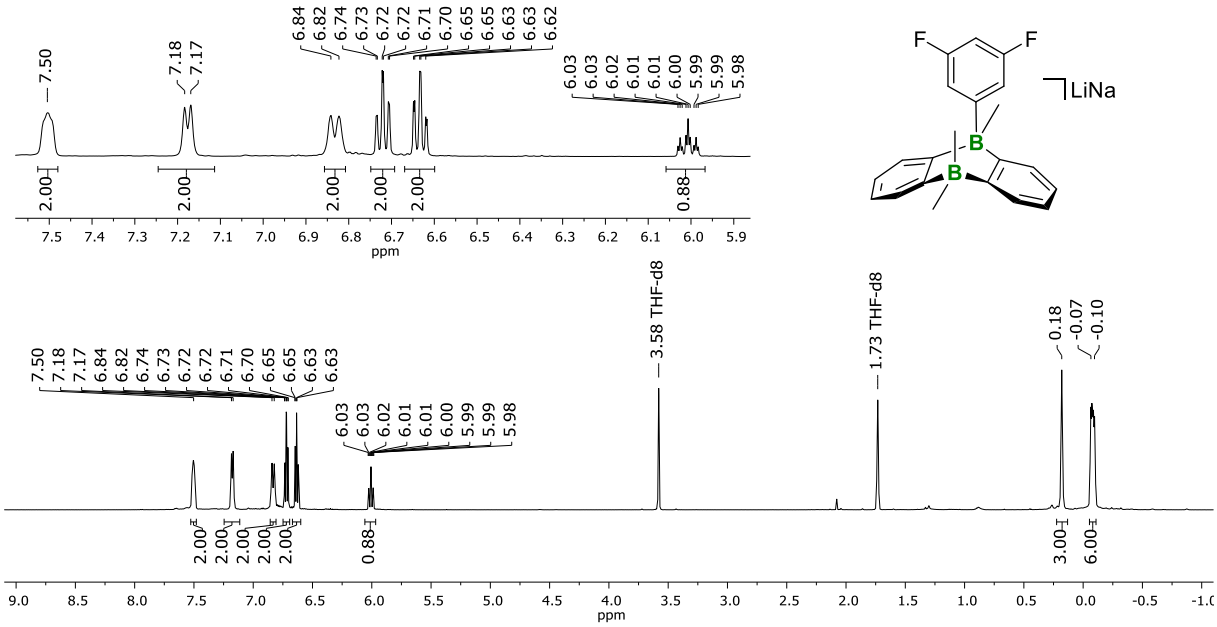

Figure S73. ^{1}H NMR spectrum (500.2 MHz, THF-d_8) of LiNa[**13**].

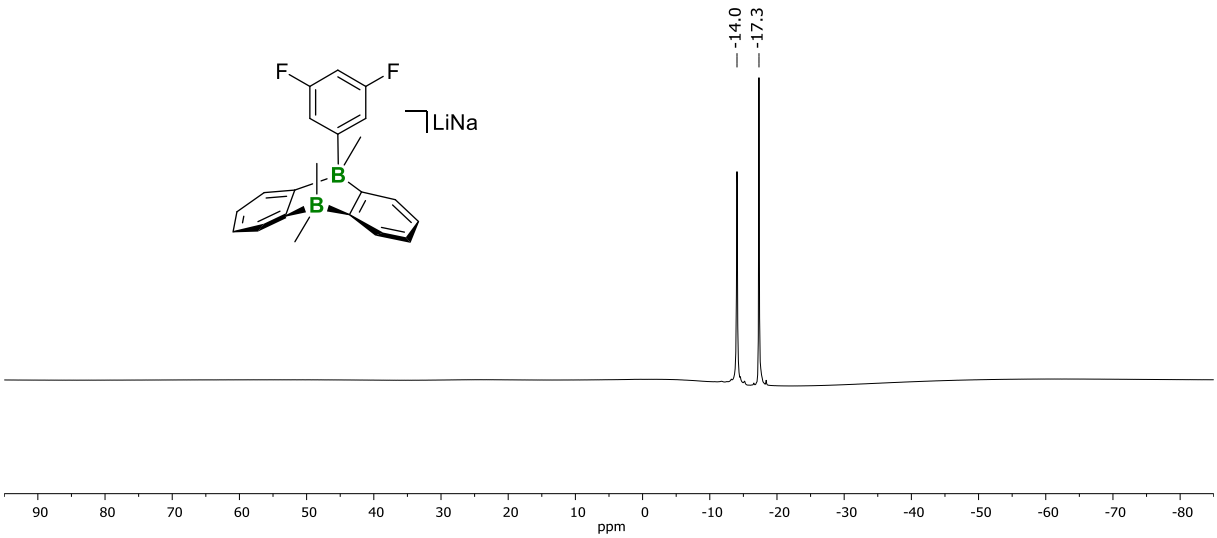

Figure S74. ^{11}B NMR spectrum (160.5 MHz, THF-d_8) of LiNa[**13**].

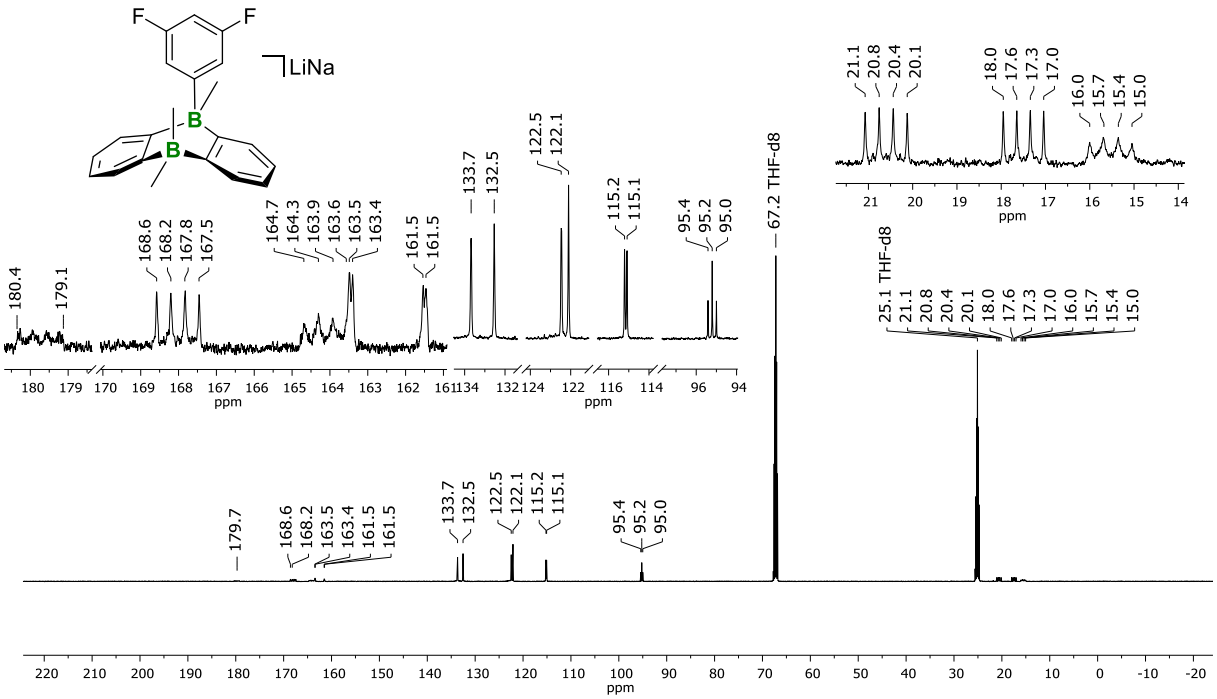

Figure S75. $^{13}C\{^{1}H\}$ NMR spectrum (125.8 MHz, THF-d_8) of LiNa[**13**].

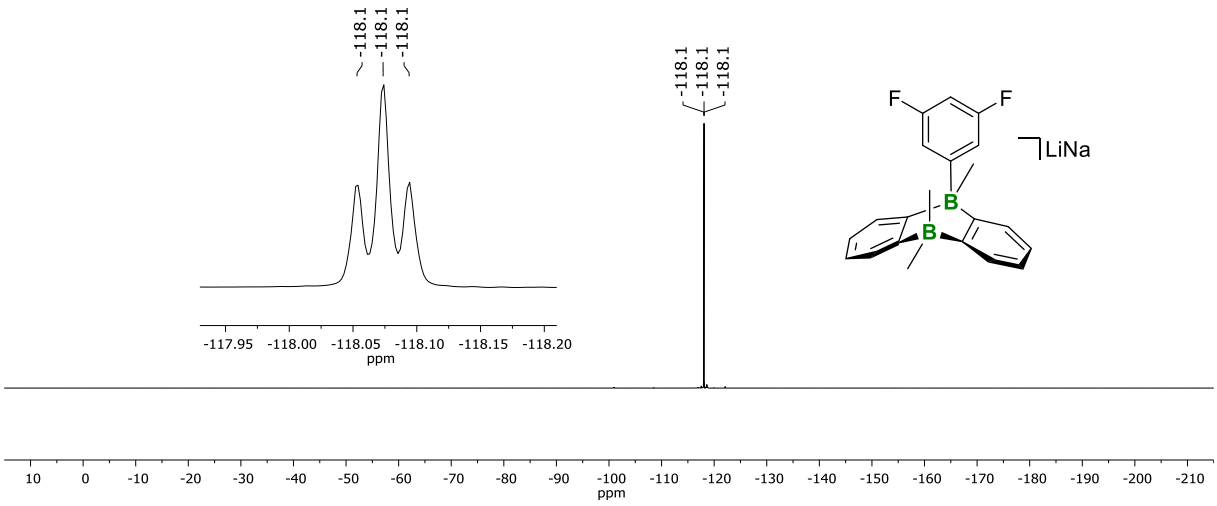

Figure S76. ^{19}F NMR spectrum (470.6 MHz, THF-d_8) of LiNa[**13**].

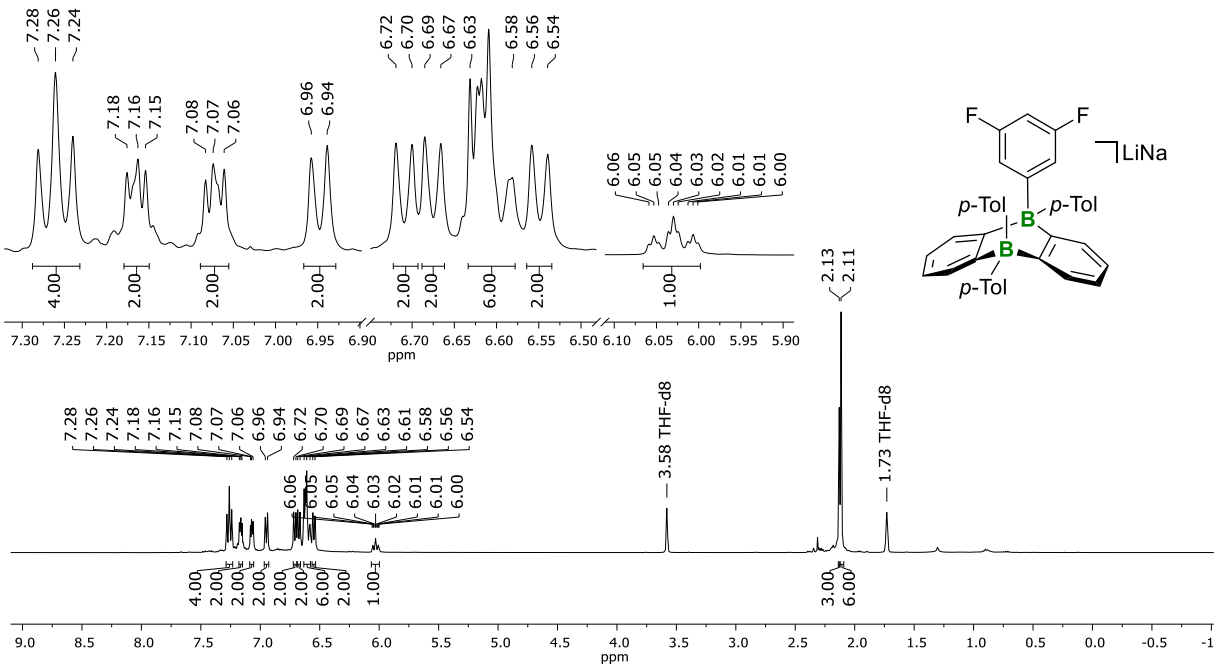

Figure S77. ^{1}H NMR spectrum (400.3 MHz, THF-d_8) recorded on the crude reaction mixture between Na[**8^{Tol}**] and *p*-tolyllithium.

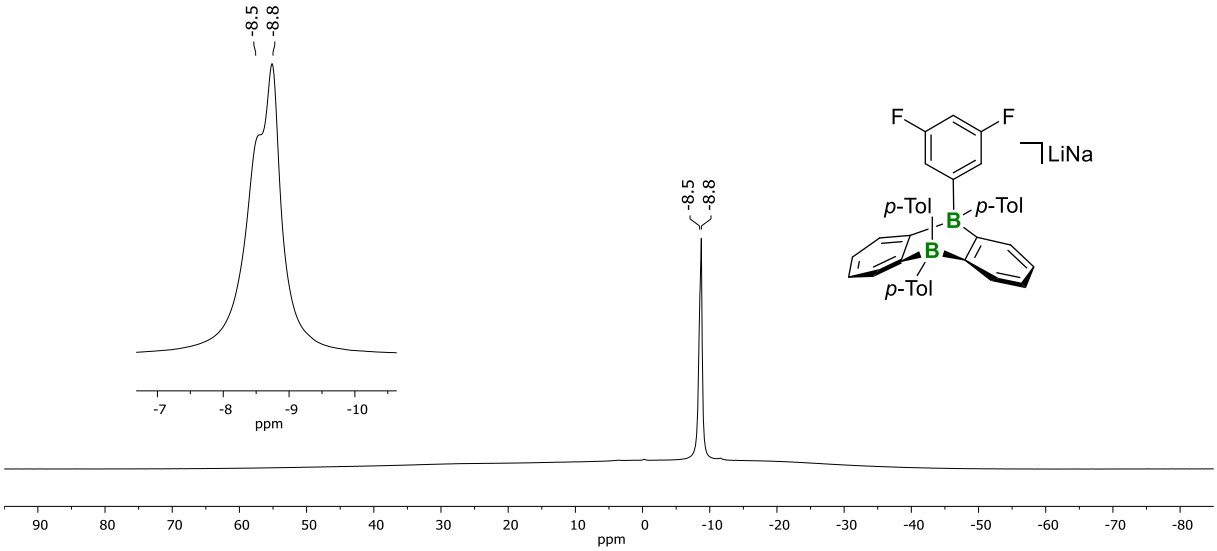

Figure S78. ^{11}B NMR spectrum (128.4 MHz, THF-d_8) recorded on the crude reaction mixture between Na[**8^{Tol}**] and *p*-tolyllithium.

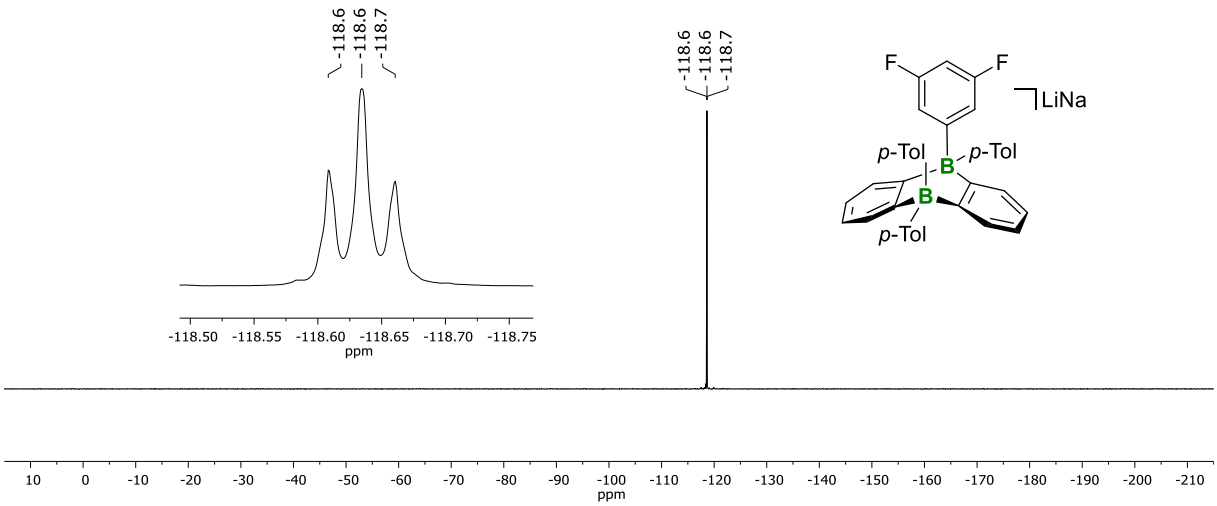

Figure S79. ^{19}F NMR spectrum (376.6 MHz, THF-d_8) recorded on the crude reaction mixture between Na[**8**$^{\mathbf{Tol}}$] and *p*-tolyllithium.

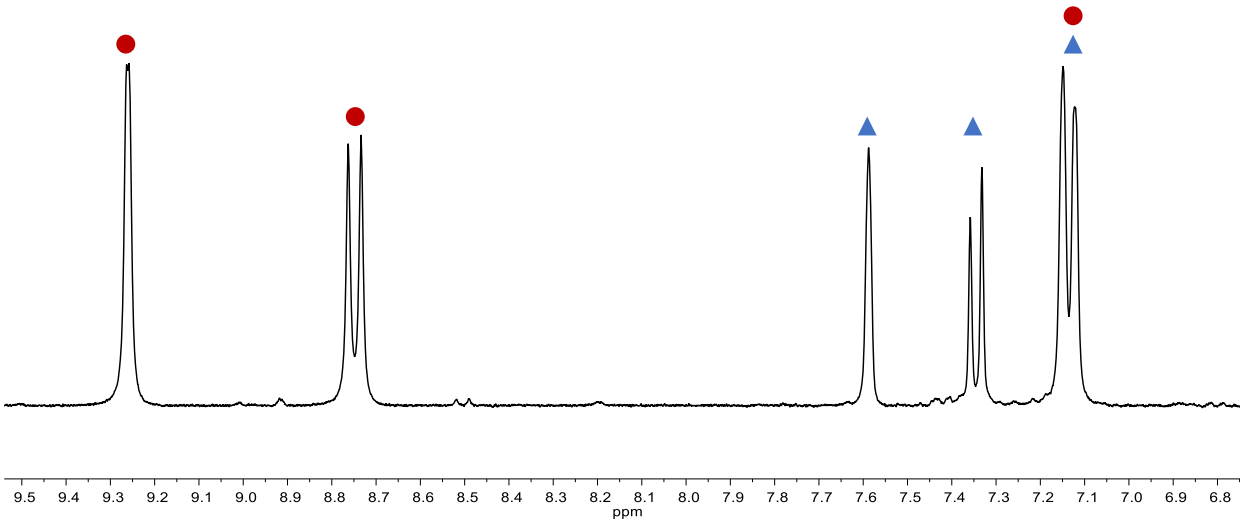

Figure S80. Aromatic region of the ^{1}H NMR spectrum (300.0 MHz, THF-d_8) recorded on the reaction mixture of an excess of Na_2[**2**] and hexafluorobenzene (cf. 1.21). Marked components: Na_2[**2'**] (●), Na[**10**](▲).

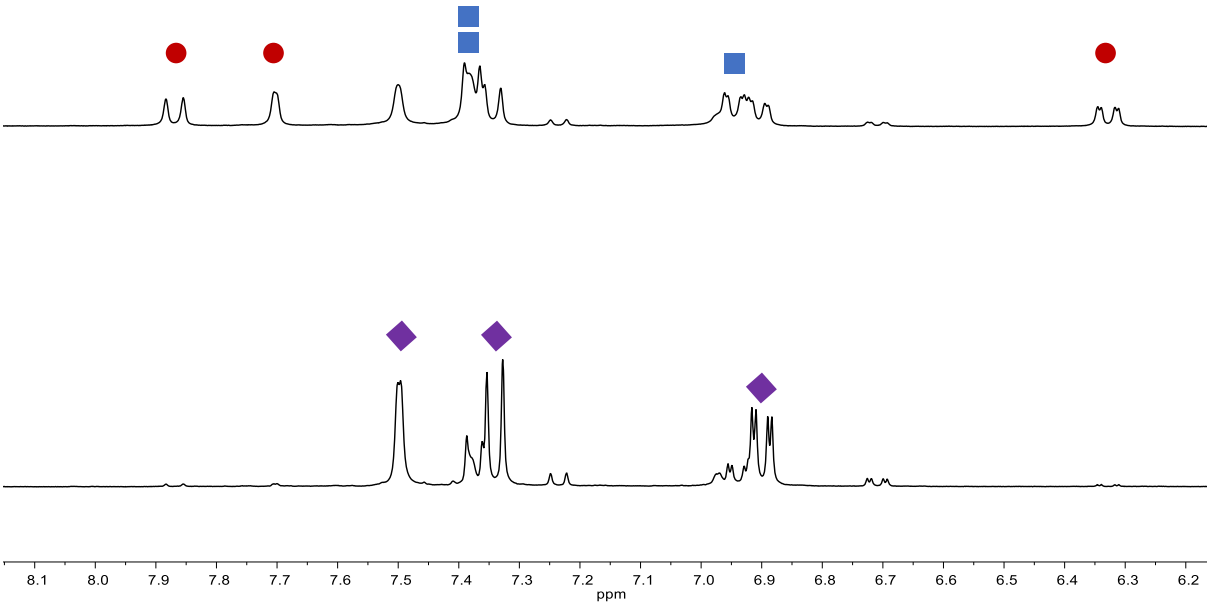

Figure S81. Aromatic regions of the ^{1}H NMR spectra (300.0 MHz, THF-d_8) corresponding to different stages of the reaction between Li_2[**3**] and 0.5 equiv hexafluorobenzene (cf. 1.23; top: after 2h, bottom: after 2d). Marked components: Li_2[**3**] (●), Li[**5**] (■), Li_2[**9**] (◆).

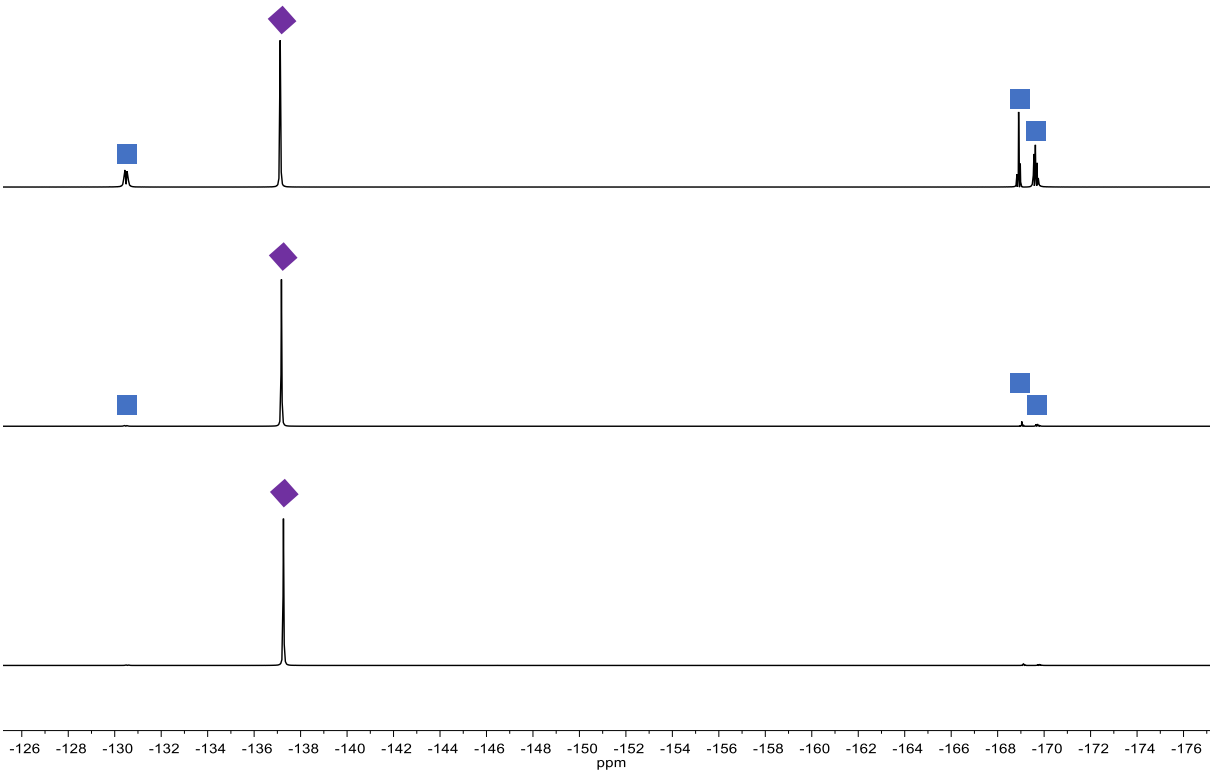

Figure S82. ^{19}F NMR spectra (282.3 MHz, THF-d_8) corresponding to different stages of the reaction between Li_2[**3**] and 0.5 equiv C_6F_6 (cf. 1.23; top: after 2h, middle: after 2d, bottom: after 3d). Marked components: Li[**5**] (■), Li_2[**9**] (◆).

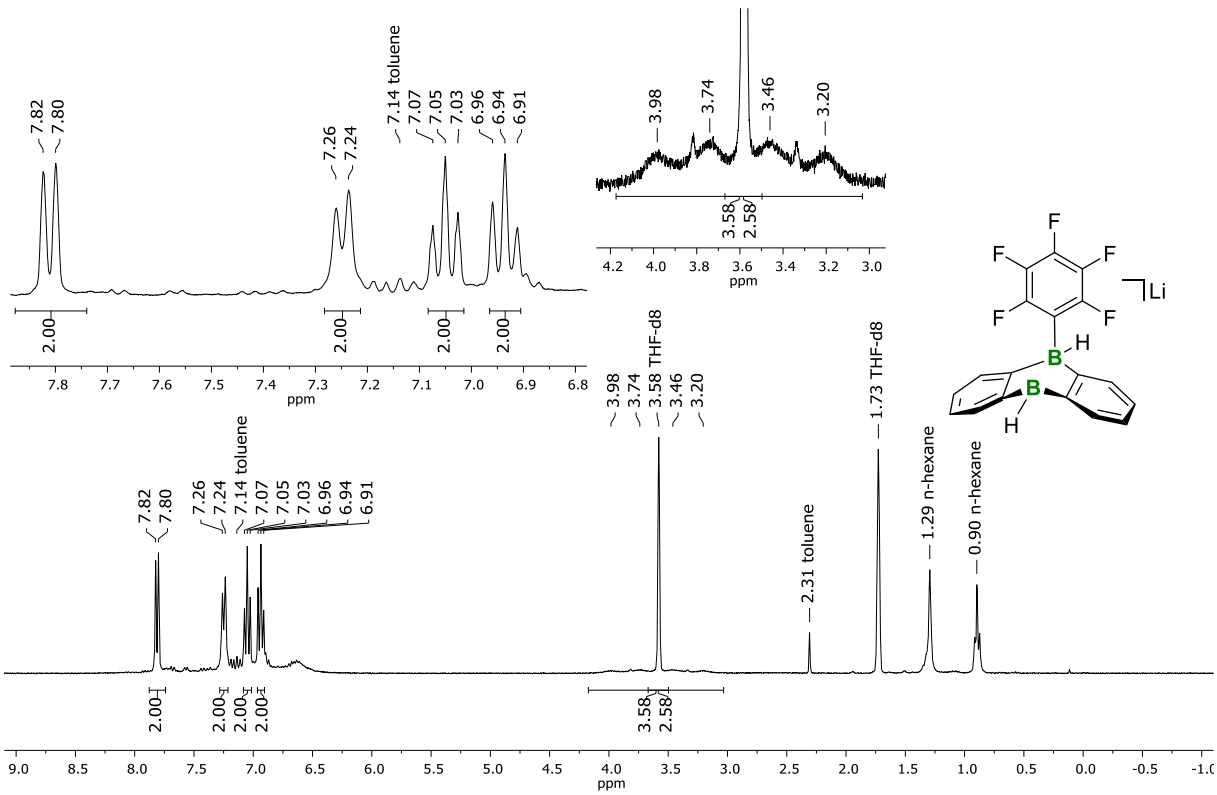

Figure S83. ^{1}H NMR spectrum (300.0 MHz, THF-d_8) recorded on the crude reaction mixture of Li_2[**4^{H}**] and hexafluorobenzene.

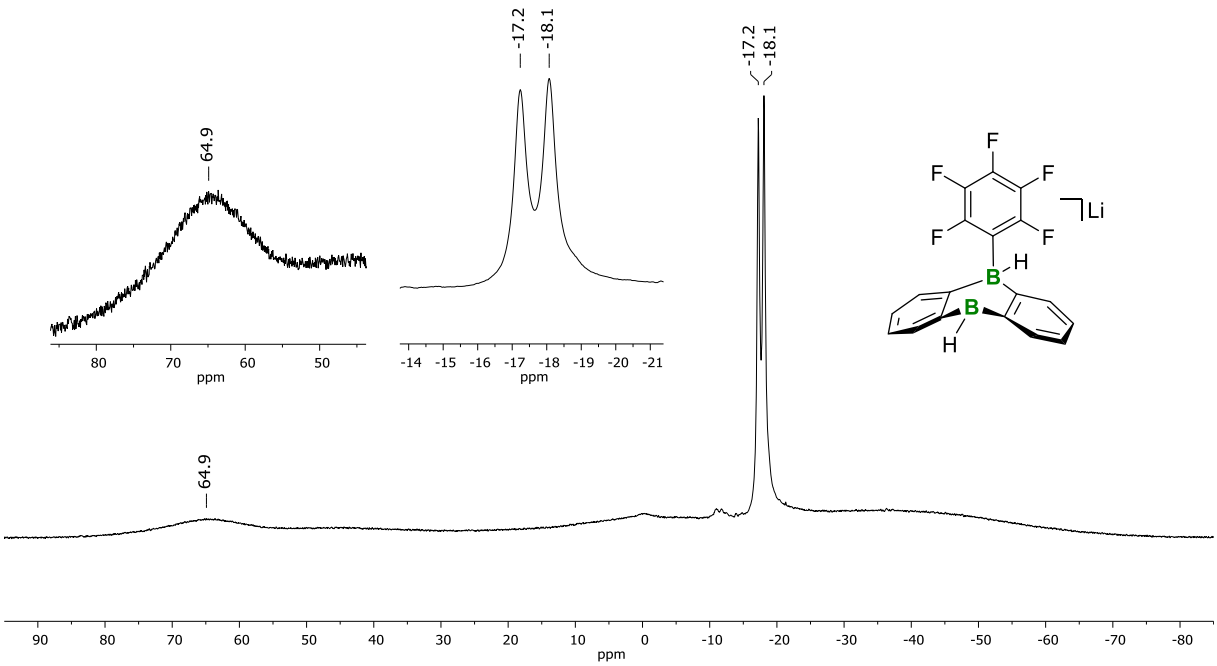

Figure S84. ^{11}B NMR spectrum (96.3 MHz, THF-d_8) recorded on the crude reaction mixture of Li_2[**4^{H}**] and hexafluorobenzene.

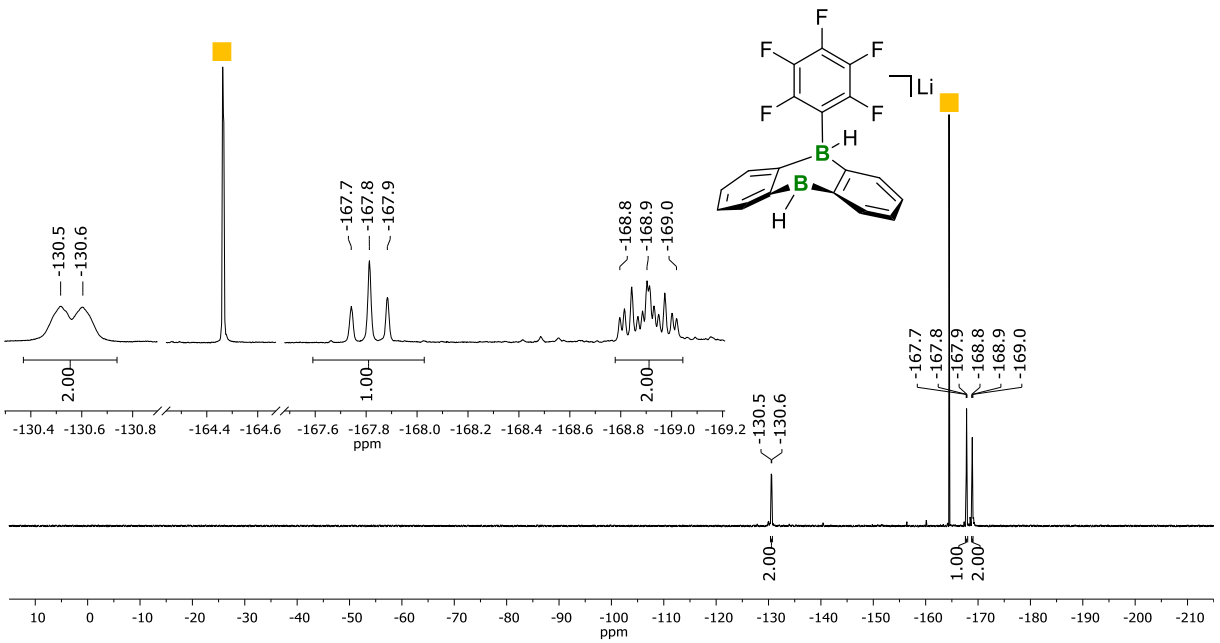

Figure S85. ^{19}F NMR spectrum (282.3 MHz, THF-d_8) recorded on the crude reaction mixture of Li_2[**4**^{H}] and hexafluorobenzene. Marked component: hexafluorobenzene (■).

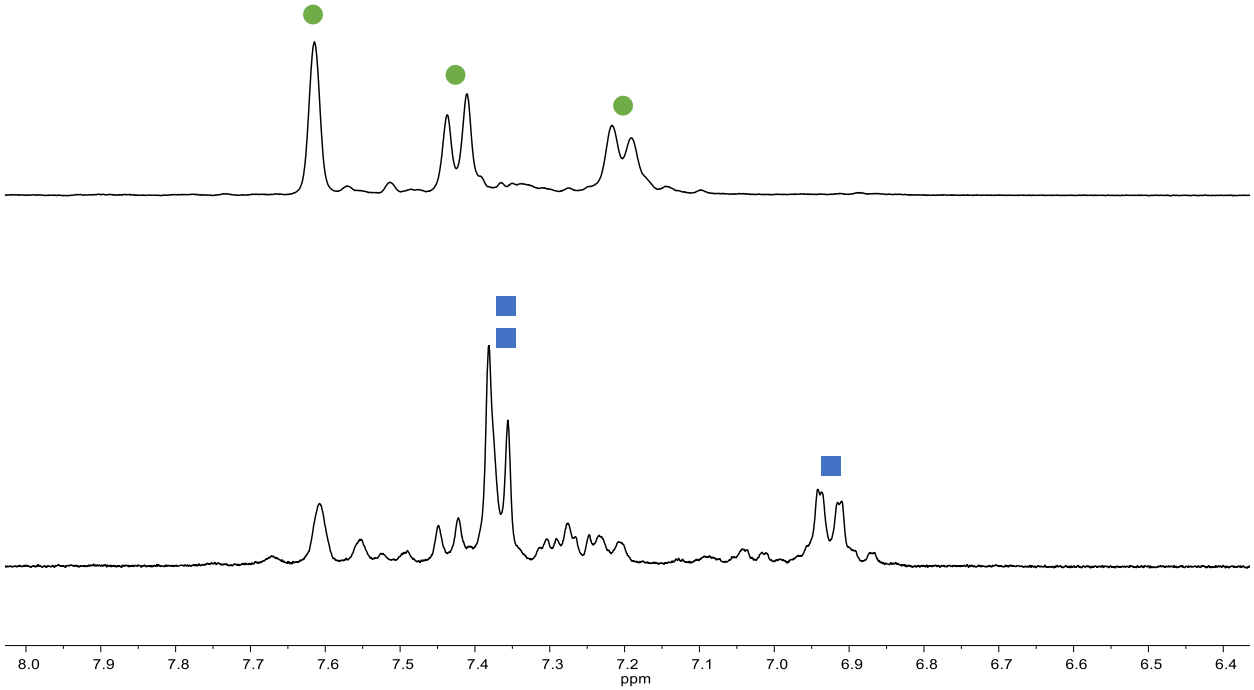

Figure S86. Aryl regions of the ^{1}H NMR spectra (300.0 MHz, THF-d_8) of **11** before (top) and after addition of LiH (bottom; cf. 1.25). Marked components: **11** (●), Li[**5**] (■).

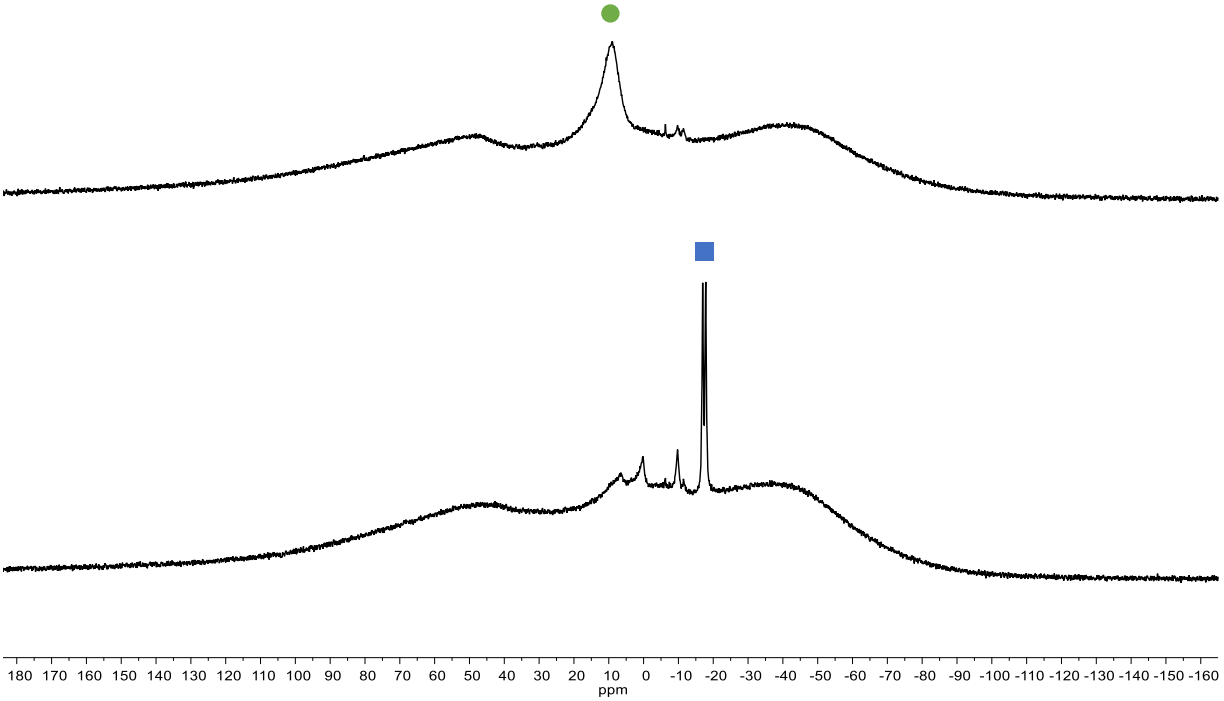

Figure S87. ^{11}B NMR spectra (96.3 MHz, THF-d_8) of **11** before (top) and after addition of LiH (bottom; cf. 1.25). Marked components: **11** (●), Li[**5**] (■).

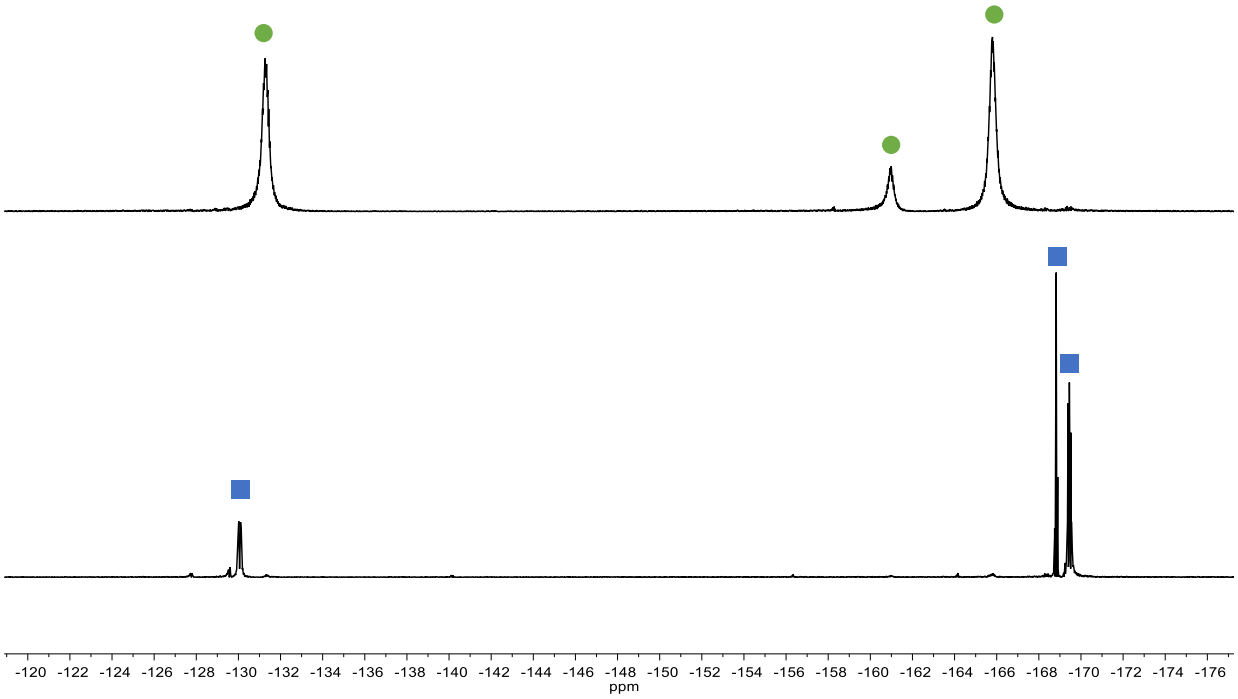

Figure S88. ^{19}F NMR spectra (282.3 MHz, THF-d_8) of **11** before (top) and after addition of LiH (bottom; cf. 1.25). Marked components: **11** (●), Li[**5**] (■).

3. X-ray crystal structure analyses

Data for all structures were collected on a STOE IPDS II two-circle diffractometer with a Genix Microfocus tube with mirror optics using MoK_α radiation (λ = 0.71073 Å). The data were scaled using the frame-scaling procedure in the *X-AREA* program system.[S9] The structures were solved by direct methods using the program *SHELXS* and refined against F^2 with full-matrix least-squares techniques using the program *SHELXL*.[S10]

CCDC 2119827–2119832 contain the supplementary crystallographic data for this paper. These data can be obtained free of charge from The Cambridge Crystallographic Data Centre via www.ccdc.cam.ac.uk/data_request/cif.

[Na(dme)$_2$(thf)$_2$][**6**]: Both *t*Bu groups are disordered over two sets of sites with site occupation factors of 0.724(6) and 0.778(11) for the major occupied sites. In one thf ligand, all methylene groups are disordered over two sets of sites with a site occupation factor of 0.642(10) for the major occupied sites. The displacement parameters of the disordered atoms were restrained to an isotropic behavior. The H atom bonded to B was isotropically refined.

[Li(12-c-4)$_2$][**7**]: The H atoms of one methyl group are disordered over two sets of sites with a site occupation factor of 0.54(5) for the major occupied sites. Both cations are located on a two-fold rotation axis. [Li(12-c-4)$_2$][**7**] and [Li(12-c-4)$_2$][**8**] form isomorphous structures.

[Li(12-c-4)$_2$][**8**]: The H atoms of one methyl group are disordered over two sets of sites with a site occupation factor of 0.60(3) for the major occupied sites. Both cations are located on a two-fold rotation axis. [Li(12-c-4)$_2$][**7**] and [Li(12-c-4)$_2$][**8**] form isomorphous structures.

[Na(thf)$_2$][**8**·py] forms a polymeric structure with chains running along the c axis (cf. Figure S93).

[Li(dme)$_3$]$_2$[**9**]·(THF)$_2$: The anion is located on a center of inversion. The H atom bonded to B was isotropically refined. One *t*Bu group is disordered over two sets of sites with a site occupation factor of 0.63(3) for the major occupied sites. The displacement parameters of the disordered atoms and the THF molecule were restrained to an isotropic behavior. The displacement parameters of the atoms in one dme ligand were restrained to be similar.

[Na(dme)(thf)$_3$][**10**]·THF: One *t*Bu group is disordered over two sets of sites with a site occupation factor of 0.765(15) for the major occupied sites. In one thf ligand, three methylene groups are disordered over two positions with a site occupation factor of 0.593(15) for the major occupied sites. The displacement parameters of the disordered atoms were restrained to an isotropic behavior. In one thf ligand, the C–C bond distances were restrained to 1.54(1)Å and all 1–3 distances were restrained to 2.30(1)Å. The contribution of unidentifiable solvent molecules was suppressed using the *SQUEEZE* routine in *PLATON*.[S11]

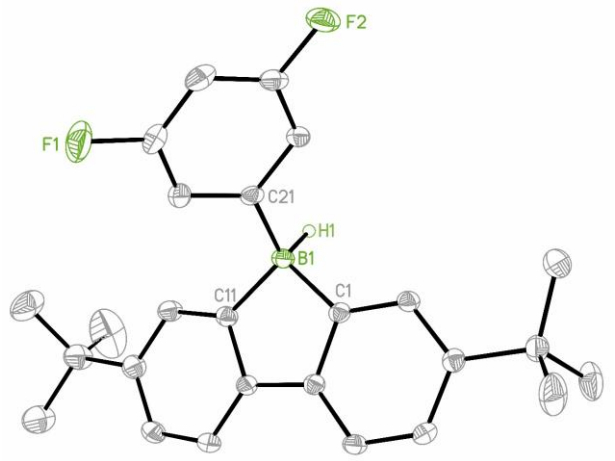

Figure S89. Molecular structure of $[Na(dme)_2(thf)_2][\mathbf{6}]$ in the solid state. Displacement ellipsoids are drawn at the 30% probability level; the $[Na(dme)_2(thf)_2]^+$ cation and all carbon-bonded hydrogen atoms are omitted for clarity. Selected bond lengths (Å) and bond angles (°): B(1)–C(1) = 1.625(3), B(1)–C(11) = 1.629(3), B(1)–C(21) = 1.625(3), B(1)–H(1) = 1.17(3); C(1)–B(1)–C(11) = 98.54(16), C(21)–B(1)–H(1) = 107.7(13).

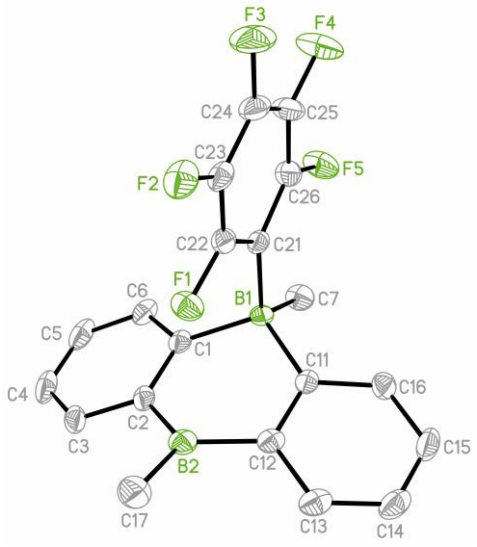

Figure S90. Molecular structure of $[Li(12\text{-c-}4)_2][\mathbf{7}]$ in the solid state. Displacement ellipsoids are drawn at the 30% probability level; the $[Li(12\text{-c-}4)_2]^+$ cation and all hydrogen atoms are omitted for clarity. Selected bond lengths (Å), atom···atom distances (Å), and bond angles (°): B(1)–C(1) = 1.643(4), B(1)–C(7) = 1.634(4), B(1)–C(11) = 1.646(4), B(1)–C(21) = 1.682(4), B(2)–C(2) = 1.556(5), B(2)–C(12) = 1.552(4), B(2)–C(17) = 1.592(5), C(1)–C(2) = 1.415(4), C(11)–C(12) = 1.418(4); B(2)···F(1) = 2.647(4); C(1)–B(1)–C(11) = 109.4(2), C(7)–B(1)–C(21) = 112.4(2), C(2)–B(2)–C(12) = 116.9(3), C(2)–B(2)–C(17) = 121.7(3), C(12)–B(2)–C(17) = 121.3(3).

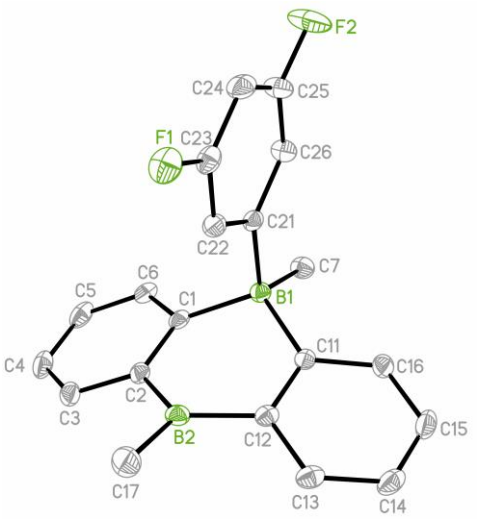

Figure S91. Molecular structure of $[Li(12\text{-}c\text{-}4)_2][\mathbf{8}]$ in the solid state. Displacement ellipsoids are drawn at the 30% probability level; the $[Li(12\text{-}c\text{-}4)_2]^+$ cation and all hydrogen atoms are omitted for clarity. Selected bond lengths (Å) and bond angles (°): B(1)–C(1) = 1.635(2), B(1)–C(7) = 1.638(2), B(1)–C(11) = 1.638(2), B(1)–C(21) = 1.6649(19), B(2)–C(2) = 1.557(2), B(2)–C(12) = 1.553(2), B(2)–C(17) = 1.583(2), C(1)–C(2) = 1.4205(19), C(11)–C(12) = 1.4223(19); C(1)–B(1)–C(11) = 109.23(11), C(7)–B(1)–C(21) = 110.08(11), C(2)–B(2)–C(12) = 117.27(12), C(2)–B(2)–C(17) = 121.27(13), C(12)–B(2)–C(17) = 121.42(13).

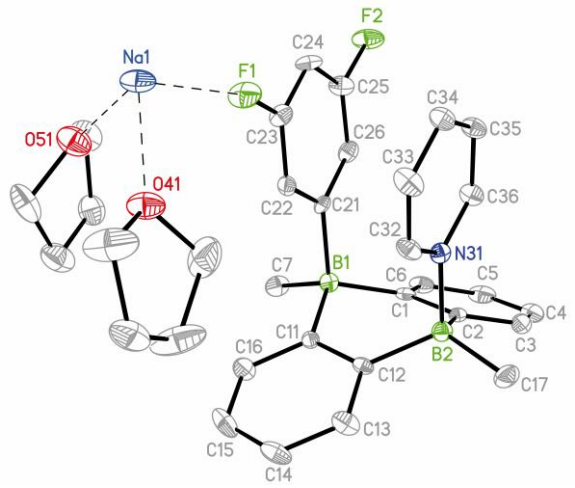

Figure S92. Molecular structure of $[Na(thf)_2][\mathbf{8}\cdot py]$ in the solid state. Displacement ellipsoids are drawn at the 30% probability level; hydrogen atoms are omitted for clarity. Selected bond lengths (Å), atom···atom distances (Å), and bond angles (°): B(1)–C(1) = 1.641(8), B(1)–C(7) = 1.651(8), B(1)–C(11) = 1.642(8), B(1)–C(21) = 1.657(8), B(2)–N(31) = 1.671(8), B(2)–C(2) = 1.625(8), B(2)–C(12) = 1.627(8), B(2)–C(17) = 1.617(8), C(1)–C(2) = 1.424(7), C(11)–C(12) = 1.418(7); F(1)···Na(1) = 2.475(4); C(1)–B(1)–C(11) = 108.7(4), C(7)–B(1)–C(21) = 105.6(4), N(31)–B(2)–C(17) = 102.4(4), C(2)–B(2)–C(12) = 109.4(4).

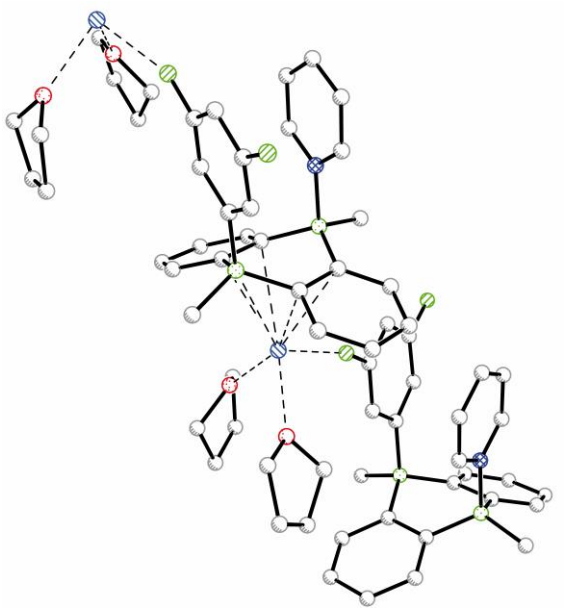

Figure S93. Description of the solid-state structure of $[Na(thf)_2][\mathbf{8}\cdot py]$: In the crystal lattice, coordination polymers are formed: Each Na^+ cation coordinates a B_2C_4 ring in an η^5 mode and one fluorine atom of a second $[\mathbf{8}\cdot py]^-$ moiety. The coordination sphere of each Na^+ cation is completed by two thf ligands.

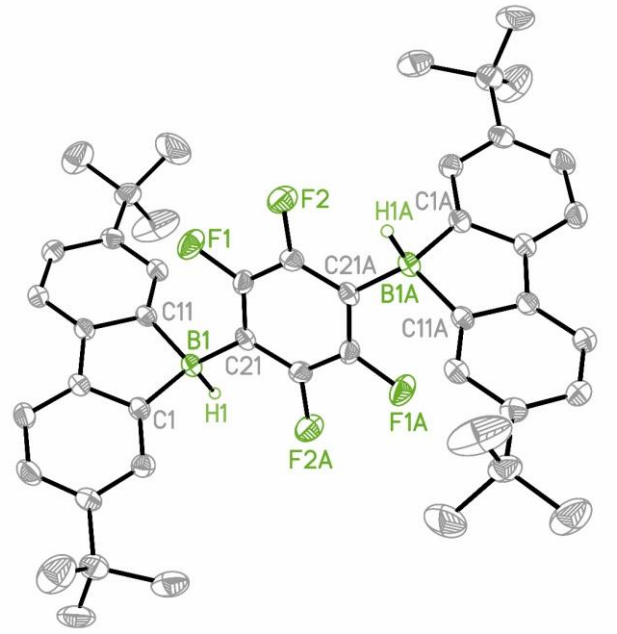

Figure S94: Molecular structure of $[Li(dme)_3]_2[\mathbf{9}]\cdot(THF)_2$ in the solid state. Displacement ellipsoids are drawn at the 30% probability level; the $[Li(dme)_3]^+$ cations, the non-coordinating THF molecules, and all carbon-bonded hydrogen atoms are omitted for clarity. Selected bond lengths (Å) and bond angles (°): B(1)–C(1) = 1.624(5), B(1)–C(11) = 1.625(5), B(1)–C(21) = 1.6242(5), B(1)–H(1) = 1.15(4); C(1)–B(1)–C(11) = 98.7(3), C(21)–B(1)–H(1) = 109(2). Symmetry transformation used to generate equivalent atoms: A: –x+2, –y+1, –z+1.

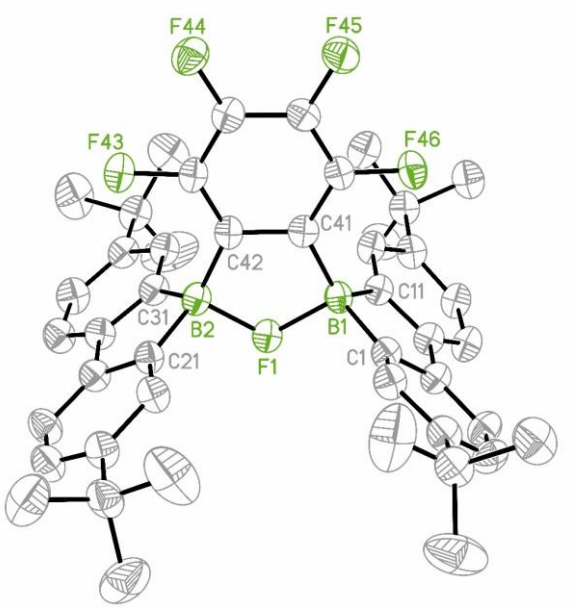

Figure S95. Molecular structure of [Na(dme)(thf)$_3$][**10**]·THF in the solid state. Displacement ellipsoids are drawn at the 30% probability level; the [Na(dme)(thf)$_3$]$^+$ cation, the non-coordinating THF molecule, and all hydrogen atoms are omitted for clarity. Selected bond lengths (Å) and bond angles (°): B(1)–C(1) = 1.588(7), B(1)–C(11) = 1.605(7), B(1)–C(41) = 1.596(7), B(2)–C(21) = 1.606(8), B(2)–C(31) = 1.620(7), B(2)–C(42) = 1.585(7), B(1)–F(1) = 1.627(6), B(2)–F(1) = 1.606(6); C(1)–B(1)–C(11) = 100.9(4), C(41)–B(1)–F(1) = 96.6(3), C(21)–B(2)–C(31) = 100.4(4), C(42)–B(2)–F(1) = 97.8(3), B(1)–F(1)–B(2) = 116.1(3).

Table S1. Selected crystallographic data for $[Na(dme)_2(thf)_2]$[**6**], $[Li(12\text{-}c\text{-}4)_2]$[**7**], and $[Li(12\text{-}c\text{-}4)_2]$[**8**].

compound	$[Na(dme)_2(thf)_2]$[**6**]	$[Li(12\text{-}c\text{-}4)_2]$[**7**]	$[Li(12\text{-}c\text{-}4)_2]$[**8**]
CCDC	2119827	2119828	2119829
formula	$C_{42}H_{64}BF_2NaO_6$	$C_{36}H_{46}B_2F_5LiO_8$	$C_{36}H_{49}B_2F_2LiO_8$
M_r	736.73	730.29	676.31
T (K)	173(2)	173(2)	173(2)
radiation, λ (Å)	Mo*K*a, 0.71073	Mo*K*α, 0.71073	Mo*K*α, 0.71073
crystal system	Triclinic	Monoclinic	Monoclinic
space group	*P* –1	*P*2/*c*	*P*2/*c*
a (Å)	10.8845(5)	14.9807(7)	14.7855(6)
b (Å)	11.5297(6)	11.3004(3)	11.3455(3)
c (Å)	19.0040(10)	21.6896(9)	21.3068(8)
α (°)	99.757(4)	90	90
β (°)	95.418(4)	102.043(3)	99.601(3)
γ (°)	111.364(4)	90	90
V (Å^3)	2157.0(2)	3591.0(2)	3524.1(2)
Z	2	4	4
D_{calcd} (g cm^{-3})	1.134	1.351	1.275
μ (mm^{-1})	0.087	0.109	0.093
F (000)	796	1536	1440
crystal size (mm)	0.27 x 0.27 x 0.25	0.21 x 0.16 x 0.13	0.19 x 0.18 x 0.08
crystal shape, color	block, colorless	block, colorless	plate, colorless
Reflections collected	26770	35548	47433
Independent reflections	8073	6742	6607
R_{int}	0.0306	0.0342	0.0394
data / restraints / parameters	8073 / 150 / 566	6742 / 0 / 473	6607 / 0 / 445
GOF on F^2	1.127	1.176	1.046
R_1, wR_2 ($I > 2\sigma(I)$)	0.0661, 0.1503	0.0701, 0.1595	0.0386, 0.0951
R_1, wR_2 (all data)	0.0857, 0.1665	0.0892, 0.1754	0.0489, 0.1027
largest difference peak and hole (e Å^{-3})	0.515, –0.319	0.385, –0.266	0.248, –0.191

Table S2. Selected crystallographic data for , $[Na(thf)_2][\mathbf{8}\cdot py]$, $[Li(dme)_3]_2[\mathbf{9}]\cdot(THF)_2$, and $[Na(dme)(thf)_3][\mathbf{10}]\cdot THF$.

compound	$[Na(thf)_2][\mathbf{8}\cdot py]$	$[Li(dme)_3]_2[\mathbf{9}]\cdot(THF)_2$	$[Na(dme)(thf)_3][\mathbf{10}]\cdot THF$
CCDC	2119830	2119831	2119832
formula	$C_{33}H_{38}B_2F_2NNaO_2$	$C_{78}H_{126}B_2F_4Li_2O_{14}$	$C_{66}H_{90}B_2F_5NaO_6$
M_r	563.25	1399.28	1118.98
T (K)	173(2)	173(2)	173(2)
radiation, λ (Å)	Mo$K\alpha$, 0.71073	Mo*K*a, 0.71073	Mo*K*a, 0.71073
crystal system	Monoclinic	Monoclinic	Triclinic
space group	$P2_1/c$	$P2_1/n$	$P\,\bar{1}$
a (Å)	17.3110(11)	11.4340(4)	15.1329(12)
b (Å)	9.3726(5)	19.5110(7)	15.4312(14)
c (Å)	18.6925(11)	18.5193(7)	17.5943(16)
α (°)	90	90	115.739(7)
β (°)	96.886(5)	90.374(3)	93.230(7)
γ (°)	90	90	112.736(6)
V (Å^3)	3011.0(3)	4131.4(3)	3286.7(5)
Z	4	2	2
D_{calcd} (g cm^{-3})	1.243	1.125	1.131
μ (mm^{-1})	0.096	0.080	0.085
F (000)	1192	1516	1200
crystal size (mm)	0.18 x 0.16 x 0.04	0.29 x 0.28 x 0.23	0.26 x 0.17 x 0.11
crystal shape, color	plate, colorless	block, light yellow	plate, colorless
Reflections collected	12823	47677	33613
Independent reflections	5611	7265	11559
R_{int}	0.0726	0.0425	0.0721
data / restraints / parameters	5611 / 0 / 370	7265 / 96 / 483	11559 / 164 / 786
GOF on F^2	1.381	1.139	1.325
R_1, wR_2 ($I > 2\sigma(I)$)	0.1304, 0.2191	0.1049, 0.2594	0.1204, 0.3236
R_1, wR_2 (all data)	0.1738, 0.2353	0.1218, 0.2732	0.1913, 0.3775
largest difference peak and hole (e Å^{-3})	0.313, –0.313	0.569, –0.495	0.861, –0.507

4. References

S1 H. Budy, T. Kaese, M. Bolte, H.-W. Lerner and M. Wagner, *Angew. Chem. Int. Ed.*, 2021, **60**, 19397–19405.

S2 J. Gilmer, H. Budy, T. Kaese, M. Bolte, H.-W. Lerner and M. Wagner, *Angew. Chem. Int. Ed.*, 2020, **59**, 5621–5625.

S3 E. von Grotthuss, S. E. Prey, M. Bolte, H.-W. Lerner and M. Wagner, *Angew. Chem. Int. Ed.*, 2018, **57**, 16491–16495.

S4 A. Lorbach, M. Bolte, H. Li, H.-W. Lerner, M. C. Holthausen, F. Jäkle and M. Wagner, *Angew. Chem. Int. Ed.*, 2009, **48**, 4584–4588.

S5 E. von Grotthuss, S. E. Prey, M. Bolte, H.-W. Lerner and M. Wagner, *J. Am. Chem. Soc.*, 2019, **141**, 6082–6091.

S6 R. J. Procter, J. J. Dunsford, P. J. Rushworth, D. G. Hulcoop, R. A. Layfield and M. J. Ingleson, *Chem. Eur. J.*, 2017, **23**, 15889–15893.

S7 G. R. Fulmer, A. J. M. Miller, N. H. Sherden, H. E. Gottlieb, A. Nudelman, B. M. Stoltz, J. E. Bercaw and K. I. Goldberg, *Organometallics*, 2010, **29**, 2176–2179.

S8 H. Budy, C. D. Buch, M. Bolte, H.-W. Lerner and M. Wagner, CCDC 2119826: CSD Communication, 2021, DOI: 10.5517/ccdc.csd.cc294vht.

S9 *X-AREA: Diffractometer Control Program System*, Stoe & Cie, Darmstadt, Germany, 2002.

S10 G. M. Sheldrick, *Acta Crystallogr. Sect. A: Found. Crystallogr.*, 2008, **64**, 112–122.

S11 A. L. Spek, *Acta Crystallogr. Sect. C Struct. Chem.*, 2015, **71**, 9–18.